Heat transfer through an electrical coil

J. Pitchford

THE UNIVERSITY OF DURHAM

HEAT TRANSFER THROUGH AN ELECTRICAL COIL

by

J. Pitchford

THESIS SUBMITTED FOR THE DEGREE OF M.Sc.

DECEMBER 1973

CONTENTS

Page

Page

Page

ACKNOWLEDGEMENTS

I should like to thank Mr. L. Morley of Teesside Polytechnic for the many hours of help and encouragement given during the preparation of this thesis.

I should also like to thank Professor H. Marsh of Durham University for the time spent in reading the draft copies and for the many helpful suggestions which were much appreciated.

J Pitchford.

ABSTRACT

A theoretical basis is laid down for determining the radial conductivity for electrical coils of cylindrical construction made from electrical grade round copper wire covered with a thin layer of plastic insulation, both with and without paper interleaving between the windings. A novel technique is used to give the radial conductivity of a coil in the form of equations which are functions of the thermal conductance of the insulation on the wire, the conductivity of the air, the maximum compression of the insulation under load, the relationship between the thermal conductance of paper and the applied load, and general dimensions. The technique approximates the lines of heat flow through the coil by a system of lines that can be analysed by one-dimensional heat transfer theory.

Methods are described for determining the properties of the constituents of the coil that are required for the calculation of the conductivity, and the results of experiments are given that show that the accuracy of the the theoretical prediction of the conductivity is better than $\pm 15\%$ of that obtained by direct test upon the coil.

The analysis for the radial conductivity of non-interleaved coils is extended to cover axial conductivity but no experimental verification is given. The use of the two conductivities, axial and radial, in obtaining the temperature distribution by numerical analysis is shown and the limitations of the analysis is discussed.

Finally a computer programme is provided for calculating the conductivity of paper interleaved coils.

INTRODUCTION.

Electrical coils are used throughout the electrical industry for producing an inductance or a short tractive force as in transformers, electromagnets, solenoids etc. The inductive effect is produced by passing a current through windings which are wrapped around a central core. An unfortunate side effect of this is the production of heat within the windings which must be removed by conduction to the outer surface and then dissipated into the surrounding medium. A review of design manuals, British Standards, text books etc., reveals that a considerable amount of work has already been carried out into the mechanism involved in the transfer of heat from the surface of a coil into the surroundings, but the techniques available for obtaining the temperature distribution within the coil are severely restricted because of the lack of a satisfactory method for predicting the apparent conductivity of the main body of the coil. The only technique that gives any indication of the temperature within a coil is that given in British Standard 171 (1970) for testing transformer coils. The technique involves determining a mean temperature in the coil by recording the change in resistance of the windings as the coil heats up. This mean temperature only bears a loose relationship to the highest temperature in the windings which would depend on the geometric shape of the coil; examples from a few text books and design manuals will illustrate the present state of knowledge on this subject. Advanced Electrical Technology by Cotton (1) makes no reference to the temperature distribution within the windings of a transformer but only refers to the surface temperature of those windings. M.G. Say, in his Electrical Engineering Design Manual (2) makes comment "That the hot spot temperature in a coil may be estimated if the coil has a simple geometric shape (see Example 3-2 and 3-3). The results, however, are not strictly reliable owing to the uncertainty of the data and the heterogeneity of the conditions; but they may be used for the purposes of comparison". Say's examples use an average on an area basis of the conductivities of all the constituents of the coil. Fink & Carrol (3) have a single paragraph on the temperature distribution within the windings of a transformer and they give an equation $T = R_t . t . D_t$ where T is the temperature drop, R_t is the thermal resistance, t is the distance through which the heat has to pass, and D_n is the heat flow, but they give no way of determining the value of R_t. A second book by Say, The Performance and Design of Alternating Current Machines (4) makes the comment "the average winding temperature is limited to about 100°C (with hot spot temperatures possibly 30 to 40°C higher)"; the average temperature he refers to is that determined by the method in BS.171. Estimates vary as to the difference between the hot spot and mean temperature. British Standard 171 recommends mean temperatures in transformer windings 45K to 55K below the maximum working temperature of the insulation as given in BS. 2757 (1956). Probably one of the most accurate techniques for obtaining the apparent thermal conductivity of the windings of a coil is given by Richter in Elektrische Maschinen (5). The technique involves assuming a change in the geometric configuration of the windings in order to make the calculation simple. The technique is dealt with in more detail in later parts of this text.

The only heat transfer literature with any reference to coils is that of Jakob, Heat Transfer Vol.1.(6) which gives mathematical analysies for determining the temperature distribution within the coil from the apparent conductivity, but the technique given for determining the apparent conductivity leaves a considerable amount to be desired and is in fact very similar to Richter's (5) technique. In a number of places Jakob (6) is inaccurate in referring to other texts and he makes comment that Moore (7) and Richter (5) have graphical techniques for determining the apparent conductivity of a coil. Examination of Moore's (7) book reveals no such technique, only an illustration of a method of drawing the lines of heat flow through a simplified coil and Richter (5) uses virtually the same technique as Jakob (6).

From the above it would seem that the outlook was extremely bleak for a coil designer. However, the empirical techniques for designing coils tend to be self correcting as regards temperature within the windings, i.e., once a successful first transformer has been designed it will be relatively easy to scale a second without knowledge of the temperature distribution within the windings. This is because a transformer coil is designed on constant surface temperature for which there is an adequate theoretical basis. Increasing the size of a transformer would involve increasing the heat output by the cube of the linear dimensions and the surface area by the square of the linear dimensions. Therefore, extra surface area will be required to maintain the same coil surface temperature as the prototype coil. This is usually obtained by splitting a large coil into small ones which of necessity would have a lower hot spot temperature than the large coil. Thus a certain amount of compensation for hot spot temperature is obtained.

The transformer designer could in fact do better than he appears to have done from the literature since it is possible to calculate the apparent conductivity from the mean temperature of the coil obtained by BS.171 test. This is unfortunately a long and complicated procedure (a method is suggested in Jakob (6) without details) and will only apply to, coils without a core, coils with a very large core and pancake coils. Even so, the effect of change in wire size cannot be predicted with present techniques. Therefore a technique for obtaining the apparent conductivity of a wound coil would have considerable application.

The conclusion is borne out by a discussion with a local manufacturer of coils (Westool Ltd.,) They commented that it would be of considerable value to be able to predict the temperature to which the hot spot of a coil would rise under a given condition of current and voltage.

This project is therefore devoted to devising a method of predicting, with reasonable accuracy, the apparent conductivity of a coil. However the number of different types of coil at present in use make it possible to cover only a small range of wire, insulations and sizes. Therefore, for the purpose of this analysis, the type of coils under consideration were made from electrical grade round copper wire with a thin layer of plastic insulation and wound on a cylindrical former with or without paper interleaving between the windings. Radial conductivity was tested fully and the analysis was extended to axial heat flow. To derive the apparent conductivity, a novel method is used whereby the true lines of heat flow through the coil are approximated by lines of heat flow that can be analysed mathematically from one dimensional heat transfer theory. In this way an algebraic solution is obtained.

In the first chapter a theory is developed from which the apparent conductivity of a coil may be obtained by the substitution of various characteristics of the constituents of the coil into certain equations. However some of the characteristics required are not available in reference literature. Therefore, in the second chapter, precise experimental methods for the determination of these characteristics are described and tested. In the third chapter the accuracy with which the method will predict the apparent radial conductivity is determined, and in the fourth chapter the technique is extended to cover axial conductivity. Finally, in a discussion, the general method is analysed and a comparison made between this and the method of Jakob (6) and Richter (5).

A considerable amount of the detail of the project is left out of the main text and put into the appendices. This was thought necessary since some of the derivation of the theory is long and complicated and not essential to the main argument. Also, the derivations of standard equations that can be obtained from other literature are not given.

CHAPTER 1.

DEVELOPMENT OF THEORY.

1.1 Basic definitions.

The main theoretical basis of this thesis, excluding that involved directly with the experimentation, is given in this chapter. Throughout a preference is given to the use of conductance rather than the more common conductivity, conductance being defined as follows:-

$$C = \frac{q}{A(\theta_2 - \theta_1)}$$

where C = conductance,

A = the area through which the heat flows,

q = the heat flow,

θ_2 and θ_1 = the temperatures at the ends of the body for which the conductance is to be found.

This preference for conductance arose because it was, in the practical sense, simpler to obtain the conductance of thin films such as paper and insulation rather than the conductivity. Also, in a number of places it was necessary to define the heat flow through non uniform sections, in which case, conductance was easier to use than the conductivity where a thickness measurement would have to be given. This was similar to the use of conductance for film coefficients where a thickness measurement is difficult to obtain. However, in some sections it was also found easier to dispense with the area measurement A in the conductance and define a new term for heat transfer, which,for want of a better name will be called the "heat rate" and will be the product of conductance and area as defined below:-

$$H = C.A = \frac{q}{(\theta_2 - \theta_1)}$$

where H = heat rate = heat flux per unit temperature difference.

Now in order to show how the heat rate will be used in the text, two theorems are given below which will be referred to in later parts of the chapter.

<u>Theorem 1.</u>

"The overall heat rate for any number of bodies in parallel with the same end temperatures is the sum of the individual heat rates for each body, provided there is no heat transfer between the bodies" .

This can be shown to be true by considering two bodies as shown in Fig. 1.1. The figure shows two bodies in parallel with perfect insulation between, to stop heat transfer from one body to the other. The ends of the bodies are immersed in a perfect conductor, the top at a temperature θ_1. the bottom at a temperature of θ_2.

Therefore the heat transfer through Body 1 will be:

$$q_1 = H_1(\theta_2 - \theta_1)$$

The heat transfer through Body 2 will be:

$$q_2 = H_2(\theta_2 - \theta_1)$$

and the total heat transfer will be:

$$q_t = q_1 + q_2$$

which makes the overall heat rate:

$$H_t = \frac{q_t}{(\theta_2 - \theta_1)} = \frac{q_1 + q_2}{(\theta_2 - \theta_1)} = H_1 + H_2 \quad .$$

thus verifying Theorem 1.

Theorem 2.

"The reciprocal of the heat rate for any number of bodies in series is the sum of the reciprocals of the heat rates for the individual bodies."

This can be shown to be true by considering Fig 1.2 which shows two bodies in series surrounded by thermal insulation and with the free surfaces at either end at temperatures of θ_1 and θ_2 respectively. Putting the overall heat transfer equal to q_t and the overall heat rate equal to H_t and the temperature at the interface equal to θ_i then:-

$$H_t = \frac{q_t}{\theta_2 - \theta_1} \qquad (1.1)$$

$$H_1 = \frac{q_t}{\theta_i - \theta_1} \qquad (1.2)$$

$$H_2 = \frac{q_t}{\theta_2 - \theta_i} \qquad (1.3)$$

Substituting Eq. 1.2 into Eq. 1.3 gives:-

$$\theta_2 - \theta_1 = \frac{q_t}{H_2} + \frac{q_t}{H_1}$$

Substituting into Eq. 1.1 gives:-

$$\frac{1}{H_t} = \frac{1}{H_1} + \frac{1}{H_2}$$

Which may be extended by inspection to any number of bodies, thus verifying the theorem.

It is worth noting that the heat rate for a body is a property of that body and is independent of temperatures within, or heat flow through, that body.

1.2 Preliminary theory.

Jakob (6) shows how the radial temperature distributions within a coil can be calculated from the conductivity of that coil. However, no reference could be found which verified that the conductivity of a coil was constant. Therefore, it was thought necessary to verify this, and in order to cover the experimental work, this preliminary theory was taken from Jakob (6).

Consider first the coil is a homogeneous thick walled cylinder with the ends covered by a perfect insulator. If a heater is placed in the core and the heat allowed to leave the outer surface of the cylinder, then after time $t = \infty$
distribution will be given by the equation:-

$$\frac{q}{2\pi . L . k} . \log_e r = -\theta + C \qquad (1.4)$$

where C is an arbitrary constant.

Thus, the temperature, as would be expected, will fall with increasing radius, and since there will be no heat transfer from the ends of the cylinder, there will be a constant temperature distribution longitudinally. If it was required to obtain the conductivity of the material of the cylinder, this could be done by taking readings of the heat input at the heater, temperature at the heater and temperature at the outside surface. Substituting these readings and the physical dimensions of the coil into Eq.1.4 would give the conductivity (k) of the cylinder. Now if the same cylinder were heated so that the heat was generated throughout the body of the cylinder and the rate of heat generation was a linear function of temperature, then from Jakob (6) the temperature distribution would be given by the equation:-

$$\theta = -\frac{\alpha}{\beta} + C_1.J_o.\left(r\sqrt{\frac{\beta}{k}}\right) + C_2.Y_o.\left(r\sqrt{\frac{\beta}{k}}\right) \qquad (1.5)$$

J_o = Bessel function (first kind; order zero)

Y_o = Bessel function (second kind; order zero)

k = conductivity

r = radius

θ = temperature

and heat generation = $(\alpha + \beta\theta)$

which could be solved by substituting for k plus the other perameters.

It will be shown in Chapters 2 and 3 that the conductivities of the type of coils tested are constant and that the apparent conductivity can be used to predict the temperature distribution in the coil when heat is flowing through the windings. The equation used for this would be Eq. 1.5 since the electrical resistance of the windings will change with temperature such that the heat generation is equal to $\alpha + \beta.\theta$

1.3 An approximate method for calculating the conductivity of non-interleaved coils.

In order to obtain the apparent conductivity of a coil (from now on called 'the conductivity') it is necessary to assume a configuration for the windings within the coil. For the purpose of the approximate method it is assumed that a cross section through the windings is as shown in Fig. 1.3 i.e., the windings are lying on top of each other in a diagonal manner. In practice, the windings cannot lie in this way for the whole of a turn, since the helix of one winding is in the opposite direction to the one below. Thus, on each turn the wire on top must overlap the wire below. Inspection of a coil indicates that this overlap takes place in about 30° of coil rotation and for the rest of the rotation the wire on top lies in the groove made by the wires below. An approximation is therefore introduced by this assumption.

A second assumption is that the coil is built up of identical rectangular blocks of unit length whose cross section is shown outlined in thick black lines in Fig 1.3 and that the lines of heat flow are as shown in the figure. In this way the conductivity of the block will be the same as the conductivity of the whole coil. In practice, the coil is not made up of rectangular blocks but of sections of a toroid; however, provided that the diameter of the coil is much larger than the diameter of the wire, the error caused by approximating a rectangular block to a section of a toroid will be small. Also, the heat flow lines in the sketch are a reasonable approximation that can be analysed mathematically but are not identical to those in practice. It must be noted that the heat flow lines do not cover the whole of the air space, but only pass through the shaded section. The error involved in neglecting this small amount of air space will be negligible since the low conductivity of air will cause most of the heat to pass through the narrowest part of the air space.

Further assumptions are:-

1) copper has infinite conductivity;

2) there is no heat transfer by convection;

3) there is no heat transfer by radiation.

Considering each of the above in turn:

1) Although copper has finite conductivity, this will be at least one order of magnitude greater than the conductivity of any of the other components. Therefore, the errors involved in assuming infinite conductivity will be small.

2) The air spaces are small. Therefore, an appreciable amount of convective heat transfer is unlikely.

3) Radiation across the air space in the coil will only have a detectable effect at much higher temperatures than are likely to be reached.

Now the conductivity of the block outlined in black in Fig 1.3, and hence the conductivity of the coil, may be found as follows:-

$$k_r = - \frac{q_b . h}{A_b(\theta_2 - \theta_1)} \qquad (1.6)$$

where k_r = the conductivity of the coil and hence of the block

q_b = the heat flow through the block

A_b = the area of the block perpendicular to the direction of the heat flow

θ_1 = the temperature at the bottom of the block

θ_2 = the temperature at the top of the block

h = the height of the block

Also, from the definition of the heat rate

$$H_{bl} = -\frac{q_b}{\theta_2 - \theta_1} \tag{1.7}$$

where H_{bl} = the heat rate for the block

Therefore, substituting Eq. 1.6 into Eq. 1.7 gives:-

$$k_r = \frac{H_{bl} \cdot h}{A_b} \tag{1.8}$$

which gives the conductivity of the coil in terms of the heat rate for the block (this equation will be used in later parts of this thesis).

Inspection of Fig.1.3 indicates that D/2 can be substituted for A_b since the block is D/2 wide and of unit length.

Therefore

$$k_r = \frac{H_b \cdot h}{D/2} \tag{1.9}$$

Now to obtain the heat rate of the whole block, the heat rate for each individual part of the block must be found.

Consider first the shaded part of Fig. 1.3. This part may be split into four identical quadrants each having the same heat rate. Therefore by obtaining the heat rate for one quadrant the heat rate for the whole of the shaded area may be found.

To obtain the heat rate for the quadrant, consider element δx in the figure.

From definition of heat rate, page 8 the heat rate for the part of the element in the air space will be:-

$$\frac{k_a.\delta x}{m'}$$

where k_a is the conductivity of the air

m' is the length of the part of the element in the air

and the heat rate for the part of the element passing through the insulation will be:-

$$\frac{C_i.\delta x}{\text{Cos}\phi}$$

where C_i is the conductance of the insulation.

Therefore, applying Theorem 2 to the two equations above will give the heat rate for the whole element thus:

$$H_x = \frac{\frac{k_a.\delta x}{m'} \cdot \frac{C_i.\delta x}{\text{Cos}\phi}}{\frac{k_a.\delta x}{m'} + \frac{C_i.\delta x}{\text{Cos}\phi}} \qquad (1.10)$$

Now from Theorem 1. the sum of the heat rates of each element over the quadrant of the shaded area will give the heat rate for the quadrant.

Eq. 1.10 can best be summed by putting δx in terms of ϕ

Therefore putting

$$x = \tfrac{1}{2}D.\text{Sin}\,\phi$$

so that

$$dx = \tfrac{1}{2}D.\text{Cos}\,\theta.d\phi$$

Substituting into Eq.1.10 and changing δx to dx gives:-

$$H_x = \frac{\frac{k_a}{m'}\,\tfrac{1}{2}D.\text{Cos}\phi.d\phi}{\frac{k_a}{m'}\,\frac{\text{Cos}\phi}{C_i} + 1} \qquad (1.11)$$

However m' varies with ϕ therefore m' must also be obtained in terms of ϕ thus

$$m' = \tfrac{1}{2}D.(1 - \text{Cos}\phi)$$

Substituting into Eq.1.11 gives:-

$$H_x = \frac{\frac{k_a}{\frac{1}{2}D.(1 - \text{Cos}\phi)}.\tfrac{1}{2}D.\text{Cos}\phi.\ d\phi}{\frac{k_a}{\frac{1}{2}D.(1 - \text{Cos}\phi)}.\frac{\text{Cos}\phi}{C_i} + 1}$$

which simplifies to

$$H_x = \frac{C_i.\text{Cos}\phi.k_a.\tfrac{1}{2}D.d\phi}{C_i.\tfrac{1}{2}D + \text{Cos}\phi(k_a - Ci.\tfrac{1}{2}D)}$$

Therefore summing H_x over the quadrant gives:-

$$\sum_{0}^{x_2} H_x = H_{1q} = \int_{\phi_1}^{\phi_2} \frac{C_i . \text{Cos}\phi . k_a . \frac{1}{2}D . d\phi}{C_i . \frac{1}{2}D + \text{Cos}\theta . (k_a - C_i . \frac{1}{2}D)}$$

where H_{1q} = the heat rate for the quadrant

x_2 = the limit of the quadrant in the x direction

θ_2 = the angular limit corresponding to x_2

θ_1 = zero, but will be retained for completeness since the integral will be used in a later part of the text,

which can be abbreviated to

$$H_{1q} = \int_{\phi_1}^{\phi_2} \frac{a . \text{Cos}\phi . d\phi}{c . \text{Cos}\phi + b} \qquad (1.12)$$

where $a = C_i . k_a . \frac{1}{2}D$

$b = C_i . \frac{1}{2}D$

$c = k_a - C_i . \frac{1}{2}D$

$\phi_2 = 30^\circ$

$\phi_1 = 0$

Integrating (the complete integration is given in App.1)

$$H_{1q} = \frac{a}{c}\left\{\phi_2 - \phi_1 - \frac{2b}{(b - c)m}\left[\text{Tan}^{-1}\left(\frac{1}{m}.\text{Tan}\tfrac{1}{2}\phi_2\right) - \text{Tan}^{-1}\left(\frac{1}{m}.\text{Tan}\tfrac{1}{2}\phi_1\right)\right]\right\} \qquad (1.13)$$

when the function $\frac{b + c}{b - c}$ is positive or

$$H_{1q} = \frac{a}{c}\left\{\phi_2 - \phi_1 - \frac{b}{(b - c)m}\left[\log_e\left(\frac{\mathrm{Tan}\frac{1}{2}\phi_2 - m}{\mathrm{Tan}\frac{1}{2}\phi_2 + m} \cdot \frac{\mathrm{Tan}\frac{1}{2}\phi_1 + m}{\mathrm{Tan}\frac{1}{2}\phi_1 - m}\right)\right]\right\} \quad (1.14)$$

when the function $\frac{b + c}{b - c}$ is negative

where m^2 = the positive value of $\frac{b + c}{b - c}$

For all practical purposes the function $\frac{b + c}{b - c}$ will be positive so the result may be simplified by eliminating Eq. 1.14. A further simplification may be obtained by substituting for ϕ_1 and ϕ_2 which results in the equation below:-

$$H_{1q} = \frac{a}{c}\left\{0.524 - \frac{2b}{(b - c)m}\left[\mathrm{Tan}^{-1}\frac{0.2679}{m}\right]\right\} \quad (1.15)$$

It can be shown, using Theorems 1 and 2, that the heat rate for the quadrant is the same as the heat rate for the whole of the shaded area, i.e., the four quadrants.

Now from the heat rate for the shaded area, the heat rate for the area bounded by thick black lines may be found. Considering again Fig. 1.3, the part of the air and insulation between the edges of the shaded area and the edges of the section is assumed to have no heat flow and will therefore have zero heat rate. The copper is assumed to have infinite conductivity and therefore it will have infinite heat rate. Combining all these according to Theorems 1 and 2 gives the heat rate of the whole section as

$$\frac{1}{H_{bl}} = \frac{1}{\infty} + \frac{1}{H_{lq} + 0 + 0} + \frac{1}{\infty}$$

where H_{bl} = the heat rate for the section in this case

Therefore

$$H_{bl} = H_{lq}$$

Now to obtain the conductivity of the coil a substitution is made into Eq.1.9 thus:-

$$k_r = \frac{a}{c}\left\{0.524 - \frac{2b}{(b-c)m}\left[\mathrm{Tan}^{-1}\frac{0.2679}{m}\right]\right\}\frac{h}{\frac{1}{2}D} \qquad (1.16)$$

where $m^2 = \dfrac{b+c}{b-c}$

$a = C_i.\frac{1}{2}D.k_a$

$b = C_i.\frac{1}{2}D$

$c = k_a - C_i.\frac{1}{2}D$

h = the radial pitch of the wires (see Fig.1.3)

Note, h would normally be taken as $D.\frac{\sqrt{3}}{2}$.

The foregoing equation can now be used to calculate the radial conductivity of a coil. An investigation into the accuracy of the equation is carried out in Chapter 2.

1.4 Theory involving the contact area.

The theory in Section 1.3 based on Fig 1.3 does not take into account any contact area between the insulation of adjacent wires since it was assumed that there would only be line contact. Pressure between the wires is in fact likely to result in some deformation of the insulation giving a finite contact area. Now the resistance to heat flow through this finite contact area will be low compared to that where the heat has to pass through an air space, since the thermal resistance of the insulation will be low compared with that of air. Therefore, a method which takes this into account should give a more accurate result than that of Section 1.3. Assuming for the present that the amount of heat which passes through the air space is negligible compared with that passing through the contact area, then the equations governing the conductivity of the coil may be derived as shown below:

As in Section 1.3, consider a block of unit length with the cross section shown in Fig 1.4, outlined in thick black lines. The figure shows the wires to have a finite contact area, the shaded area being that through which the heat flows. Under the assumptions in Case 1 and the additional assumption that the shaded area is rectangular in shape with a depth equal to twice the thickness of the insulation, a relationship can be obtained for the heat rate of the shaded area. The additional assumption made in this case is reasonable and will only cause small errors, provided (a) the contact area is small compared with the diameter of the wire and (b) the reduction in thickness of the insulation is small compared with the thickness of the insulation.

Therefore, considering the shaded area in the sketch, both top and bottom halves will have a conductance the same as the insulation C_i and the heat rate for each half will be $C_i.M$ where M is the width of the contact area.

Therefore the heat rate for the whole of the shaded area may be obtained thus:-

$$H_{2c} = \frac{(C_i.M) \, . \, (C_i \, M)}{(C_i.M) + (C_i.M)}$$

$$= \frac{C_i.M}{2} \qquad (1.17)$$

which could be used in Eq. 1.9 to obtain the conductivity of the coil. However, this will not be carried out here since the assumption that there is no heat flow through the air space is unlikely to be correct.

To take into account the heat transfer through the air space Fig 1.5 must be considered. This shows the area which must be taken into account in adlition to the shaded area in Fig. 1.4. Inspection of Fig. 1.5 shows that it is very similar to Fig. 1.3 for Section 1.3 in that the configuration of the components is the same except that the centre section is missing. However, apart from the centre section, another difference is that the centres of the wires are closer together by an ammount equal to the flattening of the insulation on each wire. Because of the similarity between Section 1.3 and this section, the solution in Section 1.3 may be used here. Considering a quadrant of the shaded area in Fig. 1.5, the heat rate of the element δx in that quadrant will be the same as for Section 1.3 and will be given by Eq. 1.10 thus:-

$$H_x = \frac{\frac{k_a}{m'} \cdot \delta x}{\frac{k_a}{m'} \cdot \frac{\cos\phi}{C_i} + 1}$$

However, in this case compared with Section 1.3, m' will be smaller by an amount equal to the reduction in the thickness of the insulation. Thus, instead of m' equalling $\frac{1}{2}D(1 - \cos\theta)$, it will equal $\frac{1}{2}D(1 - \cos\theta) - p$ where p is the reduction in the thickness of the insulation and can be calculated from M the contact area; (in a later part of this chapter the above equation is used again with respect to paper interleaved coils, in which case p will equal half the reduction in thickness of the paper)

Therefore, summing all the elements as in Section 1.3 gives:-

$$\sum_{x_1}^{x_2} H_x = H_{2q} = \int_{\phi_1}^{\phi_2} \frac{C_i . \cos\phi . k_a . \frac{1}{2}D . d\phi}{C_i . \frac{1}{2}D + \cos\phi(k_a - C_i . \frac{1}{2}D) - C_i . p}$$

However, ϕ_1 now has a different value from that in Section 1.3. It takes the value of the limit of the shaded area nearest the centre of the section and can be obtained from:

$$\sin\phi_1 = M/D$$

Therefore Eq. 1.18 is of the form -

$$H_{2q} = \int_{\phi_1}^{\phi_2} \frac{a.\cos\phi.d\phi}{c.\cos\phi + b}$$

where

$$a = C_i.k_a.\tfrac{1}{2}D$$
$$b = C_i.\tfrac{1}{2}D - C_i.p$$
$$c = k_a - C_i.\tfrac{1}{2}D$$
$$\phi_2 = 30^o$$
$$\phi_1 = \sin^{-1}M/D$$

It can be seen that this equation is the same as Eq. 1.12. Therefore, the solution will be Eq. 1.13 and Eq. 1.14. These equations are rewritten below since the constants here are different from those in Section 1.3:

$$H_{2q} = \frac{a}{c}\left\{\phi_2 - \phi_1 - \frac{2b}{(b - c)m}\left[\tan^{-1}\left(\frac{1}{m}.\tan\tfrac{1}{2}\phi_2\right) - \tan^{-1}\left(\frac{1}{m}.\tan\tfrac{1}{2}\phi_1\right)\right]\right\} \quad (1.18)$$

when function $\frac{b + c}{b - c}$ is positive or

$$H_{2q} = \frac{a}{c}\left\{\phi_2 - \phi_1 - \frac{b}{(b - c)m}\left[\log_e\left(\frac{\text{Tan}\frac{1}{2}\phi_2 - m}{\text{Tan}\frac{1}{2}\phi_2 + m} \cdot \frac{\text{Tan}\frac{1}{2}\phi_1 + m}{\text{Tan}\frac{1}{2}\phi_1 - m}\right)\right]\right\} \quad (1.19)$$

when function $\frac{b + c}{b - c}$ is negative

and where m^2 = the positive value of $\frac{b + c}{b - c}$ The values of the other constants are given above. At this point the heat rates of all parts of the section of coil under consideration have been found. Therefore the heat rate for the whole section can be obtained by combining the heat rates of each individual part. Thus, using Theorems 1 and 2 the heat rate for the whole section will be:-

$$H_{b2} = H_{2q} + H_{2c} \quad (1.20)$$

which can be used to obtain the conductivity of the coil by substitution into Eq. 1.9, giving -

$$k_r = \frac{(H_{2q} + H_{2c}).h}{D/2} \quad (1.21)$$

The above equation can now be used to calculate the conductivity of a non-interleaved coil taking into account the contact area between the wires.

1.5 A method of calculating the conductivity of paper-interleaved coils.

The previous analysis deals only with coils without paper interleaved between the windings. The introduction of paper brings another three variables into the problem. Although this may seem to increase the equations to quite unmanageable proportions, reasonable approximations can be made to reduce their complexity. The additional variables are, the thickness of the paper, the amount of compression the paper will undergo when compressed into the windings, and the thermal conductance of the paper.

The geometric arrangement of paper inter-leaved coils is assumed to be shown in Fig. 1.6. The wires are arranged diagonally as before and the tension in the windings can be seen to compress the paper. Assuming initially that no heat passes through the air spaces and the heat which passes through the rest of the coil travels along the lines of heat flow shown in the figure. Proceeding under the same assumptions as in Section 1.3, the heat rate for the shaded area in the figure may be found.

Consider an element δx in Fig. 1.6. The heat rate of that element may be derived from Theorem 2 thus:-

$$\frac{1}{H_x} = \frac{1}{C_i.\delta x.\cos\phi} + \frac{1}{C_p.\delta x} + \frac{1}{C_i.\delta x.\cos\phi} \qquad (1.22)$$

An approximation is made here that the sides of the element are parallel, in fact they are at an angle of $(D/2).\delta x.\cos\phi$ radians to each other. The error involved in using this approximation will be small, provided the thickness of the insulation is small compared with the diameter of the wire. Another approximation that must be made is to put $\cos\phi$ equal to 1 simplifying Eq. 1.22.

$$\frac{1}{H_x} = \frac{1}{C_i.\delta x} + \frac{1}{C_p.\delta x} + \frac{1}{C_i.\delta x}$$

The effect of this approximation is small provided the angle of contact around the circumference of the wire is small.

Rearranging gives:-

$$H_x = \frac{C_i.C_p.\delta x}{C_i + 2C_p} \qquad (1.23)$$

In practice C_p will vary with the amount of compression of the paper. Therefore, C_p will also vary with respect to $\bar{x}$ and this must be taken into account in the equation. To do this it is assumed that the relationship between the thickness of paper under compression and the conductivity of the paper C_p is:-

$$C_p = s + \frac{v}{y} \qquad (1.24)$$

where y is the thickness of the paper and v and s are constants obtained by experiment.

The equation is based on the assumption that the effect on conductance of a reduction in thickness of the paper by compression will be similar to that of a reduction in thickness by removal of material from the surface. When the latter is the case, the conductance will be inversely proportional to the thickness, i.e., $C_p = \frac{v}{y}$, and over a small range, when the paper is under compression, this is likely to be correct; the constant s was necessary to set the end points.

Now substituting Eq 1.24 into Eq 1.23 gives:-

$$H_x = \frac{C_i(\frac{v}{y} + s).\delta x}{C_i + 2(\frac{v}{y} + s)}$$

and rearranging:

$$H_x = \frac{(C_i.v + C_i.s.y)\delta x}{(C_i + 2s)y + 2v} \quad (1.25)$$

which gives the heat rate of the element (See Fig. 1.6)

In order to obtain the overall heat rate for the shaded section in Fig. 1.6 the heat rate for the element must be summed over that area. To do this both x and y must be obtained in terms of ϕ.

Firstly y may be obtained from basic trigonometrical relationships thus:-

$$y = B + 2(\tfrac{1}{2}D - \tfrac{1}{2}D.\cos\phi)$$

where B is the minimum distance apart of the wires.

Simplifying gives:-

$$y = B + D(1 - \cos\phi) \qquad (1.26)$$

but

$$x = \tfrac{1}{2}D.\sin\phi$$

Therefore

$$dx = \tfrac{1}{2}D.\cos\phi.d\phi \qquad (1.27)$$

Substituting Eq. 1.26 and Eq. 1.27 into Eq. 1.25 gives:-

$$H_x = \frac{\left\{C_i.v + C_i.s\left[B + D(1 - \cos\phi)\right]\right\} \tfrac{1}{2}D.\cos\phi.d\phi}{(C_i + 2s)\ B + D(1 - \cos\phi) + 2v}$$

Rearranging and simplifying gives:-

$$H_x = \frac{\tfrac{1}{2}D.C_i(v + s.B + s.D)\cos\phi - C_i.s.\tfrac{1}{2}D^2.\cos^2\phi}{C_i(B + D) + 2s(B + D) + 2v - (C_i + 2s)D.\cos\phi}.d\phi$$

which is of the form

$$H_x = \frac{e}{c}.\cos\phi + \frac{(a - \frac{e}{c}.b).\cos\phi}{b - c.\cos\phi}\ d\phi \qquad (1.28)$$

where $a = \tfrac{1}{2}D.C_i(v + s.B + s.D)$

$b = C_i(B + D) + 2s(B + D) + 2v$

$c = D(C_i + 2s)$

$e = \tfrac{1}{2}D^2.C_i.s$

Integrating Eq. 1.28 over the shaded area will give H_{3c} the heat rate for that area. However, the limits of the integral must be defined in terms of ϕ which, in turn, may be determined from the width M of the shaded area thus:-

$$\tfrac{1}{2}D.\sin\phi_2 = \frac{M}{2}$$

therefore $$\phi_2 = \sin^{-1}\frac{M}{D}$$

consequently $$\phi_1 = -\sin^{-1}\frac{M}{D}$$

Therefore summing Eq. 1.28 over the shaded area will give -

$$\sum_{-\frac{1}{2}M}^{\frac{1}{2}M} H_x = H_{3c} = \int_{\phi_1}^{\phi_2} \left(f.\cos\phi + \frac{g.\cos\phi}{b - c.\cos\phi} \right) d\phi$$

$$f = \frac{e}{c}$$

$$g = \left(a - \frac{e}{c}.b\right)$$

$$\phi_2 = -\phi_1 = \sin^{-1}\frac{M}{D}$$

However, the integration is simplified by taking it between ϕ_2 and 0, and doubling the result since the equation is symmetrical about $\phi = 0$

Therefore:-

$$H_{3c} = 2\int_{0}^{\phi_2} \left(f.\cos\phi + \frac{g.\cos\phi}{b - c.\cos\phi} \right) d\phi \qquad (1.29)$$

and the solution to the equation is

$$H_{3c} = 2\left[f.\mathrm{Sin}\phi_2 + \frac{g}{c}(V - \phi_2)\right] \qquad (1.30)$$

(Full details of the integration are given in App.1)

where $V = \dfrac{2b}{(b - c)m}\left[\mathrm{Tan}^{-1}\left(\frac{1}{m}.\mathrm{Tan}\tfrac{1}{2}\phi_2\right)\right]$

$m^2 = \dfrac{b - c}{b + c}$

Writing in full gives:-

$$H_{3c} = 2\left\{f.\mathrm{Sin}\phi_2 + \frac{g}{c}\left(\frac{2b}{(b + c)m}\left[\mathrm{Tan}^{-1}\left(\frac{1}{m}.\mathrm{Tan}\tfrac{1}{2}\phi_2\right)\right] - \phi_2\right)\right\} \qquad (1.31)$$

where $m^2 = \dfrac{b - c}{b + c}$

$f = \dfrac{e}{c}$

$g = a - \dfrac{e}{c}.b$

$\phi_2 = \mathrm{Sin}^{-1}(M/D)$

$a = \tfrac{1}{2}D.C_i(v + s.B + s.D)$

$b = C_i(B + D) + 2s(B + D) + 2v$

$c = D.(C_i + 2s)$

$e = D^2.C_i.s$

As can be seen the result is long and complicated and would be difficult to use. However a simplification is possible by approximating the circular surface of the wire to a parabola. This approximation is reasonably good provided M the contact chord is small compared with the diameter. A second approximation that must be made is to change the equation for C_p from

$$C_p = s + \frac{v}{y}$$

to

$$C_p = \frac{1}{s' + v'.y} \qquad (1.32)$$

where s' and v' are constants (different from s and v) obtained by experiment.

The error involved in this will be small when used over a limited range.

Therefore proceeding from Eq. 1.23 which is

$$H_x = \frac{C_i.C_p.\delta x}{C_i + 2C_p}$$

Substituting from Eq. 1.34 and simplifying gives:-

$$H_x = \frac{C_i.\delta x}{C_i.v'.y + C_i.s' + 2}$$

Taking the local approximation to a circle to be:-

$$y = a'.x^2 + b'$$

where a' and b' are constants which may be obtained from the conditions

$$x = 0 \text{ when } y = B$$

$$x = \frac{M}{2} \text{ when } y = T$$

where T = the maximum thickness of the paper

B = the minimum thickness of the paper

Note: y is the thickness of the paper at any point, i.e., the distance apart of the two circular wires.

Therefore,

$$H_x = \frac{C_i.\delta x}{C_i.v'.a'.x^2 + C_i(v'.b' + s') + 2}$$

which may be written in the form

$$H_x = \frac{e.\delta x}{f.x^2 + g}$$

where $f = C_i.v'.a'$

$g = C_i(v'.b' + s') + 2$

$e = C_i$

As before integrating over the shaded area in Fig 1.6 will give H_{3c}, the overall heat rate for the area.

Therefore

$$\sum_{-\frac{1}{2}M}^{\frac{1}{2}M} H_x = H_{3c'} = \int_{x_1}^{x_2} \frac{e.dx}{f.x^2 + g} \qquad (1.33)$$

where $x_2 = M/_2$

$x_1 = -M/_2$

As before the integration may be simplified thus:-

$$H_{3c'} = 2\int_{0}^{x_2} \frac{e.dx}{f.x^2 + g}$$

and the solution is:-

$$H_{3c'} = \frac{2.e}{f.m}\left[\mathrm{Tan}^{-1}\frac{x_2}{m}\right] \qquad (1.34)$$

(Full details of the integration in App.1)

where $m = \sqrt{\frac{g}{f}}$

As can be seen, the equation is simpler than the original Eq. 1.31 and will be considerably easier to use. Both original and simplified equation have alternative solutions but these do not apply to this particular problem.

Equation 1.34 could be used as it stands to obtain the conductivity of the coil, assuming no heat transfer through the air spaces. However, since the result does not give reliable predictions, no further work will be carried out in this direction. Instead the analysis will be extended to take into account the heat transfer through the air spaces.

Considering the air space alone as shown in Fig.1.7, it is assumed that the heat passes through this portion of the coil along the lines of heat flow shown in the figure. Now the heat rate for the shaded section could be found by integrating the heat rate for an element over the whole shaded area as in previous cases. Unfortunately the expression for the conductance of the element is extremely complex and the intergral would be even more so. However, by assuming a constant temperature along the dotted line in the figure, the conductance, and hence the heat rate, can be found in two parts, that is, above the line and below the line. The heat rates can then be combined to obtain the result for the whole of the shaded area. The assumption will in fact cause an error, since the dotted line will not in practice be an isothermal.

To obtain the overall heat rate, consider first the lower left hand portion of the shaded section in Fig.1.7. This is identical with the section in Section 1.4 (see Fig. 1.5 and pages 21 to 26) Therefore the heat rate for this part will be given by Eq. 1.18 and Eq. 1.19. Also, the same equations apply to the upper right hand section since this is identical but inverted. The inversion makes no difference to the result.

Consider secondly the lower right hand part of the shaded area. In this part the heat will have to pass through the insulation, the paper and then the air. Taking element δx, the conductance can be found as follows:-

The part of the element passing through the paper will have a total conductance of:-

$$\frac{C_i \cdot C_p}{C_i + C_p}$$

Let this be called C_{ip}.

It can now be considered that there are only two materials through which the heat has to pass, that of the material with a conductance C_{ip} and the air. Now if C_a (the conductance of the air) is replaced by k_a/m, the problem becomes the same as in Section 1.4 (see Fig. 1.5 and pages 21 to 26) except that the conductance C_p must be replaced by C_{ip}. Therefore, the solution must again be Eq. 1.18 and Eq. 1.19 with C_p replaced by C_{ip} thus:-

$$H_{3p} = \frac{a}{c}\left\{\phi_2 - \phi_1 - \frac{2b}{(b-c)m}\left[\mathrm{Tan}^{-1}\left(\frac{1}{m}.\mathrm{Tan}\tfrac{1}{2}\phi_2\right) - \mathrm{Tan}^{-1}\left(\frac{1}{m}.\mathrm{Tan}\tfrac{1}{2}\phi_1\right)\right]\right\} \quad (1.35)$$

when function $\frac{b+c}{b-c}$ is positive

or

$$H_{3p} = \frac{a}{c}\left\{\phi_2 - \phi_1 - \frac{b}{(b-c)m}\left[\log_e\left(\frac{\mathrm{Tan}\frac{1}{2}\phi_2 - m}{\mathrm{Tan}\frac{1}{2}\phi_2 + m} \cdot \frac{\mathrm{Tan}\frac{1}{2}\phi_1 + m}{\mathrm{Tan}\frac{1}{2}\phi_1 - m}\right)\right]\right\} \quad (1.36)$$

when function $\frac{b+c}{b-c}$ is negative where m^2 = the positive value of $\frac{b + c}{b - c}$

H_{3p} = the heat rate for the upper right hand shaded quadrant in Fig. 1.6.

$a' = C_{ip}.k_a.D_p/2$

$b' = C_{ip}.\tfrac{1}{2}D_p - C_{ip}.p$

$c' = k_a - C_{ip}.D_p/2$

$\phi_1 = \mathrm{Sin}^{-1}M/D_p$

$\phi_2 = 30^o$

D_p = diameter of wire + 2T

$p = \frac{T - B}{2}$

Note that the diameter of the wire is increased since it now has a layer of paper on the part of the surface under investigation.

To summmarise, the heat rates for all parts of the section outlined in thick black lines in Fig. 1.6 and Fig. 1.7 have been obtained and these are:-

(i) centre section shaded in Fig. 1.6 (H_{3c}) given by Eq. 1.31;

(ii) lower left and upper right quadrants in Fig. 1.7 (H_{2q}) given by Eq. 1.18 and Eq. 1.19;

(iii) lower right and upper left quadrants in Fig. 1.7 (H_{3p}), given by Eq. 1.35 and 1.36.

Now using Theorems 1 and 2 in the same way as in previous sections, the overall heat rate for the section may be found thus:-

$$H_{b3} = 2\left[\frac{H_{2q} + H_{3p}}{H_{2q}.H_{3p}}\right] + H_{3c}$$

Substituting into Eq. 1.9 gives the conductivity of the coil thus:-

$$k_r = \left\{ 2\left[\frac{H_{2q} + H_{3p}}{H_{2q}.H_{3p}}\right] + H_{3c} \right\} \frac{h}{\frac{1}{2}D} \qquad (1.37)$$

or alternativly the equation for H_{3c} may be replaced by the simplified version H_{3c}'.

The value of h in the above equation may be obtained as follows. Assuming that there is no gap between the wires in the axial direction, then from Pythagoras

$$(D + B)^2 = (\tfrac{1}{2}D)^2 + h^2$$

and

$$h = \sqrt{2D.B + B^2 + \tfrac{3}{4}D^2} \qquad (1.38)$$

1.6 Discussion on the theoretical basis

At this point equations have been derived which will give the radial conductivity of all the types of coil under consideration. The analysis is subject to a number of assumptions and it requires numerical values for the properties of most of the constituents of the coil. The basic concept behind the equations has been that the lines of heat flow through the coil can be approximated by simple geometry without significantly altering the overall conductivity. Subsequent chapters will show the accuracy obtained by this technique.

CHAPTER 2.

NON - INTERLEAVED COILS.

2.1. Introduction.

In Chapter 1. a general theory has been derived by which the radial conductivity of a non-interleaved coil can be calculated given certain thermal and physical properties of the components of the coil. In the first part of this chapter it is shown that a "conductivity" can be obtained for a coil and that it can be used in the conventional way even though it is an apparent conductivity composed of the individual conductivities of the components of the coil. Secondly, techniques will be described by which the thermal and physical properties of the components of the coil required for the calculation of the conductivity may be obtained. Finally, a comparison is made between theoretical predictions and experimental results.

2.2. Experimental verification of constant conductivity.

The equations that will be used to calculate the temperature distribution within a coil, Eq. 1.4 and Eq. 1.5, were derived for thick cylinders of homogeneous material with constant conductivity. It is therefore necessary to show that a coil has a constant conductivity in the radial direction. It was also necessary to show that this conductivity does not vary with the amount of heat generated within the windings. If both these conditions were met, then the conductivity of a coil obtained by experiment based on Eq. 1.4 could be used in Eq. 1.5 to obtain the temperature distribution in a coil with heat generation within the windings. Also, since the main theory in Chapter 1 is based on heat conduction without internal generation, both conditions must be met for the theory to be of value in predicting the temperature distribution in live coils.

In order to verify these conditions, Coil No.1 was constructed as shown in Fig. 2.1. The coil was made from 1.62 mm diameter copper wire covered with a 0.037 mm thickness of hard polyurethane insulation. The wire was wound on a 25.4 mm diameter former, 127 mm long, with thermally insulated ends. During the winding, eight 0.19 mm diameter chrome-alumel thermocouples were placed in the coil, the positions being shown in Fig. 2.1. These positions were selected so that the mechanical and thermal disturbance created by one thermocouple would have the minimum effect on the next. A sample of thermocouple wire was calibrated to read temperature. The calibration curve is shown in Fig. 2.2. After winding the coil to a diameter of 156 mm, an electrical heater was placed in the centre with the ends thermally insulated to ensure that all the heat passed through the windings. The whole unit was then wired up as shown in Fig. 2.3.

The first test to be carried out on the coil was to pass a direct current through the centre heater and allow sufficient time for the heat transfer within the coil to reach the steady state. Direct current was necessary to avoid induction from heater to windings. Readings were then taken of the voltage across, and the current through, the heater, and the temperatures at the thermocouples. Full details of the readings are given in App.2.

To obtain the conductivity of the coil from the above results, a graph was drawn of thermocouple reading against $\log_e$ of the radius, and the slope of this graph was substituted into Eq. 1.4. Full details are given in App.2 and the graph is shown in Fig. 2.4.

The conductivity obtained for Coil No.1 in this way was:-

$$k_r = 1.045 \ \text{J/m s K}$$

The second test to be carried out was to pass a current through the windings of Coil No.1 and take readings of voltage across, and current through, the windings, and the temperature at the thermocouples as before. Full details of the results of this test are given in App.2, and the temperatures are plotted against the radius in Fig. 2.5. A second set of temperature against radius results was obtained by substituting the value of conductivity obtained in the first test (k_r = 1.045 J/ m s K), the current passing through the windings, and the properties of the wire into Eq. 1.5. (full details of this calculation are given in App.2.) This second set of results is superimposed upon the first in Fig. 2.5.

2.3 Discussion on the tests for constant conductivity.

The results of these two tests indicate that the apparent conductivity of a coil can be used in the same way as the conductivity of a homogeneous cylinder. The conductivity of Coil No.1 is constant at any radius, since any change in the conductivity would be indicated by a change in the slope of the line in Fig. 2.4. The use of this conductivity for calculating the temperature distribution with a current flowing through the windings is indicated by Fig. 2.5. The two curves of this graph do not coincide but it can be seen that the conductivity would be of use in giving an indication of the temperature in a live coil. A point worthy of note is that some of the difference between the two curves is caused by the leakage of heat from the centre of the coil; this is indicated by the temperature drop between the highest temperature in the coil and the temperature in the core. The heat loss will probably be small but will contribute towards the difference in temperatures. An indication of the effect of this heat loss on the theoretical predictions is given by the the third graph in Fig. 2.5. The points for this graph were calculated in the same way as those for the theoretical graph No.2, but the boundary condition of zero heat flow, which was originally assumed to be at the core, was instead, taken from the experimental graph at a value of 30 mm. This third graph can be seen to underestimate the temperature.

The linearity of the graph in Fig. 2.4 has a second implication, i.e. the conductivity is relatively independent of the pressure between the adjacent windings. For a constant winding tension the pressure between the windings at the centre of the coil would be greater than the pressure between the windings at the outside of the coil. Therefore, since the conductivity was constant it must be independent of pressure between the windings.

2.4 Analytical prediction of k_r

As shown in the previous section of this chapter, the conductivity obtained by an experiment with central core heating could be used to predict the temperature distribution in a live coil. Therefore, if the conductivity could be derived with reasonable accuracy analytically, the prediction of the temperature distribution in the coil would be greatly facilitated.

In Chapter 1 two analytical methods were described by which the conductivity of the coil could be obtained. The methods use equations from which a result may be obtained by the substitution of certain properties of the coil. These properties are given below, together with their origin.

1) the conductivity of air - International Critical Tables.

2) the dimensions of the wire - measurement;

3) the dimension of the coil - measurement;

4) the thermal conductance of the insulation on the wire - experiment;

5) the contact area between the wires - experiment;
(this property is only required for the second method).

As can be seen, certain of these properties require experimental determination, details of which are given below:

2.5 Conductance of the insulation.

A number of methods were considered for obtaining the conductance of the insulation. Each of these will be described and the various advantages and disadvantages will be given.

Method 1. Seek information from the manufacturer. Even if available, such information will probably be very inaccurate and will require checking.

Method 2. Obtain a solid block of insulation and shape it to fit a conventional conductivity testing machine. This would be very simple practically, but the film of insulation on the wire, which is very thin, may have a conductivity that is dependent upon surface effects, e.g., air diffusion into the surface during hardening.

Method 3. Paint the insulation on to the surface of a block of good conducting material and use in a Lees' disk. Again this would be simple enough to carry out but difficulties may arise in ensuring that the layer had the same thickness as the insulation and was also uniform.

Each of the above methods entail measuring the conductance away from the wire and they all have the same basic disadvantages. Firstly, that no guarantee can be given that the conductivity of the insulation will be the same when coated on the wire as it is in the practical situation, and secondly, that the thickness of the insulation may vary, which would mean that an average conductance was required. If the conductance can be found whilst the insulation is actually on the wire, or, after being removed from the wire, then the above difficulties are avoided. The following methods were considered to satisfy these conditions and are analysed in a little more detail.

In general a method for finding the conductance of the insulation whilst it is on the wire is most likely to entail passing heat through the insulation and measuring the temperature difference across the insulation.

Method 4. Heat the copper wire by passing a current through the wire and cool the outer surface in a bath of highly agitated liquid. The temperature of the inside of the wire could then be obtained by using the copper as a resistance thermometer and the temperature of the outside of the insulation would be the temperature of the liquid. This assumes that the agitation is sufficient to ~~reduce~~ increase the heat transfer coefficient between water and the surface of the wire to a value which is infinite negligible compared with the conductance of the insulation. The disadvantage of this method is that high electrical currents are required to heat the copper since it is a good conductor of electricity.

Method 5. Calibrate a length of wire as a resistance thermometer and arrange a system so that the temperature can be recorded with respect to time. Then, plunging the wire into a highly agitated bath of hot liquid will give a recording of the rate of increase of temperature of the copper or, in other words, the rate of heat flow through the insulation. Therefore, from this recording, assuming the surface temperature of the insulation is the same as that of the liquid, the conductance of the insulation may be calculated. Again, the difficulty with this method lies in ensuring sufficient agitation to avoid surface effects from the water on the wire

Method 6. Remove the insulation from the wire and use a Lees' disk apparatus to obtain the conductance. The difficulty here lies in actually removing the insulation which is like a film of paint attached very firmly to the surface of the wire.

The method selected for use was number 5. It was thought that in addition to this primary method it was necessary to carry out a check by another method. To do this would require a method which would not be susceptible to any errors that may be involved in the primary method. Method 6 is therefore to be preferred since the other methods could suffer either from the effect of an insulating film when immersed in the fluid or a resistance thermometer error.

2.6 Basis of the primary method (Method 5).

It was assumed that the copper wire inside the insulation was a mass of material of infinite conductivity so that the temperature at the interface of copper and insulation would be the same as for the rest of the copper. Therefore, by using the copper as a resistance thermometer, the temperature at the inside face of the insulation could be obtained. It was also assumed that the bath of highly agitated water would act like an infinite-capacity heat source of infinite conductivity, so that the temperature at the interface of the liquid and insulation would be the same temperature as the main body of the liquid. Therefore, the outside temperature of the insulation may be obtained from the temperature of the main body of the liquid. Also, it was assumed that the temperature of the liquid would remain constant with respect to time.

In practice, certain errors arise from the above considerations. Firstly, the copper has an finite conductivity and the passage of heat through the insulation would cause a temperature distribution in the copper. However, since the copper is likely to have a conductivity so much greater than that of the insulation, the error would be small. Secondly, the temperature of the main body of the liquid would be different from the temperature of the surface of the insulation, since heat transfer takes place through a medium of finite conductivity. However, this temperature difference could be reduced to negligible proportions by vigorous agitation. This was shown to be so by by repeating the test with different amounts of agitation. A different result for the repeat test would indicate a temperature drop that varied with the ammount of agitation. The same result for principal and repeat test would indicate that the temperature drop was negligible. An attempt was made to calculate the heat transfer coefficient from water to wire (see App. 2). This however indicated that the error would not be inappreciable but the result was rejected in favour of the experimental check. Thirdly, the main body of the liquid would not be constant temperature but would cool down when the cool wire was placed into it; again the error would be negligible provided the mass of water was large enough.

2.7 Procedure for the primary method (Method 5).

The apparatus was set up as shown in Fig. 2.6. A length of wire to be tested was arranged to have a small constant current passing through it. The current was to have a 50 Hz ripple about 1% of the DC value in order to measure time in the final recording. The voltage across the length of wire was measured by a UV recorder. Handles were available for easy manipulation of the wire. A test was carried out as follows:-

Firstly, the copper wire was calibrated to read as a thermometer by placing it in water of fixed temperature and allowing time for all heat flow into the the wire to stop; the UV recorder would then be recording a voltage that corresponded to the temperature of the water. This process was then reppeated a number of times for various water temperatures, thus building up a temperature calibration chart.

Secondly, a vessel of boiling water and a large vessel of ambient temperature water were prepared and the temperature taken in both vessels. The wire was immersed in the boiling water until the trace on the UV recorder became steady, i.e., there was no further heat flow across the insulation. The wire was then placed in the cold water and agitated manually at a rate of two 300 mm strokes per second producing a trace on the output of the UV recorder. The process was repeated with four 300 mm strokes per second. The curves were then compared to find if there were any insulating liquid film effects and then used to calculate the conductance of the insulation.

2.8 Theoretical basis of the primary method (Method 5).

The temperature increase of the copper is given by the equation

$$\log_e \theta' = A - \frac{4k_i \cdot t}{T_i \cdot D_w \cdot \rho_c \cdot Cp_c} \qquad (2.1)$$

where

θ' = the temperature drop across the insulation,

D_w = the outside diameter of the wire excluding the insulation,

k_i = the thermal conductivity of the insulation,

T_i = the thickness of the insulation,

ρ_c = the density of copper,

Cp_c = the specific heat of copper,

A = an arbitrary constant

A full derivation of the equation is given in App.3.

It can be seen from the equation that the temperature drop across the insulation has a logarithmic relationship with time. Therefore, if the $\log_e$ of the temperature drop is plotted against time, a straight line graph should result, the slope of which is:-

$$\frac{4k_i}{T_i \cdot D_w \cdot \rho_c \cdot Cp_c}$$

thus

$$S = -\frac{4k_i}{T_i \cdot D_w \cdot \rho_c \cdot Cp_c}$$

where S is the slope of the $\log_e \theta'$ against t graph

However, since the relationship between temperature and an electrical resistance of copper wire was linear, the slope S of the $\log_e \theta'$ against t graph would be the same as the slope S' of the $\log_e C_m$ against t graph where C_m is the height of the UV recording above the steady state line of the cold water temperature. This can be shown to be so by considering:-

$$\theta' = C_m . \phi'$$

where ϕ' is a constant

Therefore, substituting into Eq. 2.1 gives

$$\log_e C_m + \log_e \phi' = A - \frac{4k_i . t}{T_i . D_W . \rho_c . Cp_W}$$

thus

$$S' = - \frac{4k_i}{T_i . D_W . \rho_c . Cp_c}$$

and

$$\frac{k_i}{T_i} = C_i = - \frac{D_W}{4} . \rho_c . Cp_c . S' \qquad (2.2)$$

Therefore the conductance of the insulation may be obtained by first plotting the $\log_e$ of the height of the trace from the UV recorder against time. The height must be measured from the datum corresponding to the temperature of the water into which the wire was plunged (the temperature of the outside of the insulation). Then substituting the slope of the graph, which should be a straight line, into Eq. 2.2 gives

C_i the conductance of the insulation.

An interesting point here is that the conductance has been found without actually calibrating the resistance thermometer. It is sufficient to know that the resistance temperature relationship was linear. This was checked prior to carrying out the experiment to exclude errors due to non-linearities in the electronic equipment.

2.9 Results from a test on the wire from Coil No.1.

Reproductions of the trace obtained from the UV recorder can be seen in Fig.2.7. (Unfortunately the original was too faint to reproduce. A print of a typical recording is shown in Fig. 2.9). The resultant logarithmic graph is shown in Fig. 2.8. The slope of the logarithmic graph was found to be -2.44. Substituting this into Eq. 2.2 gives a value of conductance for the insulation of:-

$$C_i = 33.9 \times 10^2 \ \text{J/m}^2\text{s K}$$

Full details of the calculation are given in App.3.

Discussion.

The two curves shown in Fig. 2.7 consist of three main parts, a horizontal part, a shallow sloping part and a steeply sloping part, (the horizontal part is not shown but can be seen in Fig. 2.9 which is a print of a typical recording) and which is asymptotic to the datum line corresponding to the water temperature. The horizontal part corresponds to the temperature of the hot water, the shallow sloping part corresponds to the passage of the wire through the air prior to immersion in the cold water, i.e. cooling in air, and the steeply sloping part corresponds to the immersion of the wire in the highly agitated water. It can be seen that both graphs are identical, indicating that the temperature drop between the main body of the liquid and the surface is negligible compared with the temperature drop across the insulation. Another indication of the lack of insulating water film is the straightness of the $\log_e$ graph; any film on the surface of the wire would tend to vary in thermal conductance during the period of the test and this variation would be indicated by a lack of linearity in the log graph.

It is worth noting that the <u>conductivity</u> of the insulation could have been obtained here but if this had been done the result would not have been of the same accuracy as that of the <u>conductance</u> which has in fact been found. This is because the calculation for conductivity would require a thickness for the insulation which would involve further errors mainly due to the thickness being non-uniform. This non-uniformity of the thickness of the insulation, although likely to alter the local thermal conductance from place to place on the wire, will not affect the final result since the length of the wire in the test was sufficient to obtain a good mean and it is this that is required to calculate the conductivity of the coil.

Further slight errors may have been involved through a loss of heat through the ends of the wire and a loss where the voltage connections were made. This loss would be of negligible proportions since the wire was long, compared with its diameter (approximately 1 metre; the calculations are independent of length) and the length of wire affected by the loss from the ends would be a limited number of wire diameters.

It was initially thought that boiling water would provide sufficient agitation to reduce the heat transfer coefficient between the water and the surface of the insulation to negligible proportions but this was found not to be the case.

2.10 Preliminary work on the secondary method (Method 6).

At this point errors may have arisen that have not yet been accounted for and it was necessary to carry out an independent secondary test. The method to be used for this test will be Method 6.

In order to use Method 6 a sample of insulation was required that had been removed from the wire. Examination of the wire indicated that the insulation could not be scraped from the wire without damage. Therefore, after an investigation into a number of methods, it was considered that the only one capable of producing a satisfactory sample would be where the copper was dissolved electrolytically from the centre of the insulation. The equipment used for this is shown in Fig. 2.10. The figure shows a hollow cathode of smaller diameter than the inside of the insulation. The cathode was supplied with a fully saturated solution of aqueous sodium chloride and the copper wire was made the anode of a 24 volt supply.

The copper was removed from the insulation by feeding the cathode on to the wire by hand. As the cathode approached the copper wire, a current started to flow through the electrolyte and the distance between the cathode and anode could be judged by the current. Therefore, by maintaining a constant current, a constant feed rate could be obtained. The optimum condition for maximum rate of removal of copper was to obtain maximum current through the electrolyte. However, excessive current tended to make the electrolyte boil and cause a short circuit. The maximum current obtainable in practice was 0.6 A which corresponded to a feed rate of 0.6 mm per hour. The maximum length of insulation obtained was 30 mm. At this length sparking occurred which damaged the end of the insulation. The reason for this was thought to be that at 30 mm depth of penetration of the cathode into the insulation, the electrolyte flowing down the inside of the cathode received heat from the hot electrolyte passing up the annular space between the cathode and the insulation, thus causing the electrolyte to boil at a lower current. Another difficulty that occurred was the precipitation of salt on the inside of the cathode. This was avoided by mixing the solution at a slightly cooler temperature than that at which it was to be used.

The tube of insulation produced by this method could be split along its length to produce a flat piece of insulation approximately 5 mm wide by 30 mm long.

2.11 Basis of the secondary method (Method 6).

At this stage it was necessary to design equipment to obtain the thermal conductance of the sample of insulation obtained as above. The equipment selected for this was of the Lees' disk type, although a special design was required because of the small size of the sample. However, in general the equipment had to consist of two good conducting plates between which the sample of insulation could be held while heat was passed through it. Also, temperature indication was required on both plates, and heat losses had to be kept to a minimum. A number of designs of Lees' disk equipment were tried and it was found from initial trials that an essential property of the Lees' disk for this application was that it must exert a considerable pressure on the sample of insulation in order to obtain good contact between the insulation and both plates of the

Lees' disk. The reason for this was simply that the sample was originally cylindrical and tended to crinkle when flattened. A considerable pressure was therefore required to remove the distortion. The equipment used is shown in Fig. 2.11 and consisted of two 4.66 mm copper bars each with one end ground flat and the other tapered down to a $1\frac{1}{2}$ mm sphere. Each bar had a thermocouple soldered close to the face so that the temperature of the face could be measured. The copper bars could be pressed tightly together with the sphere at each end centralising the loading, and in order to provide a temperature difference across the faces, heat was put in at the end of one bar by transferring through a 1.626 mm diameter copper wire from a heat source. The amount of heat passing into the bars was measured by placing two thermocouples a known distance apart along the copper wire, and from the temperature drop along this wire, the heat flow could be measured. Heat was removed from the other copper bar by a water jacket and the whole apparatus was enclosed in insulating material.

2.12 Procedure for the secondary method (Method 6).

A test was carried out on the equipment as follows:

A sample of insulation was placed between the faces of the copper bars and a load was exerted across the ends of the bars. Thermal insulating material was then placed round the whole apparatus. The cooling water was turned on and heat applied to the ends of the copper wire supplying heat to one of the copper bars. Time was allowed for the heat flow to reach steady state and then readings from all the thermocouples were taken. This process was repeated for different samples of insulation and at various loadings on the ends of the copper bars.

2.13 Theoretical basis of secondary method (Method 6.)

The heat flow through the sample of insulation is given by:-

$$Q = (\theta_{d1} - \theta_{d2}).C_i.A_d \qquad (2.3)$$

where

Q = heat flow through the apparatus,

θ_{d1} = temperature of the hot face,

θ_{d2} = temperature of the cold face,

A_d = area of the face,

C_i = conductance of the insulation.

The heat flow through the copper wire is given by:-

$$Q = \frac{k_w}{L_w} . (\theta_{w1} - \theta_{w2}) . A_w$$

where

θ_{w1} = temperature at the hot end of the copper wire,

θ_{w2} = temperature at the cold end of the copper wire,

A_w = cross section area of the wire,

L_w = distance between the thermocouples,

k_w = conductivity of copper.

Substituting for Q above gives:-

$$\frac{k_w}{L_w} . (\theta_{w1} - \theta_{w2}) . A_w = (\theta_{d1} - \theta_{d2}) . C_i.A_d$$

Therefore

$$C_i = \frac{k_w(\theta_{w1} - \theta_{w2})A_w}{L_w(\theta_{d1} - \theta_{d2})A_d} \qquad (2.4)$$

2.14 Results of Method 6 for the insulation from Coil No.1.

Six tests were carried out on three samples of insulation at two different loads, and the conductance of the insulation was calculated for each test, (full details are given in App.3.) The resultant conductances are given below:-

Test.	Conductance.		Load.	Average conductance.
1	30.6×10^2	J/m^2s^oK	5 kg	
2	33.8×10^2	"	5 kg	31.7×10^2 J/m^2s K
3	30.6×10^2	"	5 kg	
4	29.8×10^2	"	10 kg	
5	28.5×10^2	"	10 kg	29.6×10^2 J/m^2s K
6	30.5×10^2	"	10 kg	

2.15 Discussion on the tests using Method 6.

The results show a slight inverse correlation with pressure. This is unlikely and is probably by chance since an increase in pressure on the sample would tend to have the following effects:-

a) The contact between the copper and the insulation would improve.

b) The insulation would be slightly reduced in thickness.

Both these effects would tend to increase the value of conductance obtained from the test.

The above results are a little lower than the result of

$$C_i = 33.9 \times 10^2 \ J/m^2s \ K$$

obtained previously in the primary experiment, but the discrepancy is well within the experimental error of both tests. The main reasons for the error are:

a) a poor contact between the copper bars and the insulation;

b) slight variation in the diameter of the copper wire used to measure the heat flow.

c) the result was obtained from a short length of insulation, whereas the primary method gave a mean result over a considerable length of insulation and if the short section happened to be thicker than the average, this could account for the error.

The results do indicate however that the error involved in either test is likely to be small.

For the rest of the project the primary experiment was used to establish the conductance of the insulation. This was because of its applicability to small wire sizes and its ability to give a mean value for the conductance, when the thickness of the insulation varied along the length of the wire.

2.16 Substitution into the main theory to obtain the conductivity of Coil No.1.

The information available at this point is sufficient for substitution into Eq. 1.16 to obtain the radial conductivity of the coil. The equation is based on the assumption of line contact only between one wire and the next within the coil.

Substituting the values of:-

$$C_i = 33.9\text{x}10^2 \ \ J/m^2 s\ K$$

$$k_a = 2.94\text{x}10^{-2} \ \ J/m\ s\ K$$

$$D = 1.7\ mm$$

into Eq. 1.16 gives a value for conductance of

$$\underline{k_r = 0.925 \ \ J/m\ s\ K}$$

(Full details of the calculation are given in App.4).

which compares well with the value of

$$\underline{k_r = 1.045 \ \ J/m\ s\ K}$$

obtained by direct test on the coil.

2.17 Discussion on the results for the conductivity of Coil No.1.

The results above show that Eq. 1.16 is likely to give a good indication of the conductivity of the coil. However, an error is involved, the greater part of which is believed to be due to the assumption that line contact exists between one wire and the next within the coil. If this is the case, then the error involved could be quite large when the contact area was large. This is because a finite contact area between one wire and the next would have less thermal resistance than the air space which is assumed in this equation. The error would also be increased by improved conductance of the insulation since this would reduce further the thermal resistance of the contact area. For these reasons it was thought worth while to investigate the effect of the contact area.

2.18 Investigation into the contact area.

To provide a starting point for the investigation, an assumption had to be made about the relationship between the contact area and the load between the wires. It was assumed that this relationship would be as shown in Fig. 2.12, i.e. that at low loads the contact area would increase for an increase in load, but after the load reached a certain value no further measurable increase in contact area would take place. This would mean that there would be a limiting load beyond which the contact area would be constant. If this assumption was correct, then it could be considered that the tension in the windings of the coil was sufficient to produce a loading between one wire and the next, greater than the limiting load, thus giving maximum contact area. Therefore the contact area would be constant throughout the coil.

It was necessary to verify this assumption, and to do this tests were carried out in an attempt to illustrate the limiting load effect. The first test attempted was to cement two pieces of the wire into the jaws of a pair of pliers so that when the jaws were squeezed together the wires were pressed against each other longitudinally. The ends of the wires were ground flat and polished, so that by looking through a microscope the compression of the insulation could be observed. This was not entirely successful since although the compression could be observed, magnification of involuntary movements hindered viewing.

In the second experiment an attempt was made to obtain the contact area between two steel rollers under load. The basis of the method was that the electrical resistance of the contact area between two parallel rollers under load was in some way related to the area of contact. Since only the maximum contact area was of interest it was not necessary to know the relationship between contact area and resistance only that one was constant at the same time as the other.

The apparatus to carry out this experiment is shown in Fig. 2.13. Rollers were placed in an insulated "Vee" block to hold them square. A constant current was passed from one roller to the next and the potential across the joint face measured. Loads could be added to the top roller by means of weights acting on a lever.

A test was carried out by adding weights to the top roller. After the addition of each weight, the potential across the contact face of the rollers was taken. Then on removing the weights the potential was again taken at each weight. The resulting graph of potential against load is shown in Fig. 2.14. Inspection of the graph indicates that a limiting load exists past which any further increase in load will not increase the contact area. No attempt was made to relate the limiting load on the rollers to that in the coil.

2.19 Determination of the contact area between the wires in Coil No.1.

A number of methods for obtaining the contact area were tried with varying degrees of success. Some of the less successful methods are described here in brief with the most reliable method given in detail.

In general it was considered that the amount of flattening of the insulation that occurred when one wire was pressed against the next could be reproduced by pressing the wire against a hard flat surface of high Youngs modulus. This is illustrated in Fig. 2.15. Pressing the wires together will result in an arrangement that is symmetrical about the line of contact. Therefore if one wire is replaced by a flat rigid surface the other wire is unaffected.

The first attempt to obtain the contact area entailed pressing the wire against an inked steel surface so that a print could be obtained of the contact area between the insulation and the surface. The wire under test was wrapped around a steel drum and loaded by means of hanging weights from the ends of the wire. After removing the wire from the inked drum a print should be left of the contact area. Difficulties arose with this method due to smudging of the impression when the wire was removed. A second method was tried whereby the wire was loaded against a flat inked plate, but again the same difficulties arose.

It was concluded from the first two attempts that the most important part of a test of this type was the removal of the wire from the plate on which the impression was made.In order to achieve this, the method described below was used.

2.20 Basis of the method to obtain the contact area between the wires in Coil No.1.

This method entailed the wrapping of the wire round a steel drum and rolling the drum across an inked plate. In this way, as the drum was rolled, the wire was neatly removed from the print on the plate. However, the conditions in the test were far removed from the conditions inside the coil where one wire is pressed against the next; within the coil the contact area will be flat with parallel sides, whereas in the test the contact area between insulation and plate at any instant would be flat with elliptical boundaries. Although these differences exist it is assumed that the minor axis of the ellipse will be the same length as the distance between the parallel sides of the contact area in the coil. In other words, the print on the plate will give a good estimate of the coil contact area. This can be shown to be a reasonable assumption by considering the shape of the ellipse. If the diameter of the drum on which the wire is wound is 30 times the width of the contact area then the major axis of the ellipse will be approximately $5\frac{1}{2}$ times the minor axis, which means that the centre portion of the ellipse close to the minor axis will have edges that are almost parallel. Therefore, over this section the loading is very similar to the loading in the coil itself, and since a limiting loading is likely to occur, then the result from this test will give a good indication of the contact area.

The equipment used to obtain the contact area is shown in Fig.2.16 and consists of a drum around which is wrapped two lengths of the wire to be tested. The drum can be rolled across a flat piece of inked glass to leave a print in the ink that can be viewed through a microscope. It was considered that the Young's modulus of glass was sufficiently greater than that of the insulation to make any deformity of the glass negligible.

2.21 Procedure for obtaining the contact area.

The drum with the wire wrapped round it was rolled over the surface of the inked glass, (engineers' marking ink was used) under two different loads. The width of the print left in the ink was then measured by viewing through a microscope, and using a measuring device attached to the microscope; (a Vickers' pyramid hardness testing machine microscope was used since this had the required measuring device).

2.22 Results of tests to obtain the contact area.

For the wire used in Coil No.1, the width of print left in the ink was 0.178 mm, and both impressions at different loadings were the same, indicating that limiting conditions had been reached.

2.23 Substitution into the main theory to obtain the conductivity of Coil No.1.

At this point sufficient information was available for substitution into Eq. 1.21. This equation is an extension of Eq. 1.16 and takes into account the effect of contact area.

Therefore substituting the values of:-

$$C_i = 33.9\text{x}10^2 \ \text{J/m}^2 \text{ s K}$$

$$k_a = 2.94\text{x}10^{-2} \ \text{J/m s K}$$

$$D = 1.7 \text{ mm}$$

$$M = 0.178 \text{ mm}$$

give a result of

$$k_r = 0.995 \quad \text{J/m s K}$$

(full details in App.4).

Which compares extremely well with the experimental conductivity of

$$k_r = 1.045 \quad \text{J/m s k}$$

obtained by direct experiment.

2.24 Discussion on the results for the conductivity of Coil No.1 using contact area.

It can now be considered that a satisfactory theoretical basis has been found for predicting the thermal conductivity of an electrical coil without paper interleaving between the windings. Although the result obtained theoretically is within 5% of the result obtained experimentally, it is not thought that this is a typical accuracy. As a guide, taking into account later work in this text, the author believes that with care the results obtained from this method would be within ± 15%. The method using Eq. 1.21 will give a more reliable result than Eq. 1.16 but the latter could be of great value provided that care is taken in assessing its applicability to the coil. For hard, thin, poorly conducting insulation Eq. 1.16 would give a reasonable result.

CHAPTER 3.

PAPER INTERLEAVED COILS.

3.1 Introduction.

In the first part of Chapter 1 the general theory for calculating the conductivity of non-interleaved coils was derived, and in Chapter 2 this was tested against an actual coil. In the latter part of Chapter 1 the theory was extended to cover paper interleaved coils and in this chapter the extended theory will be tested against a number of actual coils. Also, techniques will be described by which the properties of the paper, required for the calculation of the conductivity, may be obtained.

3.2 Experimental verification of constant conductivity.

The initial experiments on the interleaved type of coil were the same as that carried out on the non-interleaved type as described at the beginning of Chapter 2. The experiments are described here in brief since similar experiments have already been described in detail.

Firstly, a coil (Coil No.2) was made with thermocouples throughout and with a heater at the centre. A test was carried out by heating the coil from the centre and taking readings from the thermocouples. Drawing a $\log_e$ radius v temperature graph (Fig. 3.1) and substituting the slope into Eq. 1.4 resulted in a value for radial conductivity of -

$$k_r = 0.53 \quad J/\,m\,s\,K$$

Full details of the calculation are given in App.5. Conclusions drawn from this result are the same as for Coil No.1, namely, that the conductivity of the coil was constant throughout and independent of winding tension.

Secondly, the coil was heated by passing a current through the windings. Temperatures taken at the thermocouples were plotted against the radius (see Fig. 3.2). A second set of temperature v. radius results was obtained by substituting the conductivity from the first test into Eq.1.5 together with the current through the windings and the properties of the wire. The second set of results were superimposed upon the first (see Fig. 3.2). The similarity between the graphs indicated that the conductivity derived in the first experiment can be used to predict the temperature distribution in the live coil. Full details of both these tests can be seen in App.5.

In Chapter 1 the method given for predicting the conductivity of paper interleaved coils requires the substitution of certain physical and thermal characteristics of paper and wire into an equation (Eq. 1.37). Methods for obtaining the characteristics of the wire are given in the previous chapter, and methodsfor obtaining the characteristics of the paper are described in the following part of the present chapter. These characteristics are the conductance of the paper in its normal condition, the conductance of the paper at maximum compression (this will be described at a later stage), and the contact area between wire and paper.

3.3 Contact area between wire and paper.

The contact area is formed by the pressure between the windings deforming the paper so that a finite area of contact exists between wire and paper. For the purpose of the present work, the contact area is defined as the chord of contact between paper and insulation across a section of wire, per unit length; this is referred to as M in the theory and was found to be one of the most difficult parameters to obtain.
The initial experiments took the form of pressing inked wires into the paper and measuring the mark so left. Although a result could be obtained by this method, repeats of the tests were not consistent and a

reliable indication of the contact area could not be obtained. Therefore a different line of attack was considered.

3.4 Basis of the method for determining contact area.

It was assumed that the behaviour of the paper under load was as shown in Fig. 2.12, i.e. the stress-strain curve for a piece of paper across its thickness would be asymptotic to a certain value corresponding to the minimum thickness of the paper. It was further assumed that within the coil the paper was at maximum compression. This would be so if the loading within the coil was above the point marked L in Fig. 2.12. Under these conditions the contact area can be calculated from the minimum thickness of the paper.

3.5 Procedure to obtain the minimum thickness of the paper.

A device was constructed, as shown in Fig. 3.3, which consisted of a support block which held the paper against the marking table, a loading bar which could be slotted through the support block to press on the paper, and a dial gauge to measure the displacement of the loading bar. Weights could be added to the loading bar to increase the load on the paper.

An experiment was carried out by first setting up the apparatus without any paper, in order to obtain a zero reading on the dial gauge. Paper was then put into the apparatus and weights added to the loading bar. For each load the displacement of the loading bar was recorded. This would be a displacement above a zero reading, decreasing as the load increased. Weights were added until no further change in displacement took place.

A test carried out on the paper from Coil No. 2 gave a graph of displacement against load as shown in Fig. 3.4 (a table of results is given in App.5). This indicates that a load is reached beyond which there will be no further reduction in thickness. It is therefore considered that this condition arises within the windings of the coil and that the loading between the windings is sufficient to reduce the paper to its thinnest, a value of:-

$$B = 0.102 \text{ mm} \qquad \text{(see Fig. 3.4).}$$

3.6 Calculation of the contact area.

Within the coil, the paper and wire have a configuration as shown in Fig.1.6, i.e., the paper will be compressed between two adjacent wires so that the distance apart of the wires will be equal to the mimimum thickness obtained above. Now it can be seen from Fig.1.6 that the paper is in contact with at least one wire for the whole of its width but there are only limited sections of the paper where it is in contact with both adjacent wires at the same time and it is the chord across these sections that is called the contact area, marked M in the figure. Now M can be calculated from the minimum thickness B as shown below:-

$$\left[\frac{M}{2}\right]^2 = \frac{(T - B)}{2}.\left[D - \frac{(T - B)}{2}\right]$$

Where T is the thickness of the paper in its uncompressed condition. On simplifying

$$M = 2\sqrt{\frac{(T - B)}{2}.\left[D - \frac{(T - B)}{2}\right]} \qquad (3.1)$$

Thus the contact area can be obtained and for Coil No.2 has a value of:-

$$M = 0.2998 \text{ mm}$$

(Full details in App.5. page 127)

3.7 Conductance of the paper.

The thermal conductance of the paper was obtained by using a standard Lees' disk.

A test was carried out on the equipment by inserting the test paper, switching on the water and electricity, and allowing time for the equipment to reach a steady state temperature. Readings were then taken of the temperature at each face of the disk and the voltage and current to the heater. From these results the conductance could be calculated in the normal way. A test carried out on the paper from Coil No.2 gave a conductance of -

$$C_{p1} \quad = \quad 4.76 \times 10^2 \quad J/m^2\ s\ K$$

Full details of the calculation are given in App.5.

3.8 Conductance of the paper under compression.

In the theory of Chapter 1, the relationship between thickness of the paper and thermal conductance is required and is assumed to be:-

$$C_p = \frac{1}{s' + v'.y}$$

where s' and v' are constants. One of these constants can be obtained from the conductance of the paper at maximum thickness, but for the other a conductance at a different thickness is required.

It was found that after the paper had been compressed to its thinnest and the load removed, the paper only recovered slightly, if any, in thickness. Therefore, obtaining the conductance at this point would satisfy the condition for the second constant in the theory.

This was done by compressing the paper to its thinnest, releasing the load, measuring the thickness and carrying out a second Lees' disk experiment. On completion of the experiment the thickness of the paper was again checked.

The result of a test on the paper from Coil No.2 gave a value of conductance of $C_{p2} = 8.1 \times 10^2 \; J/m^2 s\, K$

at a thickness of 0.102 mm

(full details in App.5).

3.9 Substitution into theory to obtain the conductivity of Coil No.2.

At this point methods have been described by which all the information required to calculate the conductivity of a paper interleaved coil may be obtained. Therefore, in order to test the theoretical basis for the calculations, the conductivity of Coil No.2 was calculated and compared with the value of conductivity obtained by direct experiment in the first part of this chapter. The characteristics of the paper have been found in this chapter; the conductance of the insulation on the wire was found by the method described in Chapter 2. (full details of all the experiments and calculations are given in App. 5).

The theoretical basis to be used will be the simplified version resulting in Eq. 1.37 from Chapter 1. Therefore on substituting the following values:-

$C_i = 51.8 \times 10^2$ J/m²s K

T = 0.1472 mm

B = 0.102 mm

$C_{p1} = 4.76 \times 10^2$ J/m²s K

$C_{p2} = 8.1 \times 10^2$ J/m²s K at 0.102 mm

D = 1.016 mm

$k_a = 2.94 \times 10^{-2}$ J/m s K

into Eq. 1.37 gives a value for the conductivity of the coil of

$$k_r = 50.08 \times 10^{-2} \quad \text{J/m.s.K}$$

Full details in App 5.

which compares extremely well with the value of

$$k_r = 53 \times 10^{-2} \quad \text{J/ m s K}$$

obtained by direct experiment on the coil.

3.10 Discussion on the results for the conductivity of Coil No.2.

The above results indicate that a satisfactory theoretical basis has been found for calculating the radial conductivity of a paper interleaved coil. However, the result does not give an indication of the accuracy of the method since the accuracy of the above result may not be typical. It was therefore necessary to confirm the accuracy of the method by further experimentation with different coils.

3.11 Determination of the accuracy of the method for obtaining the conductivity of paper interleaved coils.

Because of the number of variables involved (6), a considerable number of tests would be required to show the effect on accuracy of a change in each variable. It was therefore decided to examine a number of coils over a range of wire sizes which would give some indication of the accuracy of the method and avoid involvment in a great amount of repetitive work.

Seven different coils were made with thermocouples and a heater as for Coil No. 2. Each coil was made with a different paper, with three of the coils made from one wire size and four from another.

3.12 Proceedure for testing the accuracy of the method for obtaining the conductivity of paper interleaved coils

Each coil was tested by the method described at the begining of Chapter 2 (pages 39 to 41) to obtain the radial conductivity. The characteristics of the wire and the paper were found by the methods described in Chapters 2 and 3. These were then substituted into Eq. 1.37 to obtain the theoretical radial conductivity of each coil. The conductivity obtained by each method was then compared by plotting one against the other. A perfect agreement between experiment and theory would be indicated by a straight line, passing through the origin with a slope of 45°. The scatter of the points about this line would indicate the accuracy of the theoretical calculations.

Full details of the tests carried out on the seven coils are given in App. 6. The conductivities obtained by both methods are plotted in Fig. 3.7.

3.13 Discussion on the accuracy of the method for obtaining the conductivity of paper interleaved coils.

Inspection of Fig. 3.7 shows that reasonably good agreement is obtained between theory and practice, and over the range of variables involved, a maximum error of ± 15% could be expected with this method.

CHAPTER 4.

EXTENSION OF THE THEORY TO COVER AXIAL HEAT FLOW.

4.1 Introduction.

In the previous chapters it has been shown that the radial conductivity of a coil can be obtained with reasonable accuracy. However, it is by no means certain that the axial conductivity will have the same value as the radial conductivity. Therefore, it is proposed in this chapter to extend the theory to cover axial conductivity. Also, a method will be given whereby the overall temperature distribution under conditions of two dimensional heat transfer can be obtained.

4.2 Axial conductivity of non-interleaved coils.

It is assumed in general that when heat flows radially through a coil, the heat paths are as shown in Fig. 4.1. Comparing this with Fig. 4.2 for axial heat flow it can be seen that some of the heat travels through the coil by the same method as for radial heat flow. However, an additional factor is at work when the heat flows axially. Therefore, consider a typical section in the coil to be as shown in Fig. 4.3 and consider the part of that section outlined in thick black lines to be the same as all other sections within the coil. Now in the same way as in Chapter 1, assuming that the lines of heat flow are as shown in the figure, the axial conductivity of the coil may be found by obtaining the heat rate for the section outlined in thick black lines and substituting into Eq. 1.8.

Inspection of the individual shaded sections in the figure reveals that they are the same as those which have already been analysed in Chapter 1. The centre section marked 1 in the sketch is identical with that in Section 1.4; therefore, the value of the heat rate for this section will be H_{b2} as given by Eq. 1.20. The outside sections marked 2 and 3 may be joined together to form a section identical with the shaded area in Section 1.3 and the heat rate will therefore be given by H_{b1} as in Eq. 1.15.

Now if it is assumed that the temperatures at either side of the section outlined in thick black lines in Fig.4.3 are constant, it can be seen by inspection that the overall heat rate is given by:-

$$H_{ba} = H_{b1} + H_{b2} \qquad 4.1$$

where H_{ba} is the heat rate in the axial direction for a typical block in the coil.

This assumption is reasonable since the top part of the left hand side of the section is in the copper, which, having a very high conductivity will be at constant temperature. The bottom part may be considered at constant temperature since it is a dividing line perpendicular to the direction of heat flow separating two identical sections. The part in the middle where the insulation passes through the edge of the section is obviously not at constant temperature but if it is considered that the line itself is a very thin piece of insulating material then the problem is not altered significantly and the constant temperature condition may be assumed without serious error.

The conductivity of the coil may now be obtained from Eq. 1.8

$$k = \frac{H_b . h}{A_b}$$

Now it can be seen from Fig. 4.3 that for the case in question h and A_b will take up the following values:-

$$h = D/2$$

$$A_b = \frac{D\sqrt{3}}{2}$$

therefore

$$k_a' = \frac{H_{ba}}{\sqrt{3}} \qquad (4.2)$$

In order to give some indication of the relative magnitudes of the axial conductivity compared with the radial, the axial conductivity was calculated for Coil No. 1. Full details are given in App. 7

The resulting axial conductivity was:-

$$\underline{k_{a'} = 0.64 \text{ J/m s K}}$$

whereas the radial conductivity was:-

$$\underline{k_r = 0.996 \text{ J/m s K}}$$

4.3 Discussion on axial conductivity

The axial conductivity of the coil was obtained by a method similar to that used for the radial conductivity, although the axial method is in two independent parts. The calculation on Coil No. 1 showes the axial conductivity to be lower than the radial. Errors may be involved in the calculation of H_{bl} in that it is assumed that there is no gap axially between the wires, whereas, in practice a gap exists and will reduce the value of H_{bl}, making the value of axial conductivity lower than that given. If the axial gap between the wires is known, then with a small change in the theory a modified value of H_{bl} can be obtained to give a more accurate value of axial conductivity.

The axial conductivity of a paper interleaved coil can also be obtained in a similar manner.

No experimentation has been carried out with respect to the axial conductivity of either type of coil. Therefore no experimental verification of the technique for obtaining the axial conductivity is available at present.

4.4 Combined axial and radial heat flow through a coil.

If it is assumed that the radial and axial conductivities of a coil can be found with reasonable accuracy, then, in order that these may be of any practical value, a method must be found for calculating the temperatures within the coil from these conductivities. The relaxation method was thought to be the best way of determining these. The derivation of a method of relaxation for two dimensional polar coordinates with two different conductivities is given below.
It is assumed that the coil is homogeneous with differing conductivities in the axial and radial directions. Therefore considering an element of coil shown in Fig. 4.4 theheat transfer through the left hand curved face

$$= k_r . \frac{\partial\theta}{\partial r} . (r . \delta\phi . \delta z)$$

Heat transfer through the right hand curved face

$$= k_r . \left(\frac{\partial\theta}{\partial r} + \frac{\partial^2\theta}{\partial r^2} . \delta r\right)(r . \delta\phi . \delta z + \delta r . \delta\phi . \delta z)$$

Heat transfer through the near face

$$= k_{a'}.\frac{\partial\theta}{\partial z}.(r.\delta\phi.\delta r)$$

Heat transfer through the far face

$$= k_{a'}.(\frac{\partial\theta}{\partial z} + \frac{\partial^2\theta}{\partial z^2}. z)(\delta r.r.\delta\phi)$$

The heat transfer through the top and bottom element is assumed to be zero because of the exelent conductivity of copper.

Now, summing all these quantities entering the element should give zero, thus:-

$$k_r.\frac{\partial\theta}{\partial r}.(r.\delta\phi.\delta z) - k_r(\frac{\partial\theta}{\partial r} + \frac{\partial^2\theta}{\partial r^2}.\delta r)(r.\delta\phi.\delta z + \delta r.\delta\phi.\delta z)$$

$$+ k_{a'}.\frac{\partial\theta}{\partial z}.(r.\delta\phi.\delta r) - k_{a'}(\frac{\partial\theta}{\partial z} + \frac{\partial^2\theta}{\partial z^2}.\delta z)(\delta r.r.\delta\phi)$$

$$+ q_g(\delta r.r.\delta\phi.\delta z) \quad = \quad 0$$

Simplifying and moving to the limit gives:-

$$k_r.\frac{\partial^2\theta}{\partial r^2} + k_r.\frac{1}{r}.\frac{\partial\theta}{\partial r} + k_{a'}.\frac{\partial^2\theta}{\partial z^2} + q_g \quad = \quad 0$$

Which is the general equation for heat transfer within the coil.

Converting this to a finite difference equation gives:-

$$k_r.\frac{(\theta_1 + \theta_3 - 2\theta_o)}{a^2} \quad + \quad k_r.\frac{1}{r}.\frac{(\theta_1 - \theta_3)}{2a}$$

$$+ \quad k_{a'}.\frac{(\theta_4 + \theta_2 - 2\theta_o)}{a^2} \quad + \quad q_g \quad = \quad 0$$

where a = the pitch of the grid

θ_o = temperature at the node

θ_1 & θ_3 = the temperature above and below the node respectivly

θ_2 & θ_4 = the temperatures to the right and left of the node

r = the radius of the node

q_g = heat generation per unit volume

Note: the axis of the coil is taken as horizantal.

Now the value of q_g for the coil will not be constant since the electrical resistance of the copper in the windings will vary with temperature according to the equation

$$q_g = \alpha + \beta.\theta_o$$

Therefore, this must be substituted into the finite difference equation to give:-

$$k_r.\frac{(\theta_1 + \theta_3 - 2\theta_o)}{a^2} + k_r.\frac{1}{r}.\frac{(\theta_1 - \theta_3)}{2a} + k_{a'}.\frac{(\theta_4 + \theta_2 - 2\theta_o)}{a^2} + \alpha + \beta.\theta_o = 0$$

The above equations can now be used with the appropriate boundary conditions to obtain the temperature distribution throughout the coil. The heat transfer through a core or fixture attached to the coil would be an added difficulty but this was thought to be outside the scope of this project.

CHAPTER 5.

DISCUSSION AND CONCLUSIONS.

The whole of this dissertation may be considered as a preliminary investigation into methods of predicting the temperatures within an electrical coil that is heated due to the dissipation of electrical energy as heat within the windings. Literature surveys have indicated that the only work of any significance that has been carried out up to the present, is that described in Jakob (6) and Richter (5), (comparison between Jakob's method and the one in this text is given at the end of this discussion). The method used here was not a development of an existing technique but the foundation of a new technique which has the potential for development over a far wider range of coils than have been investigated here.

The theoretical basis for this thesis was decided upon after first investigating a considerable number of simpler methods. Averages of the conductivities of all the constituents were not thought to be of value. The assumption that the air spaces act as regions of zero conductivity was tried but very little agreement was obtained. A statistical approach was considered but discarded since firstly, any prediction from this type of method would have a probability of being too greatly in error, and secondly, the number of experimental results necessary to obtain a reasonable correlation would have been considerably greater than the number required here.

The method used was the result of an analysis of the heat flow through a section of the coil. It was realised that a purely numerical analysis could have been used to obtain the temperatures through a small section of the coil, and provided a computer was used, the temperatures throughout the whole coil could have been obtained in the same way. However, although this would have given the temperatures within the coil (it is by no means certain that a successful analysis could have been carried out, since the problem of various conductivities in series and parallel would have been extremely complex) it would have been very difficult to glean any further information about the coil from this technique. Whereas, in an algebraic analysis, general information such as the relative effect of different dimensions and different conductivities can be readily obtained. However, it was realised that a comprehensive algebraic analysis, which would have involved analysis of two dimensional heat transfer through various conducting materials was out of the question. Therefore a compromise was attempted by approximating the lines of heat flux for a numerical analysis to a system that could be analysed by one dimensional heat transfer. The result would be algebraic and would have the consequent advantages of simplicity and flexibility.

The decision to use conductances rather than the more conventional conductivity was arrived at by virtue of the fact that the whole of the analysis could be carried out (using conductance) without reference to the thickness of the insulation. In this way one variable, which could only be obtained with doubtful accuracy was eliminated.

The assumed configuration of the windings, one winding lying in the groove left by the two windings below, was thought to be the closest approximation to an actual coil that could be successfully analysed. In practice the windings cannot lie on top of each other in this way for the whole of a turn, since the helix of one winding is in the opposite direction to the one below. Thus on each turn, the wire on top must, at some point, pass over the wire below, but for most of the diameter the wire on top lies between the wires below. An error is therefore involved in this assumption which is likely to make the theoretical value of conductivity greater than the actual, since the regions of overlap, having a greater proportion of air space, will have a lower conductivity. The regions of overlap are well distributed throughout the coil since in one layer of windings the 30° of overlap is not situated axially along the coil but follows a helix around the coil, and in the next layer the overlap is unlikely to be directly over the previous overlap since the space between one winding and the next at an overlap is greater than in other parts of the coil; hence the winding layer on top is almost certain to fall into the grooves left by the winding below at the point of overlap. An indication of the error caused by the overlap can be estimated by assuming that the regions of overlap have zero conductivity and since they occupy an area of 30° at each layer, the total volume of overlap will be 30/360 or 8.3% of the total volume of the windings. Therefore, the maximum error that would be expected would be 8.3% and since the regions of overlap will have an appreciable conductivity the error from this source will probably be considerably less than this amount.

The complexity of the final equations was unfortunate since it makes the calculations involved in obtaining a result long and difficult with a possibility of numerical error but no method could be found to simplify them without limiting their scope. It was thought at one point that the approximation used for the heat transfer through the paper, i.e.

approximating the surface of the wire to a parabola, could be used for the air spaces. This was rejected on the grounds that most of the heat would pass through the thinnest part of the airspace, where any dimensional inaccuracy, although small compared with the diameter, would be large compared with the air space and could well cause a large error in the conductivity.

However for anyone wishing to obtain the conductivity of a paper interleaved coil by this method, a computer programme has been written see App.8.

The approximate method of obtaining the conductivity of the non interleaved coils (Eq. 1.16) could well be of considerable value because of its relative simplicity and limited data requirements.
It may also have application to non cylindrical coils but no experimental information is available on this.

It is important to note that the theory fits the experimental results without the need for any arbitrary correction factors. Therefore although the tests carried out cover only a small range of papers and wire sizes, it is very likely that the method will be applicable to a much wider range of coils than has been tested provided the materials of the coil are compatible with the assumptions in the theory. It is thought that one of the more important assumptions is that the interleaving paper must have a well defined minimum thickness. If the paper does not, or if the loading to reach the minmum thickness is large, then the resulting coil could well have a variable conductivity since changes in the loading between the wires would alter the contact area and hence the conductivity. Extremely hard papers may deform the insulation on the wire, but with slight modifications to the equations this could be taken into account.

Errors could arise with coils that are short compared with the diameter since at the ends of the coil the windings are not as orderly as in the centre and would probably have a lower conductivity at this point. With long coils, the part of the coil that has this low conductivity would be small and could be neglected.

The scope of the equations is limited by the assumptions used in their deriviation. These limitations are detailed below:-

1) the thickness of the insulation on the wire must be small compared with the diameter of the wire;

2) the reduction of the thickness of the insulation due to the pressure of one winding on the next must be small compared with the uncompressed thickness of the insulation;

3) the diameter of the wire must be small compared with the diameter of the coil;

4) the coil must be wound at such a tension that the pressure of one winding on the next is above the limiting load for which an increase in load will not cause an increase in contact area;

5) only radial conductivity can be found in this way, axial conductivity will be a different value;

6) the wire must be copper, or another good conductor of heat;

7) the coil must be long compared with the diameter of the wire;

8) the paper must have a well defined minimum thickness.

It is unfortunate that most of the limitations do not have a precise numerical value - they must nevertheless be accepted and until further work is carried out numerical limitations cannot be given. Although there are a considerable number of limitations, most commercially available coils will fall within the scope of the method. The coil used in the initial experiment was large compared with the coils used in the final experiment. This was primarily because it was thought that the properties of the materials would be easier to obtain when larger samples were available. However, it does show the size range for which the techniques are valid, although there is no reason why this should be the limitation to the range.
The single coil used in the first experiment was not duplicated because of the difficulty of making non-interleaved coils of good quality. The single result from the non-interleaved coil makes it difficult to draw any conclusions as to the general accuracy of the method with this type of coil. However, the same technique used on paper-interleaved coils gave good results for an intrinsically more difficult problem. This suggests that the accuracy of the calculation for non-interleaved coils would also be very good.

The method for obtaining the conductivity of the interleaved coils gave results that were better than $\pm$ 15% of the experimental result. This may be considered the best that could be obtained for a heat transfer calculation with such complex geometry.

Certain errors would be involved in the experimental derivation of the conductivity but these were thought to be small. Repeat tests were carried out with good agreement. Also, the calculation involved the use of the slope of a straight line which tended to average out small errors in single readings. It was thought that the experimental conductivity would be obtained to better than $\pm$ 3%.

As mentioned previously, the only other methods available for calculating the conductivity of a coil without recourse to actual experimental tests on the coil is that of Jakob(6) and Richter (5). Both methods involve assuming that the section of the wire is square with appropriate dimensions so that the same number of windings fit into the same space as the original coil. Under these assumptions the conductivity of the coil may easily be calculated. The conductivity for Coil No.1 was calculated in this way giving a result of

$$k_r \doteq 1.84 \quad J/ m\ s\ K$$

which does not compare at all well with the value of

$$k_r = 1.045 \quad J/ m\ s\ K$$

obtained by direct experiment. However it is the author's opinion that although not mentioned specifically, Jakob (6) only intended the method to be used on cotton covered wires, which would probably give a better result. Richter's (5) method was originally derived for rectangular wires but he says that it can be used on round wires by assuming that the wire is square! Using Richter's (5) method, the conductivities were calculated for Coils 2 to 8 and the calculated conductivities compared with the experimental results in Fig. 5.1. Comparing Fig. 5.1 and Fig. 3.7, it can be seen that Richter's (5) method does not give the accuracy obtained with the method adopted in this text.

Chapter 3 shows how the technique can be extended to cover axial conductivity. No experimental verification is given for the result and it is the author's opinion that account will have to be taken of the axial gap between the wires before a reasonable accuracy will be obtained. The modification to the equation in order to introduce a term for the axial gap would be relatively simple but predicting the dimensions of the gap would be considerably more difficult.

The method given for the calculation of the temperatures within the coil under conditions of both axial and radial heat transfer is a standard technique but one which is usually given for constant conductivity in both directions. Therefore, for completeness, the equations were derived.

APPENDIX 1

Solution of integrals

Contents | | Page

APPENDIX 1

Solution of integrals

Equation 1.12

$$H_{1q} = \int_{\phi_1}^{\phi_2} \frac{a.\cos\phi.d\phi}{c.\cos\phi + b}$$

can be reduced to

$$H_{1q} = \frac{a}{c}\left[\phi_2 - \phi_1 - \int_{\phi_1}^{\phi_2} \frac{b.d\phi}{b + c.\cos\phi}\right]$$

Let

$$U = \int_{\phi_1}^{\phi_2} \frac{b.d\phi}{b + c.\cos\phi}$$

so that substituting for

$$t = \tan\tfrac{1}{2}\phi$$

gives

$$U = \frac{2}{b - c}\int_{\eta_1}^{\eta_2} \frac{dt}{\frac{b + c}{b - c} + t^2}$$

where $\eta_1 = \tan^{-1}\tfrac{1}{2}\phi_1$

$\eta_2 = \tan^{-1}\tfrac{1}{2}\phi_2$

From this point two alternative solutions arise depending on whether $\frac{b + c}{b - c}$ is positive or negative.

Consider firstly $\frac{b + c}{b - c}$ to be positive

Putting

$$m^2 = \frac{b + c}{b - c}$$

so that

$$U = \frac{2}{b - c}\int_{\eta_1}^{\eta_2} \frac{dt}{t^2 + m^2}$$

substituting for

$$t = m.\mathrm{Tan}\Phi$$

gives

$$U = \frac{2}{b - c}\int_{\pi_1}^{\pi_2} \frac{\Phi.d\Phi}{m}$$

where $\pi_1 = \mathrm{Tan}^{-1}\frac{1}{m}.\mathrm{Tan}\tfrac{1}{2}\Phi_1$

$\pi_2 = \mathrm{Tan}^{-1}\frac{1}{m}.\mathrm{Tan}\tfrac{1}{2}\Phi_2$

therefore

$$U = \frac{2}{b - c}.\frac{1}{m}\left[\pi_2 - \pi_1\right]$$

Substituting gives

$$H_{1q} = \frac{a}{c}\left\{\Phi_2 - \Phi_1 - \frac{2b}{(b - c)m}\left[\mathrm{Tan}^{-1}\left(\frac{1}{m}.\mathrm{Tan}\tfrac{1}{2}\Phi_2\right) - \mathrm{Tan}^{-1}\left(\frac{1}{m}.\mathrm{Tan}\tfrac{1}{2}\Phi_1\right)\right]\right\}$$

Consider secondly $\frac{b + c}{b - c}$ to be negative.

Putting

$$m^2 = -\left[\frac{b + c}{b - c}\right]$$

gives

$$U = \frac{2}{b - c}\int_{\eta_1}^{\eta_2} \frac{dt}{t^2 - m^2}$$

Therefore

$$U = \frac{1}{(b - c)m} \log_e \frac{\eta_2 - m}{\eta_2 + m} \cdot \frac{\eta_1 + m}{\eta_1 - m}$$

Substituting gives

$$H_{1q} = \frac{a}{c}\left\{ \phi_2 - \phi_1 - \frac{b}{(b - c)m}\left[\log_e\left(\frac{\mathrm{Tan}\frac{1}{2}\phi_2 - m}{\mathrm{Tan}\frac{1}{2}\phi_2 + m} \cdot \frac{\mathrm{Tan}\frac{1}{2}\phi_1 + m}{\mathrm{Tan}\frac{1}{2}\phi_1 - m}\right)\right]\right\}$$

Equation 1.29

$$H_{3c} = 2\int_0^{\phi_2}\left(f.\mathrm{Cos}0 + \frac{g.\mathrm{Cos}\phi}{b - c.\mathrm{Cos}\phi}\right)d\phi$$

can be reduced to

$$H_{3c} = 2f.\mathrm{Sin}\phi_2 + 2\int_0^{\phi_2}\frac{g.\mathrm{Cos}\phi.d\phi}{b - c.\mathrm{Cos}\phi}$$

Putting

$$V = \int_0^{\phi_2}\frac{g.\mathrm{Cos}\phi.d\phi}{b - c.\mathrm{Cos}\phi}$$

and simplifying gives

$$V = \frac{g}{c}\left[-\phi_2 + \int_0^{\phi_2}\frac{b.d\phi}{b - c.\mathrm{Cos}\phi}\right]$$

Putting

$$U = \int_0^{\phi_2}\frac{b.d\phi}{b - c.\mathrm{Cos}\phi}$$

gives

$$U = \frac{2b}{b + c}\int_0^{\phi_2}\frac{dt}{\left[\frac{b - c}{b + c}\right] + t^2}$$

Substuting for

$$m^2 = + \frac{b - c}{b + c}$$

gives the same solution as for U in Eq. 1.12. Therefore substituting for H_{3c} gives:-

$$H_{3c} = 2f.\sin\phi + 2.\frac{g}{c}\left\{-\phi_2 + \frac{2b}{b + c}.\frac{1}{m}\left[\tan^{-1}\left(\frac{1}{m}.\tan\tfrac{1}{2}\phi_2\right)\right]\right\}$$

The alternative solution with $m^2 = -\left[\frac{b - c}{b + c}\right]$ does not apply

Equation 1.33

$$H_{3c'} = 2\int_0^{x_2} \frac{e.dx}{fx^2 + g}$$

Putting

$$m^2 = \frac{g}{f}$$

gives

$$H_{3c'} = \frac{2}{f}\int_0^{x_2} \frac{e.dx}{x^2 + m^2}$$

which has the solution

$$H_{3c'} = \frac{2}{f}.\frac{e}{m} \tan^{-1}\left(\frac{x_2}{m}\right)$$

APPENDIX 2

Experimental results from Coil No. 1

Contents | Page

APPENDIX 2.

Experimental results from Coil No. 1.

Results of the first test carried out on Coil No.1.

In this test the coil was heated with the central heater. Time was allowed for the coil to reach steady state and then readings were taken of the power input to the coil and voltage at each thermocouple. The voltage was then plotted against the $\log_e$ of the radial position of that thermocouple. (This is equivalent to a temperature v log radius graph since the voltage from the thermocouples was proportional to the temperature over the range used). The slope of the graph was then used to calculate the conductivity of the coil by substitution into Eq. 1.4.

Length of coil = 127 mm

Voltage across and current through the heater = 10.54 volts and 2.6 amps.

Readings from the coil:

Voltage at thermocouple. mV	Radius of thermocouple. mm	Log. of radius.
3.39	22.22	3.1
2.96	30.01	3.404
2.66	35.75	3.57
2.522	40.6	3.704
2.125	55.0	4.0
1.97	62.0	4.127
1.85	68.55	4.228
1.74	74.5	4.31

Ten thermocouples were originally put into the coil but two failed to work. Plotting these results gives the graph in Fig. 2.4 which has a slope of −0.73. This slope can be changed into a temperature v log radius slope by multiplying by the number of mV per K which equals 0.0419 (see calibration curve for the thermocouples Fig. 2.2) thus:-

$$\text{slope} = -0.0303$$

Now from Eq. 1.4 the slope of the temperature log radius graph equals:-

$$-\frac{k_r.L.2.\pi}{q}$$

Therefore

$$k_r = -\frac{\text{slope}.q}{L.2.\pi}$$

and substituting gives:-

$$\underline{k_r = 1.045 \quad J/m\ s\ K}$$

Results of the second test carried out on Coil No.1.

In this test the coil was heated by passing a current through the windings. Time was allowed for the coil to thermally reach steady state. Readings were then taken of power input to the coil and the voltage at each thermocouple.

Diameter of the coil = 156 mm

Length of the coil = 127 mm

Voltage and current through the heater = 2.05 amps and 18 volts.

Readings from the coil:

Voltage at thermocouple mV	Temperature at thermocouple. K	Radius of thermocouple mm
3.15	75.4	22.22
3.19	76.4	30.01
3.17	75.8	35.75
3.18	76	40.6
3.0	71.6	55.0
2.86	68.6	62.0
2.74	65.6	68.55
2.6	62.2	74.5

These results are plotted in Fig. 2.5

<u>Calculation of the temperature distribution in Coil No.1 under the conditions of heat generation within the coil.</u>

Current passing through the windings	I	=	2.05 A.
Electrical Resistance of the windings	R	=	$7.05\ (1 + 0.00352\theta)\ \Omega$
Thermal conductivity		=	1.045 J/ m s K
Length of coil		=	127 mm
Diameter of coil		=	156 mm
Diameter of core		=	25.4 mm

Using Eq. 1.6:

$$\theta = \frac{-\alpha}{\beta} + C_1.J_o.\left(r\sqrt{\frac{\beta}{k_r}}\right) + C_2.Y_o.\left(r\sqrt{\frac{\beta}{k_r}}\right)$$

Where heat generation $= (\alpha + \beta\theta)$

which can be obtained from

$$\frac{I^2.R}{\text{volume}} = \frac{(2.05)^2 x 7.05 x (1 + 0.00352\theta)}{\frac{(156)^2 - (25.4)^2}{4}\ 127 x 10^{-9}}$$

$$= (1.258 + 0.443\theta) x 10^2$$

therefore

$$\alpha = 1.258 x 10^2$$

and

$$\beta = 0.443 x 10^2$$

Calculating

$$\sqrt{\frac{\beta}{k_r}} = 6.5$$

Now since r has a maximum value in this case of 78×10^{-3}m the function $r\sqrt{\frac{\beta}{k_r}}$ will have a maximum value of 0.56. Therefore terms in J_o and Y_o

$$J_o = 1 - x^2 + \frac{x^4}{2^2 . 4^2} + \frac{x^6}{2^2 . 4^2 . 6^2}$$

$$Y_o = \frac{2}{\pi} (\log x + \gamma) J_o$$

$$x = r\sqrt{\frac{\beta}{k_r}}$$

having x to greater powers than 2 may be neglected; therefore the Bessel equation may be simplified to the following:-

$$0 = -\frac{\alpha}{\beta} + (1 - \frac{x^2}{4})(C_1 + C_2(2.\log_e\frac{x}{2} + \gamma))$$

Now in order to obtain values for the constants $\frac{d\theta}{dx}$ is required

Note: $\frac{d\theta}{dx}$ does not introduce an x^2 term from the original equation since the next term in the series is x^4.

$$\frac{d\theta}{dx} = C_2 \left[\frac{2}{\pi x} - x\left(\gamma + \frac{1}{2\pi} + \frac{2}{\pi}.\log_e\frac{x}{2}\right)\right] - C_1.x$$

Now substituting the conditions of

θ = 62.2°C at r = 75.4 mm

(This condition is obtained from the temperature at a thermocouple but could be the surface temperature in practice).

and

$$\frac{d\theta}{dx} = 0 \quad \text{at} \quad r = 12.7 \text{ mm}$$

(No heat transfer to the core)

Therefore, for the first condition

$$x = \frac{75.4}{10^3} \times 6.5$$

$$= 4.9 \times 10^{-1}$$

for the second condition

$$x = \frac{12.7}{10^3} \times 6.5$$

$$= 8.268 \times 10^{-2}$$

Substituting into the simplifyed equation gives:-

$$C_1 = 368.16$$

$$C_2 = 3.01$$

Therefore writing the equation in full

$$\theta = -284.1 + (1 - \frac{x^2}{4}) \left[368.16 + 3.01(\frac{2}{\pi}.\log_e \frac{x}{2} + 0.5772) \right]$$

Now substituting for r in the above equation gives:-

r	θ
12.7 mm	80.9 K
20 mm	80.2 K
30 mm	79.5 K
40 mm	77.5 K
50 mm	73.6 K
60 mm	69.8 K
70 mm	64.3 K
78 mm	60.5 K

The above calculation was repeated but with the condition $\frac{d\theta}{dx} = 0$ at r = 12.7 mm changed to $\frac{d\theta}{dx} = 0$ at r = 30 mm which corresponds to the actual readings from the coil (see Fig. 2.5).

The results obtained were as follows:-

r	θ	
30 mm	74	K
40 mm	73.2	K
50 mm	71.1	K
60 mm	67.6	K

These points are plotted in Fig. 2.5.

Calculation of the heat transfer coefficient from water to the surface of the wire used to construct Coil No. 1

This heat transfer coefficient may be calculated using the equation from Coulson & Richardson (8)

$$Nu = 0.26.(Re)^{0.6}.(Pr)^{0.3}$$

where Nu = Nusselt number

Re = Reynolds number

Pr = Prandtl number

which gives the heat transfer coefficient to a single round bar of infinite length when water is passed at constant velocity across the bar in the direction perpendicular to the axis.

This is not identical to the conditions in the test to find the conductance of the insulation, since the wire is not straight and the velocity is not constant, but the result will give some indication of the magnitude of the coefficient to expect.

Data	Symbol	Value	Units
Diameter of the wire	D	1.7×10^{-3}	m
Specific heat of water	Cp_w	4.1868×10^{3}	J/kg K
Thermal conductivity of water	k_w	0.607	J/m s K
Viscosity of water	η	0.55	Ns/m^2
Density of water	ρ_w	1000	kg/m^3
Velocity	V	1.2	m/s
Heat transfer coefficient	h_w	-	J/m^2sK

Calculating numbers

$$Re = \frac{V.D}{\eta} = 3710$$

Note: This is turbulent since turbulence begins at 200 for a bar

$$Pr = \frac{\eta.Cp_w}{k_w} = 3.79$$

therefore

$$Nu = \frac{h_w.D}{k_w} = 0.26(3710)^{0.6}.(3.79)^{0.3}$$

so that

$$\underline{h_w = 20.1x10^3 \ J/m^2s \ K}$$

This value of heat transfer coeficient is only a factor of six greater than the value of conductance found for the insulation and could lead to an error of 16% in the value obtained. However the check carried out during the experiment and confirmation of Method 6 for obtaining the conductance indicate that error involved is considerably smaller than that indicated here.

APPENDIX 3

Calculations involving the conductance of the insulation

Contents

APPENDIX 3.

Calculations involving the conductance of the insulation.

Derivation of Eq. 2.1.

$$\log_e \theta' = A - \frac{4 k_i . t}{T_i . Cp_c . \rho_c}$$

Consider a unit length of wire. If the surface temperature of the insulation is raised above the temperature of the copper, the heat flow into the copper can be equated to the heat flow through the insulation thus:-

$$\pi . \frac{D_w^2}{4} . \rho_c . Cp_c . \frac{d\theta'}{dt} = - \frac{\theta' . \pi . D_w . k_i}{T_i}$$

Where
D_w = Diameter over the copper
ρ_c = Density of copper
Cp_c = Specific heat of copper
T_i = Thickness of insulation
k_i = Conductivity of insulation
θ' = Temperature drop across the insulation

Therefore

$$\frac{D_w}{4} . \rho_c . Cp_c . \frac{d\theta'}{dt} + \frac{\theta' . k_i}{T_i} = 0$$

Solving for θ' gives:

$$\theta' = A' . e^{-\left(\frac{4 k_i . t}{T_i . D_w . \rho_c . Cp_c}\right)}$$

Where A' is an arbitrary constant

Taking logs

$$\log_e \theta' = \log_e A' - \frac{4k_i \cdot t}{T_i \cdot D_w \cdot \rho_c \cdot Cp_c}$$

$$\log_e \theta' = A - \frac{4k_i \cdot t}{T_i \cdot D_w \cdot \rho_c \cdot Cp_c}$$

Calculation of the conductance of the insulation on the wire from the graph obtained by UV recorder for Coil No.1.

The curve obtained from the UV recorder is reproduced in Fig.2.7. The original graph had small cyclic oscillations on the curve which represented 1/50 s. Taking the height of the main curve above the datum at each fifth oscillation gives the height of the curve at 1/10 s intervals, thus:-

Height of curve.	Time.	$\log_e$ of height.
cm	s	
5.23	0.1	1.65441
4.22	0.2	1.44
3.28	0.3	1.188
2.58	0.4	0.95
2.0	0.5	0.693
1.6	0.6	0.47
1.23	0.7	0.207
1.0	0.8	0.000

Now plotting the $\log_e$ of the height of the curve against time gives the graph in Fig 2.8 which is a straight line which has a slope of −2.44. Substituting this slope into Eq. 2.2 will give the conductance of the insulation thus:-

Diameter of wire (excluding insulation)	1.626 mm
Specific heat of copper	0.3815×10^3 J/kg K
Density of copper	8.95×10^3 kg/m^3

Eq. 2.2

$$C_i = -\frac{D_w}{4}.\rho_c.Cp_c.S'$$

$$\underline{C_i = 33.9\text{x}10^2 \ \text{J/m}^2\text{s K}}$$

<u>Results of the test on the small Lees' disk.</u>

Test	θ_{d1}	θ_{d2}	θ_{w1}	θ_{w2}	Load.
1	19.3	16.55	31.5	20.97	5 kg
2	18.85	16.43	30.5	20.25	5 kg
3	25.1	17.39	57.8	27.9	5 kg
4	18.82	16.08	30.5	20.26	10 kg
5	19.3	16.43	30.75	20.5	10 kg
6	25.1	17.62	56.6	27.9	10 kg

Substitution into the equation

$$C_i = \frac{k_w(\theta_{w1} - \theta_{w2}).A_w}{L_w(\theta_{d1} - \theta_{d2}).A_d}$$

where

$k_w = 387$ J/ m s K

$L_w = 61.8$ mm

$A_w = 2.09$ mm^2

$A_d = 16.4$ mm^2

gives:-

Test				
1	C_i	=	30.6×10^2	J/m^2 s K
2	C_i	=	33.8×10^2	J/m^2 s K
3	C_i	=	30.6×10^2	J/m^2 s K
4	C_i	=	29.8×10^2	J/m^2 s K
5	C_i	=	28.5×10^2	J/m^2 s K
6	C_i	=	30.5×10^2	J/m^2 s K

APPENDIX 4

Calculation of the conductivity of Coil No. 1

Contents

APPENDIX 4.

Calculation of the conductivity of Coil No.1.

Calculation of the conductivity of Coil No.1 from Eq. 1.16 as given below:-

$$k_r = \frac{a}{c}\left[0.524 - \frac{2b}{(b-c)m}\left(\mathrm{Tan}^{-1}\frac{0.2679}{m}\right)\right]\frac{h}{\frac{1}{2}D}$$

where $m = \sqrt{\dfrac{b+c}{b-c}}$

$a = C_i.\frac{1}{2}D.k_a$

$b = C_i.\frac{1}{2}D$

$c = k_a - C_i.\frac{1}{2}D$

$h = \frac{\sqrt{3}}{2}.D$

Data	Symbol	Value	Units	Source.
Conductance of the insulation	C_i	$33.9\text{x}10^{2}$	$J/m^2 s\ K$	App. 3
Diameter of wire over the insulation.	D	1.7	mm	measurement
Conductivity of air	k_a	$2.94\text{x}10^{-2}$	J/m s K	Int.Crit.Tables.

$a = 84.6 \times 10^{-3}$

$b = 28.8 \times 10^{-1}$

$c = 28.5 \times 10^{-1}$

$m = 7.14 \times 10^{-2}$

therefore

$$\mathrm{Tan}^{-1}\frac{0.2679}{m} = 1.31$$

and

$$\frac{2b}{(b - c)m} \cdot \mathrm{Tan}^{-1} \frac{0.2679}{m} = 18.5$$

Therefore

$$\underline{k_r = 0.925 \text{ J/m s K}}$$

Calculation of the conductivity of Coil No. 1 using Eq. 1.21 as given below

$$k_r = (H_{2q} + H_{2c}) \cdot \frac{h}{\frac{1}{2}D}$$

where

$$H_{2q} = \frac{a}{c}\left\{ \phi_2 - \phi_1 - \frac{2b}{(b-c)m}\left[\mathrm{Tan}^{-1}\left(\frac{1}{m}.\mathrm{Tan}\tfrac{1}{2}\phi_2\right) - \mathrm{Tan}^{-1}\left(\frac{1}{m}.\mathrm{Tan}\tfrac{1}{2}\phi_1\right)\right]\right\}$$

$$H_{2c} = \frac{C_i . M}{2}$$

$$m = \sqrt{\frac{b+c}{b-c}}$$

$$a = C_i . k_a . \tfrac{1}{2}D$$

$$b = C_i(\tfrac{1}{2}D - p)$$

$$c = k_a - C_i . \tfrac{1}{2}D$$

$$\phi_2 = 30^{\circ}$$

$$\phi_1 = \mathrm{Sin}^{-1}(M/D)$$

$$h = \frac{\sqrt{3}}{2} . D$$

$$p = \frac{M^2}{4} . \frac{1}{D}$$

Data	Symbol	Value	Units	Source
Conductance of the insulation	C_i	33.9×10^{-2}	$J/m^2 s\ K$	App. 3
Diameter of the wire over the insulation	D	1.7	mm	measurement
Conductivity of air	k_a	2.94×10^{-2}	J/m s K	Int. Crit. Tables
Contact area	M	0.178	mm	experiment. (see page 62)

Calculating

$$a = 84.6 \times 10^{3}$$

$$b = 28.8 \times 10^{-1}$$

$$c = -28.5 \times 10^{-1}$$

$$p = 0.466 \times 10^{-5}$$

$$m = 7.14 \times 10^{-2}$$

$$\phi_1 = 0.1048 \text{ (Radians)}$$

$$\tan^{-1} \frac{1}{m}.\tan\tfrac{1}{2}\phi_2 = 1.31 \text{ (Radians)}$$

$$\tan^{-1} \frac{1}{m}.\tan\tfrac{1}{2}\phi_1 = 0.64 \text{ (Radians)}$$

$$H_{2q} = 2.72 \times 10^{-1}$$

$$H_{2c} = 3.02 \times 10^{-1}$$

$$\underline{k_r = 0.995 \text{ J/m s K}}$$

APPENDIX 5

Experimental results and calculations for Coil No. 2

Contents

Page

APPENDIX 5.

Experimental results and calculations for Coil No.2.

Results of the first and second tests carried out on Coil No.2.

Tests carried out as in App.2.

Length of coil 63.5 mm

Diameter of coil 36.8 mm

First Test.

Voltage and current through central heater = 4.86 V. 1.475 A.

Readings from coil:-

Voltage at thermocouples.	Radius of thermocouples.	Log of radius.
mV	mm	
3.191	7.14	1.966
2.845	9.32	2.232
2.464	12.35	2.514
2.1	15.44	2.737
1.92	17.41	2.857

Plotting these results gives graph in Fig. 3.1

The slope of the graph = − 0.702.

This slope can be changed into a temperature v $\log_e$ radius slope by multiplying by the number of mV per K = 0.0419 (see calibration curve for the thermocouple).

Which gives the slope to be 0.702 x 0.0419 = − 0.0294.

Substituting the above results into Eq. 1.4 gives:-

$$k_r = 0.53 \quad J/m\ s\ K$$

Results of the temperature distribution in Coil No.2 when current was passed through the windings.

Readings from the coil:-

The test on the coil was carried out in the same way as described in App.2.

Voltage at thermocouples.	Temperatures at thermocouples.	Radius of thermocouples.
mV	K	mm
3.56	82.5	7.14
3.62	83.2	9.32
3.675	83.8	12.35
3.8	85.2	15.44
3.82	85.4	17.41

Calculating the temperatures from Eq. 1.5.

The temperatures are calculated in the same way as in App.2.

Temperature.	Radius.
K	mm
86.2	3.175
86	5
85.1	10
83.5	15
82.0	18.4

Plotting the above results gives the graphs in Fig. 3.2.

Results of the compression test on the paper in Coil No.2.

In this test the paper was compressed in the apparatus shown in Fig.3.3. The following results give the thickness of the paper under different loads. Two tests were carried out on the same paper.

Load. kg	1st Test. Thickness. mm	2nd Test. Thickness. mm
0	0.1472	0.1472
0.545	0.132	0.125
2.353	0.122	0.122
4.163	0.114	0.112
5.973	0.112	0.107
7.783	0.105	0.107
9.597	0.102	0.102
11.403	0.102	0.102

These results are plotted in Fig. 3.4.

The minimum thickness to which the paper can be compressed = 0.102 mm

Calculation of the conductance of paper used in Coil No.2.

Results from the Lees' disk.

Voltage across heater in Lees' disk	=	4.21 V
Current through heater in Lees' disk	=	0.86 A.
Readings of thermocouple on cold face of Lees' disk	=	0.25 mV.
Readings of thermocouple on warm face of Lees' disk	=	0.88 mV.
Area of faces of Lees' disk.	=	5.06×10^{-4} m^2

Temperature difference across the paper can be found from the difference in the thermocouple voltages divided by the mV per K, thus:-

$$\frac{(0.88 - 0.25)}{0.0419}$$

$$= 15.05 \text{ K}$$

Heat transfer through the paper is given by voltage x current thus:-

$$4.21 \times 0.86 = 3.63 \text{ J/s}$$

therefore thermal conductance of paper

$$= \frac{3.63}{15.05 \times 5.06 \times 10^{-4}}$$

$$C_{pl} = 4.76 \times 10^2 \quad \text{J/m}^2\text{s K}$$

Calculation of the conductance of paper used in Coil No.2 after it has been compressed to its thinnest.

Results from Lees' disk.

Voltage across the heater in Lees' disk	=	0.84 V.
Current through the heater in Lees' disk	=	4.26 A.
Readings of thermocouples on the cold face of Lees' disk	=	0.16 mV.
Readings of thermocouples on warm face of Lees' disk	=	0.53 m V.
Area of faces of disk	=	5.06×10^{-4}

As in previous calculation:

Temperature across paper

$$= \frac{0.53 - 0.16}{0.0419}$$

$$= 8.85 \text{ K}$$

Heat transfer through the paper

$$= 0.84 \times 4.26 = 3.58.$$

Thermal conductance of paper

$$= \frac{3.58}{8.85 \times 5.06} \times 10^{-4}$$

$$C_{p2} = 8.1 \times 10^{2} \quad \text{J/m}^2 \text{ s K}$$

Calculation of the conductance of the insulation on the wire from the graph obtained by UV recorder for Coil No.2.

The curve obtained from the UV recorder is reproduced in Fig. 3.5. The original graph had small cyclic oscillations on the curve above the datum. Each fifth oscillation gives the height of the curve at 1/10 s intervals, thus:-

Height of curve.	Time.	$\log_e$ of height.
cm	s	
0.3	0.48	− 1.20398
0.5	0.4	− 0.69351
0.95	0.3	− 0.05130
1.8	0.2	0.58779
3.435	0.1	1.20896
4.8	0	1.56862

Now, plotting the $\log_e$ of height against time gives the graph in Fig. 3.6 which is a straight line of slope − 6.31. Substituting this slope into Eq. 2.2 will give the conductance of the insulation thus:-

Diameter of wire (excluding insulation)	=	0.965 mm
Specific heat of copper	=	0.3185×10^3 J/kg K
Density of copper	=	8.95 kg/m^2

Eq. 2.2

$$C_i = -\frac{D_w}{4} \cdot \rho_c \cdot Cp_c \cdot S'$$

$$C_i = 51.8 \times 10^{-2} \ \mathrm{J/m^2 s\,K}$$

Calculation of the conductivity of Coil No.2 from Eq 1.37.

Eq. 1.37 is given as follows:-

$$k_r = \left\{ 2 \left[\frac{H_{2q} \cdot H_{3p}}{H_{2q} + H_{3p}} \right] + H_{3c'} \right\} \frac{h}{\frac{1}{2}D}$$

Note: The simplified version has been used, i.e., H_{3c} is replaced by $H_{3c'}$

Each of the above terms will be calculated separately below:

The data required for calculating these terms is as follows:-

Data Name	Symbol	Value	Units	Source.
Conductance of insulation.	C_i	51.8×10^2	$J/m^2\ s\ K$	App. 5
Thickness of paper	T	0.1472	mm	App. 5
Thickness of paper under maximum compression	B	0.102	mm	App. 5
Conductance of paper uncompressed		4.76×10^2	$J/m^2\ s\ K$	App. 5
Conductance of paper under maximum compression		8.1×10^2	$J/m^2\ s\ K$	App. 5
Diameter of wire over insulation	D	1.016	mm	Measurement
Conductivity of Air	k_a	2.94×10^2	J/m s K	Int. Crit. Tables.

<u>To obtain $H_{3c'}$</u>

From Eq. 1.34

$$H_{3c'} = \frac{2e}{f.m}\left[\mathrm{Tan}^{-1}\frac{(x_2)}{(m)}\right]$$

where

$$x_2 = M/2$$

$$m = \sqrt{\frac{g}{f}}$$

$$e = C_i$$

$$f = C_i.v'.a'$$

$$g = C_i(v'.b' + s) + 2$$

and a' & b' can be found from

$$y = a'.x^2 + b'$$

when $x = 0,\ y = B$

and $x = \frac{M}{2},\ y = T$

also, v' & s' can be found from

$$C_p = \frac{1}{s' + v'.y}$$

when $C_p = C_{p1},\ y = T$

and $C_p = C_{p2},\ y = B$

Calculating M

From Eq. 3.1

$$M = 2\sqrt{\frac{(T-B)}{2} \cdot \left\{D - \frac{(T-B)}{2}\right\}}$$

therefore

$$\underline{M = 0.2998 \text{ mm}}$$

Calculating a' & b'

Substituting the conditions of

$$x = 0 \text{ at } y = B$$

$$\text{and} \quad x = \frac{M}{2} \text{ at } y = T$$

into

$$y = a'.x^2 + b$$

gives

$$a' = \frac{T - B}{(M/2)^2} \qquad \text{and} \qquad b' = B$$

therefore

$$\underline{a' = 2.0115 \times 10^3} \text{ and } \underline{b' = 0.102 \times 10^{-3}}$$

Calculating v' & s'

Substuting the conditions of

$$C_p = C_{p1} \text{ at } y = T$$

$$\text{and} \quad C_p = C_{p2} \text{ at } y = B$$

into

$$y = \frac{1}{s' + v'.y}$$

gives

$$v' = \frac{C_{p2} - C_{p1}}{C_{p2} . C_{p1} . (T - B)}$$

therefore

$$\underline{v' = 19.165}$$

also

$$s' = \frac{1}{C_{p1}} - T.v'$$

therefore

$$\underline{s' = 0.721 \times 10^{-3}}$$

Calculating g

$$g = C_i.(v'.b' + s') + 2$$

therefore

$$\underline{g = 8.3833}$$

Calculating f

$$f = C_i.v'.a'$$

therefore

$$\underline{f = 199.691 \times 10^{6}}$$

Calculating m

$$m = \sqrt{\frac{g}{f}}$$

therefore

$$\underline{m = 0.20491 \times 10^{-3}}$$

Calculating x_1

$$x_1 = \frac{M}{2}$$

therefore

$$\underline{x_1 = 0.1499 \times 10^{-3}}$$

Calculating $H_{3c'}$

$$H_{3c'} = \frac{2e}{f.m}\left[\mathrm{Tan}^{-1}\left(\frac{x_2}{m}\right)\right]$$

therefore

$$\underline{H_{3c'} = 0.1605 \ \ J/s\,K}$$

This value of $H_{3c'}$ is the heat rate for the part of the coil where the paper is in contact wiht the wire above it and the wire below as illustrated in Fig. 1.6.

To obtain H_{2q}

From Eq. 1.19

$$H_{2q} = \frac{a}{c}\left\{\phi_2 - \phi_1 - \frac{b}{(b-c)m}\left[\log_e\left(\frac{\mathrm{Tan}\frac{1}{2}\phi_2 - m}{\mathrm{Tan}\frac{1}{2}\phi_2 + m} \cdot \frac{\mathrm{Tan}\frac{1}{2}\phi_1 + m}{\mathrm{Tan}\frac{1}{2}\phi_1 - m}\right)\right]\right\}$$

where $a = C_i . k_a . \frac{1}{2}D$

$b = C_i . \frac{1}{2}D - C_i . p$

$c = k_a - C_i . \frac{1}{2}D$

$\phi_2 = 30^c$

$\phi_1 = \mathrm{Sin}^{-1}(M/D)$

$p = \frac{T - B}{2}$

$m = \sqrt{\frac{b+c}{c-b}}$

Note that Eq. 1.19 has been used rather than Eq. 1.18 since $\frac{b+c}{b-c}$ is negative

Calculating a

$$a = C_i . k_a . \tfrac{1}{2}D$$

therefore

$$\underline{a = 7.7365 \times 10^2}$$

Calculating b

$$b = C_i \tfrac{1}{2}D - C_i . p$$

therefore

$$\underline{b = 25.143 \times 10^{-1}}$$

Calculating c

$$c = k_a - C_i . \tfrac{1}{2}D$$

therefore

$$\underline{c = -26.016 \times 10^{-1}}$$

Calculating ϕ_1

$$\phi_1 = \text{Sin}^{-1}(M/D)$$

therefore

$$\underline{\phi_1 = 0.301 \text{ Radians}}$$

Calculating m

$$m = \sqrt{\frac{b + c}{c - b}}$$

therefore

$$\underline{m = 0.13063}$$

Calculating H_{2q}

$$H_{2q} = \frac{a}{c}\left\{\phi_2 - \phi_1 - \frac{b}{(b-c)m}\left[\log_e\left(\frac{\mathrm{Tan}\frac{1}{2}\phi_2 - m}{\mathrm{Tan}\frac{1}{2}\phi_2 + m}\cdot\frac{\mathrm{Tan}\frac{1}{2}\phi_1 + m}{\mathrm{Tan}\frac{1}{2}\phi_1 - m}\right)\right]\right\}$$

therefore

$$\underline{H_{2q} = 16.937 \times 10^{-2} \quad \mathrm{J/s\ K}}$$

This value of H_{2q} is the heat rate for the part of the coil where the heat flows from the copper through the insulation and into the air space as illustrated in Fig. 1.7

<u>To obtain H_{3p}</u>

From Eq. 1.35

$$H_{3p} = \frac{a}{c}\left\{\phi_2 - \phi_1 - \frac{2b}{(b-c)m}\left[\mathrm{Tan}^{-1}\left(\frac{1}{m}.\mathrm{Tan}\tfrac{1}{2}\phi_2\right) - \mathrm{Tan}^{-1}\left(\frac{1}{m}.\mathrm{Tan}\tfrac{1}{2}\phi_1\right)\right]\right\}$$

where

$$a = C_{ip}.k_a.\tfrac{1}{2}D_p$$

$$b = C_{ip}.\tfrac{1}{2}D_p - C_{ip}.p$$

$$c = k_a - C_{ip}.\tfrac{1}{2}D_p$$

$$\phi_2 = 30^\circ$$

$$\phi_1 = \mathrm{Sin}^{-1}(M/D_p)$$

$$m = \sqrt{\frac{b+c}{b-c}}$$

$$C_{ip} = \frac{C_i.C_{pl}}{C_i + C_{pl}}$$

$$p = \frac{T - B}{2}$$

Note that Eq. 1.35 has been used rather than Eq. 1.36 since $\frac{b + c}{b - c}$ is positive

Calculating C_{ip}

$$C_{ip} = \frac{C_i . C_{pl}}{C_i + C_{pl}}$$

therefore

$$\underline{C_{ip} = 4.3594 \times 10^2}$$

Calculating a

$$a = C_{ip}.k_a.\tfrac{1}{2}D_p$$

therefore

$$\underline{a = 8.39746 \times 10^{-3}}$$

Calculating b

$$b = C_{ip}.\tfrac{1}{2}D_p - C_{ip}.p$$

therefore

$$\underline{b = 2.73596 \times 10^{-1}}$$

Calculating c

$$c = k_a - C_{ip}.\tfrac{1}{2}D_p$$

therefore

$$\underline{c = 2.5628 \times 10^{-1}}$$

Calculating m

$$m = \sqrt{\frac{b + c}{b - c}}$$

therefore

$$\underline{m = 0.18105}$$

Calculating H_{3p}

$$H_{3p} = \frac{a}{c}\left\{\phi_2 - \phi_1 - \frac{2b}{(b - c)m}\left[\mathrm{Tan}^{-1}\left(\frac{1}{m}.\mathrm{Tan}\tfrac{1}{2}\phi_2\right) - \mathrm{Tan}^{-1}\left(\frac{1}{m}.\ \mathrm{Tan}\tfrac{1}{2}\phi_1\right)\right]\right\}$$

therefore

$$\underline{H_{3p} = 6.5 \times 10^{-2}\ \ \mathrm{J/s\ K}}$$

This value of H_{3p} gives the heat rate of the part of the coil where heat flows from copper through insulation and paper, and into the air space as illustrated in Fig. 1.7

Finally to obtain k_r

From Eq. 1.37

$$k_r = \left\{ 2 \left[\frac{H_{2q} \cdot H_{3p}}{H_{2q} + H_{3p}} \right] + H_{3c'} \right\} \frac{h}{\frac{1}{2}D}$$

Calculating h

From Eq. 1.38

$$h = \sqrt{2B.D + B^2 + \frac{3}{4}D^2}$$

therefore

$$h = 0.99085 \text{ mm}$$

therefore

$$k_r = 49.6 \times 10^{-2} \text{ J/m s K}$$

APPENDIX 6.

Results of tests on various coils.

In this appendix the results of tests on seven independent paper interleaved coils are given.

The tests carried out on each coil were:-

1. To obtain the radial conductivity of the coil by the direct experimental method described at the beginning of Chapter 2.

2. To obtain all the characteristics of the constituents of the coil required to calculate the radial conductivity of the coil by the method described at the end of Chapter 1.

The results for each coil are given on a separate page.

COIL No.2.

Dimensions.

Diameter	=	36.88	mm
Length	=	63.5	mm
Diameter of wire over insulation	=	1.016	mm
Diameter of wire excluding insulation	=	0.965	mm
Thickness of paper	=	0.1472	mm
Thickness of paper under maximum compression.	=	0.102	mm

Properties.

Conductance of insulation	=	51.8×10^{2} J/m^{2} s K
Conductance of paper uncompressed	=	4.76×10^{2} J/m^{2} s K
Conductance of paper compressed to 0.102 mm	=	8.1×10^{2} J/m^{2} s K

Results.

Radial conductivity obtained by experiment:

$$k_r = 53 \times 10^{-2} \text{ J/m s k}$$

Radial conductivity obtained by calculation:

$$k_r = 49.6 \times 10^{-2} \text{ J/m s K}$$

COIL No.3.

Dimensions.

Diameter	=	34.5 mm
Length	=	63.5 mm
Diameter of wire over insulation	=	0.762 mm
Diameter of wire excluding insulation	=	0.711 mm
Thickness of paper	=	0.1472 mm
Thickness of paper under maximum compression.	=	0.102 mm

Properties.

Conductance of insulation	=	55.4×10^2 J/m^2 s K
Conductance of paper uncompressed	=	4.76×10^2 J/m^2 s K
Conductance of paper compressed to 0.102 mm	=	8.1×10^2 J/m^2 s K

Results.

Radial conductivity obtained by experiment:

$$k_r = 39.5 \times 10^{-2} \quad \text{J/m s K}$$

Radial conductivity obtained by calculation:

$$k_r = 45.0 \times 10^{-2} \quad \text{J/m s K}$$

COIL No. 4

Dimensions

Diameter	=	35.3 mm
Length	=	63.5 mm
Diameter of wire over insulation	=	1.016 mm
Diameter of wire excluding insulation	=	0.965 mm
Thickness of paper	=	0.1016 mm
Thickness of paper under maximum compression	=	0.0788 mm

Properties

Conductance of insulation	=	55.4×10^2 J/m^{2}s K
Conductance of paper uncompressed	=	6.67×10^2 J/m^{2}s K
Conductance of paper compressed to 0.795 mm	=	11.8×10^2 J/m^2 s K

Results

Radial conductivity obtained by experiment

$$k_r = 55 \times 10^{-2} \quad \text{J/m s K}$$

Radial conductivity obtained by calculation

$$k_r = 52.2 \times 10^{-2} \quad \text{J/m s K}$$

COIL No.5.

Dimensions.

Diameter	=	35.6 mm
Length	=	38.1 mm
Diameter of wire over insulation	=	0.762 mm
Diameter of wire excluding insulation	=	0.711 mm
Thickness of paper	=	0.0814 mm
Thickness of paper under maximum compression.	=	0.0674 mm

Properties.

Conductance of insulation	=	55.4×10^2 J/m^2 s K
Conductance of paper uncompressed	=	11.07×10^2 J/m^2 s K
Conductance of paper compressed to 0.0674.	=	13.35×10^2 J/m^2 s K

Results.

Radial conductivity obtained by experiment:

$$k_r = 46.5 \times 10^{-2} \text{ J/ m s K}$$

Radial conductivity obtained by calculation:

$$k_r = 51.2 \times 10^{-2} \text{ J/m s K}$$

COIL No. 6.

Dimensions

Diameter	=	39.5	mm
Length	=	63.5	mm
Diameter of wire over insulation	=	1.016	mm
Diameter of wire excluding insulation	=	0.965	mm
Thickness of paper	=	0.295	mm
Thickness of paper under maximum compression	=	0.234	mm

Properties

Conductance of insulation	=	51.8×10^{2} J/m^{2}s K
Conductance of paper uncompressed	=	0.2195×10^{2} J/m^{2} K
Conductance of paper compressed to 0.234mm	=	0.254×10^{2} J/m^{2} K

Results

Radial conductivity obtained by experiment

$$k_r = 36.1 \times 10^{-2} \quad J/m\ s\ K$$

Radial conductivity obtained by calculation

$$k_r = 35.0 \times 10^{-2} \quad J/m\ s\ K$$

COIL No.7.

Dimensions.

Diameter	=	37 mm
Length	=	63.5 mm
Diameter of wire over insulation	=	1.016 mm
Diameter of wire excluding insulation	=	0.965 mm
Thickness of paper uncompressed	=	0.1142 mm
Thickness of paper under maximum compression	=	0.0814 mm

Properties.

Conductance of insulation	=	51.8×10^2 $J/m^2 s K$
Conductance of paper uncompressed	=	6.544×10^2 $J/m^2 s K$
Conductance of paper compressed to 0.965 mm	=	10.732×10^2 $J/m^2 s K$

Results.

Radial conductivity obtained by experiment:

$$k_r = 59.5 \times 10^{-2} \ J/m\ s\ K$$

Radial conductivity obtained by calculation:

$$k_r = 54.6 \times 10^{-2} \ J/m\ s\ K$$

COIL No.8.

Dimensions.

Diameter	$\simeq$	26 mm
Length	=	38.1 mm
Diameter of wire over insulation	=	0.762 mm
Diameter of wire excluding insulation	=	0.711 mm
Thickness of paper	=	0.0864 mm
Thickness of paper under maximum compression	=	0.0564 mm

Properties.

Conductance of insulation	=	55.4×10^2 J/m^2 s K
Conductance of paper uncompressed	=	7.7×10^2 J/m^2 s K
Conductance of paper compressed	=	15.5×10^2 J/m^2 s K

Results.

Radial conductivity obtained by experiment:

$$k_r = 65.5 \times 10^{-2} \text{ J/m s K}$$

Radial conductivity obtained by calculation:

$$k_r = 60.3 \times 10^{-2} \text{ J/m s K}$$

APPENDIX 7

To obtain the axial conductivity of Coil No. 1 by substitution into Equation 4.2

$$k_{a'} = \frac{H_{ba}}{\sqrt{3}}$$

where $$H_{ba} = H_{b1} + H_{b2}$$

Now H_{b1} may be obtained directly from App. 4 that is,

$$\underline{H_{b1} = 0.535 \quad J/s\ K}$$

and H_{b2} may be obtained directly from App. 4 that is,

$$\underline{H_{b2} = 0.575 \quad J/s\ K}$$

therefore

$$\underline{H_{ba} = 1.109 \quad J/s\ K}$$

and

$$\underline{\underline{k_r = 0.64 \quad J/m\ s\ K}}$$

APPENDIX 8.

A computer programme for the calculation of the conductivity of paper interleaved coils.

The computer programme at the end of this appendix will calculate the conductivity of paper interleaved coils by the method given at the end of Chapter 1. The programme is written in Fortran 1V as used on an IBM 1130 and requires input and output through a card reader and a 1132 printer respectively.

The programme will take an input from the cards of the following numerical values:-

Conductance of the insulation (J/m^2 s K).

Thickness of the paper (mm).

Thickness of the paper under maximum compression (mm).

Conductance of the paper at full thickness (J/m^2 s K).

Conductance of the paper under maximum compression (J/m^2 s K).

Diameter of the wire over the insulation (mm).

Conductivity of air (J/m s K).

The figures in brackets give the units that must be used.

The input format is given in statement No.1 in the programme and is:-

FORMAT (F8.1, 2F7.4, 2F8.1, F7.4, F8.6) .

On receiving the above information the programme will print out on the line printer the input data in the above format and two lines below will print out the radial conductivity of the coil in the form below:-

RADIAL CONDUCTIVITY = XXX J/METRE SEC DEG K

where XXX represents the calculated value of the conductivity.

After printing out the value of conductivity the programme will read the next card in the card reader. If this card is a negative integer number the programme will return control to the monitor. If the card is blank or any positive integer, the programme will read the next card and calculate a second conductivity from the data thereon. Therefore any number of calculations may be carried out in this way.

The programme follows basically the same calculation as carried out in App.6, and with reference to this appendix the programme may easily be followed.

```
// JOB T

LOG DRIVE   CART SPEC   CART AVAIL   PHY DRIVE
  0000        0003        0003         0000

V2 M10   ACTUAL  8K  CONFIG  8K

// FOR
*ONE WORD INTEGERS
*IOCS(CARD,1132 PRINTER)
* LIST SOURCE PROGRAM
      REAL KA,M,M1,KR,MDUM,M2
   10 READ(2,1)CI,T,B,CP1,CP2,D,KA
      WRITE(3,1)CI,T,B,CP1,CP2,D,KA
    1 FORMAT(F8.1,2F7.4,2F8.1,F7.4,F8.6)
      D=D/10**(+3)
      B=B/10**(+3)
      T=T/10**(+3)
      M=2*SQRT(((T-B)/2)*(D-(T-B)/2))
      ADASH=(T-B)/((M/2)**2)
      BDASH=B
      VDASH=(CP2-CP1)/((T-B)*CP1*CP2)
      SDASH=(1/CP1)-(T*VDASH)
      G1=CI*(VDASH*BDASH+SDASH)+2
      F1=CI*VDASH*ADASH
      M1=SQRT(G1/F1)
      X11=M/2
      H3CDS=(2*CI/(F1*M1))*(ATAN(X11/M1))
      I=1
    7 A2=CI*KA*D/2
      B2=CI*D/2-CI*((T-B)/2)
      C2=KA-CI*D/2
      PHI12=ATAN(M/SQRT(D**2-M**2))
      MDUM=(B2+C2)/(B2-C2)
      IF(MDUM)2,2,3
    2 M2=SQRT(-MDUM)
      H=(A2/C2)*(0.50956-PHI12-(B2/((B2-C2)*M2))*(ALOG((SIN(0.25478)-M2*
     CCOS(0.25478))/(SIN(0.25478)+M2*COS(0.25478))*(SIN(PHI12/2)+M2*COS
     C(PHI12/2))/(SIN(PHI12/2)-M2*COS(PHI12/2)))))
      GO TO 4
    3 M2=SQRT(MDUM)
      DDUM=ATAN((1/M2)*(SIN(0.5*PHI12))/COS(0.5*PHI12))
      CDUM=ATAN((1/M2)*((SIN(0.25478))/COS(0.25478)))
      H=(A2/C2)*(0.50956-PHI12-(2*B2/((B2-C2)*M2))*(CDUM-DDUM))
    4 GO TO(5,6),I
    5 I=2
      H2Q=H
      CI=(CI*CP1)/(CI+CP1)
      D=D+2*T
      GO TO 7
    6 H3P=H
      SMALH=SQRT(2*B*D+B**2+((D-2*T)**2)*0.75)
      KR=(2*(H2Q*H3P)/(H2Q+H3P)+H3CDS)*SMALH*2/(D-2*T)
      WRITE(3,8)KR
    8 FORMAT(/'  RADIAL CONDUCTIVITY = ',F9.3,' J/METRE SEC DEG K '///)
      READ(2,9)J
    9 FORMAT(I5)
      IF(J)11,10,10
   11 CONTINUE
      CALL EXIT
      END
```

This card provides a print of this programme and will not normally by required.

LIST OF TERMS.

A	Area.	m^2
A_b	Cross section area of a block taken perpendicular to the direction of heat flow. The block is considered to be a macro element in the coil.	m^2
A_d	Area of the face of the small Lees' disk.	m^2
App.	Abbreviation for appendix.	
A_w	Cross section area of the wire used to feed heat into the small Lees' disk.	m^2
B	Minimum thickness of the interleaving paper in the coil	m
C	Thermal conductance defined as heat flow per unit area, unit time, degree of temperature difference across the material.	J/m^2 s K
C'	Arbitrary constant.	
C_i	Thermal conductance of the insulation on a wire	J/m^2 s K
C_{ip}	Combined thermal conductance of a layer of paper and a layer of insulation from a wire.	J/m^2 s K
C_m	The height of the UV recording above the steady state line of the cold water temperature.	mm

C_p	Thermal conductance of the interleaving paper.	J/m^2 s K
Cp_c	Specific heat of copper.	J/kg K
Cp_w	Specific heat of water.	J/kg K
D	Diameter of a wire over the insulation.	m
D_p	The diameter of a wire that has been wrapped in a layer of paper.	m
D_w	The diameter of a wire excluding the insulation.	m
Eq.	Abbreviation for equation.	
Fig.	Abbreviation for figure.	
H	Heat rate defined as heat flow per unit time, degrees of temperature difference across a body.	J/s K
H_1	Heat rate of body No.1.	J/s K
H_2	Heat rate of body No.2.	J/s K
H_{1q}	Heat rate of the quadrant in Section 1.3.	J/s K
H_{2q}	Heat rate of the quadrant in Section 1.4.	J/s K
H_{2c}	Heat rate of the centre part of the section in Section 1.4.	J/s K

H_{3c}	Heat rate of the centre part of the section in Section 1.5.	J/s K
$H_{3c'}$	Heat rate of the centre part of the section in Section 1.5 calculated by the simplified method.	J/s K
H_{3p}	Heat rate of the quadrant containing the paper.	J/s K
H_b	Heat rate of a block which is considered to be a typical macro element in a coil.	J/s K
H_{b1}	Heat rate of the block in Section 1.3.	J/s K
H_{b2}	Heat rate of the block in Section 1.4.	J/s K
H_{b3}	Heat rate of the block in Section 1.5.	J/s K
H_{ba}	Heat rate of the block under axial heat flow.	J/s K
H_t	Total heat rate	J/s K
H_x	Heat rate of element δx	J/s K
h	Height of a typical section in a coil measured in the direction of the heat flow.	m
I	Electrical current.	A
J_o	Bessel function (first kind; order zero).	
k	Thermal conductivity.	J/m s K

k_a	Thermal conductivity of air.	J/m s K
$k_{a'}$	Apparent axial thermal conductivity.	J/m s K
k_i	Thermal conductivity of the insulation on the wire.	J/m s K
k_r	Apparent radial thermal conductivity.	J/m s K
k_w	Thermal conductivity of the wire leading heat into the small Lees' disk.	J/m s K
L	Length of coil.	m
L_w	Length of wire.	m
m'	Length of an element in the air space.	m
M	Contact area measured as the chord of contact between one wire and the next, or a wire and the interleaving paper.	m
N_u	Nusselt number $\frac{h_w \cdot D}{k_{w'}}$	
P_r	Prandtl number $\frac{\nu \cdot Cp_w}{k_{w'}}$	
p	The amount of depression in the insulation on the wire or in the paper caused by the tension in the windings.	m
Q	Heat flow through the small Lees' disk	J/s

q	Heat flow	J/s
q_1	Heat flow through body 1.	J/s
q_2	Heat flow through body 2.	J/s
q_b	Heat flow through a block which is considered to be a typical macro element in a coil.	J/s
q_g	Heat generated per unit volume.	$J/m^2 s$
q_t	Total heat flow.	J/s
R_e	Reynolds number $\frac{V.D.}{\nu}$	
S	The slope of the $\log_e \theta'$ against t graph.	
S'	The slope of the $\log_e C_m$ against t graph.	
s	A constant in the expression for the thermal conductance of paper.	-
s'	A constant in the approximate expression for the thermal conductance of paper.	
T	Thickness of paper.	m
T_i	Thickness of insulation.	m
t	Time.	s

v	A constant in the expression for the thermal conductance of paper.	
v'	A constant in the approximate expression for the conductance of paper.	
x_1	A linear limit of integration in the x direction.	m
x_2	A linear limit of integration in the x direction.	m
Y_o	Bessel function. (2nd kind; order zero).	
x,y & z	Space coordinates.	m
α	Electrical resistance of copper wire at 273 K	Ω
β	Change in resistance of copper wire per 273 K	Ω/K
η	Viscosity of water	Ns/m^2
θ	Temperature.	K
θ_1	Temperature at one end of a body.	K
θ_2	Temperature at the other end.	K
θ'	Temperature difference across the insulation on a wire.	K

θ_{d1}	Temperature at the hot face of the small Lees' disk .	K
θ_{d2}	Temperature at the cold face of the small Lees' disk.	K
θ_{w1}	Temperature at the hot end of the wire leading into the small Lees' disk	K
θ_{w2}	Temperature at the cold end of the wire leading heat into the small Lees' disk	K
ρ_w	Density of water	kg/m^3
ρ_c	Density of copper	kg/m^3
ϕ	Angle	Radians
ϕ_1	Angular limit of integration	Radians
ϕ_2	Angular limit of integration	Radians
ϕ'	A constant	

BIBLIOGRAPHY.

(1) Cotton , H., Electrical Technology (Isaac Pitman & Sons, 1957).

(2) Say, M.G., Electrical Engineering Design Manual (Chapman & Hall, 1962).

(3) Fink, D.G. and Carroll, J.M., Standard Handbook for Electrical Engineers, Tenth Edition (McGraw-Hill, 1968).

(4) Say, M.G., The Performance and Design of Alternating Current Machines (Isaac Pitman & Sons, 1968).

(5) Richter, R., Electriche Maschinen Vol.1. (Julius Springer, 1924).

(6) Jakob, M., Heat Transfer Vol.1. (Wiley, 1949).

(7) Moore, A.D., Fundamentals of Electrical Design, (McGraw-Hill, 1927).

(8) Coulson, J.M. and Richardson, J.F., Chemical Engineering Vol.1. (Pergamon, 1956).

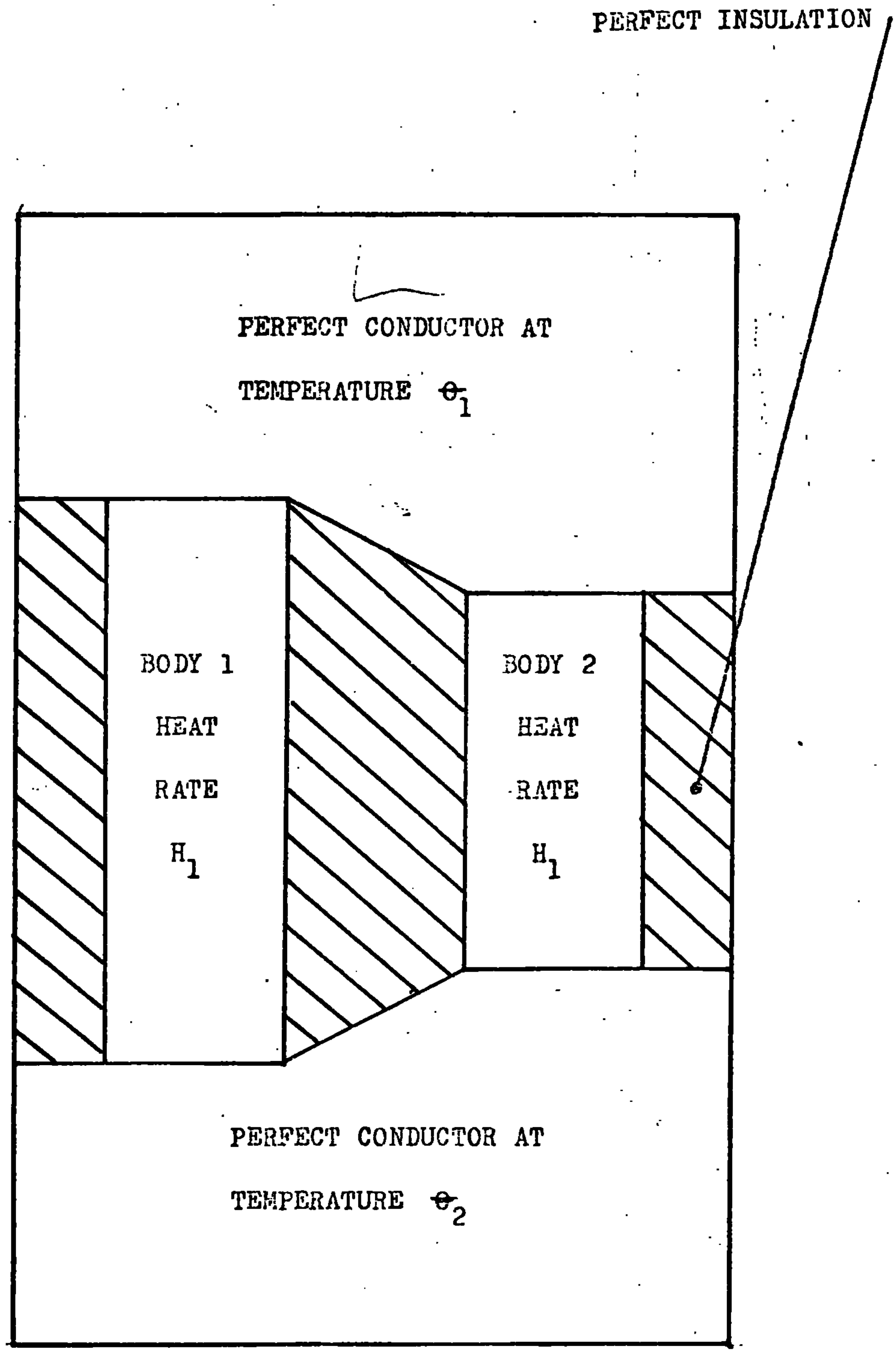
PERFECT INSULATION
PERFECT CONDUCTOR AT
TEMPERATURE θ1
BODY 1
HEAT
RATE
H1
BODY 2
HEAT
RATE
H1
PERFECT CONDUCTOR AT
TEMPERATURE θ2

FIG. 1.1

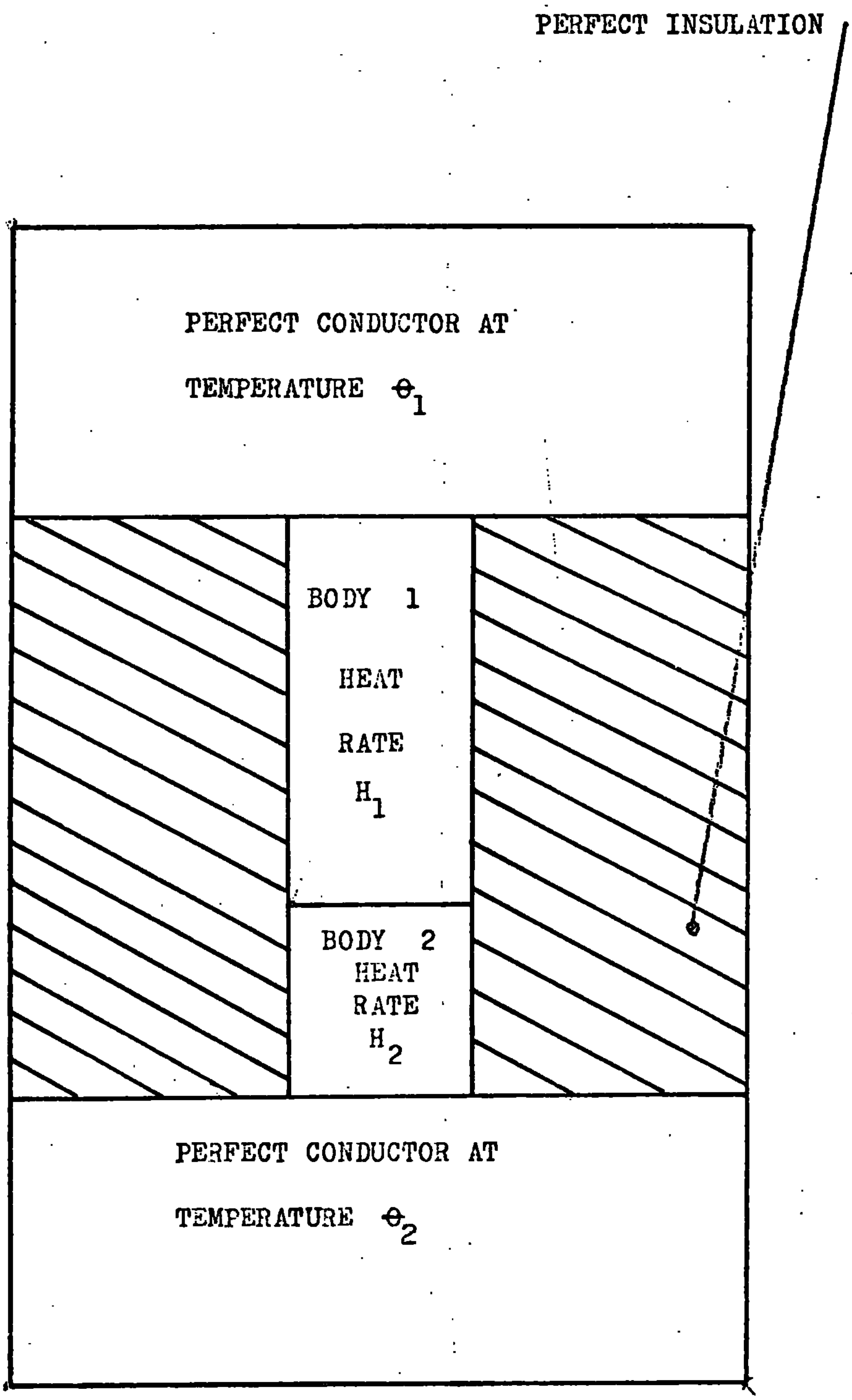
PERFECT INSULATION
PERFECT CONDUCTOR AT
TEMPERATURE θ_1
BODY 1
HEAT
RATE
H_1
BODY 2
HEAT
RATE
H_2
PERFECT CONDUCTOR AT
TEMPERATURE θ_2

FIG. 1.2

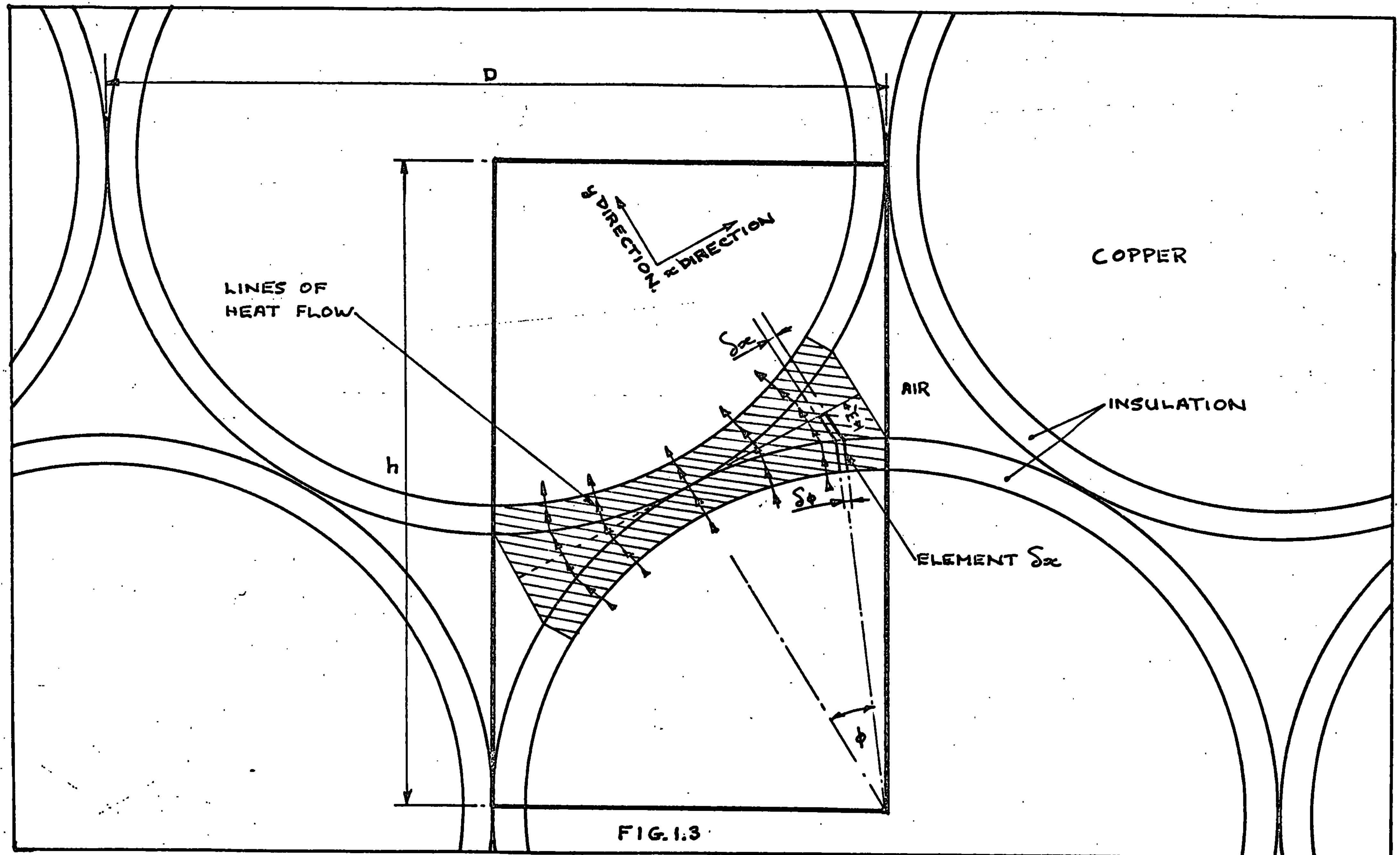
D
h
y DIRECTION
x DIRECTION
COPPER
LINES OF
HEAT FLOW
δx
AIR
INSULATION
δφ
ELEMENT δx
φ
FIG. 1.3

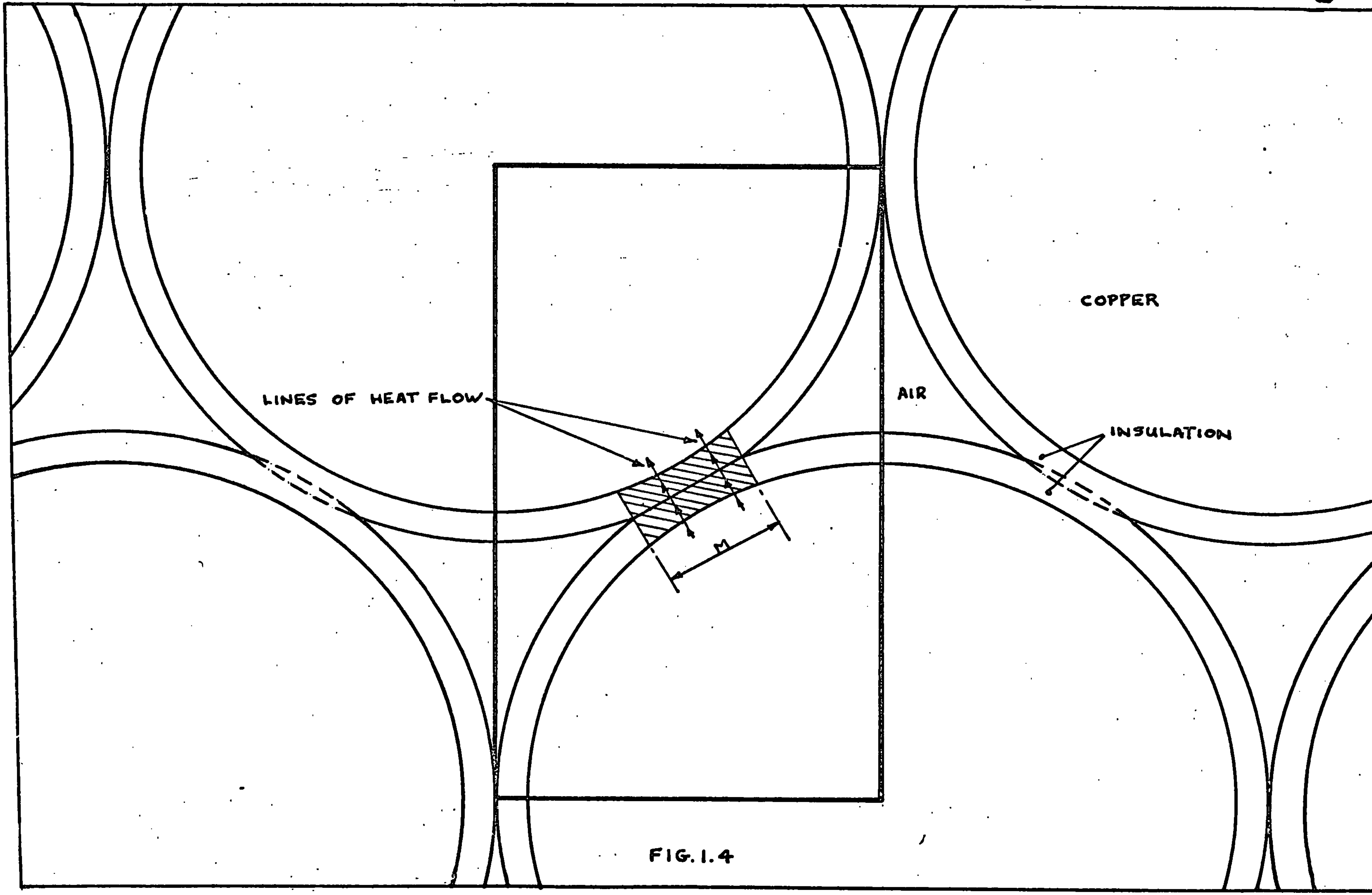

FIG. 1.4

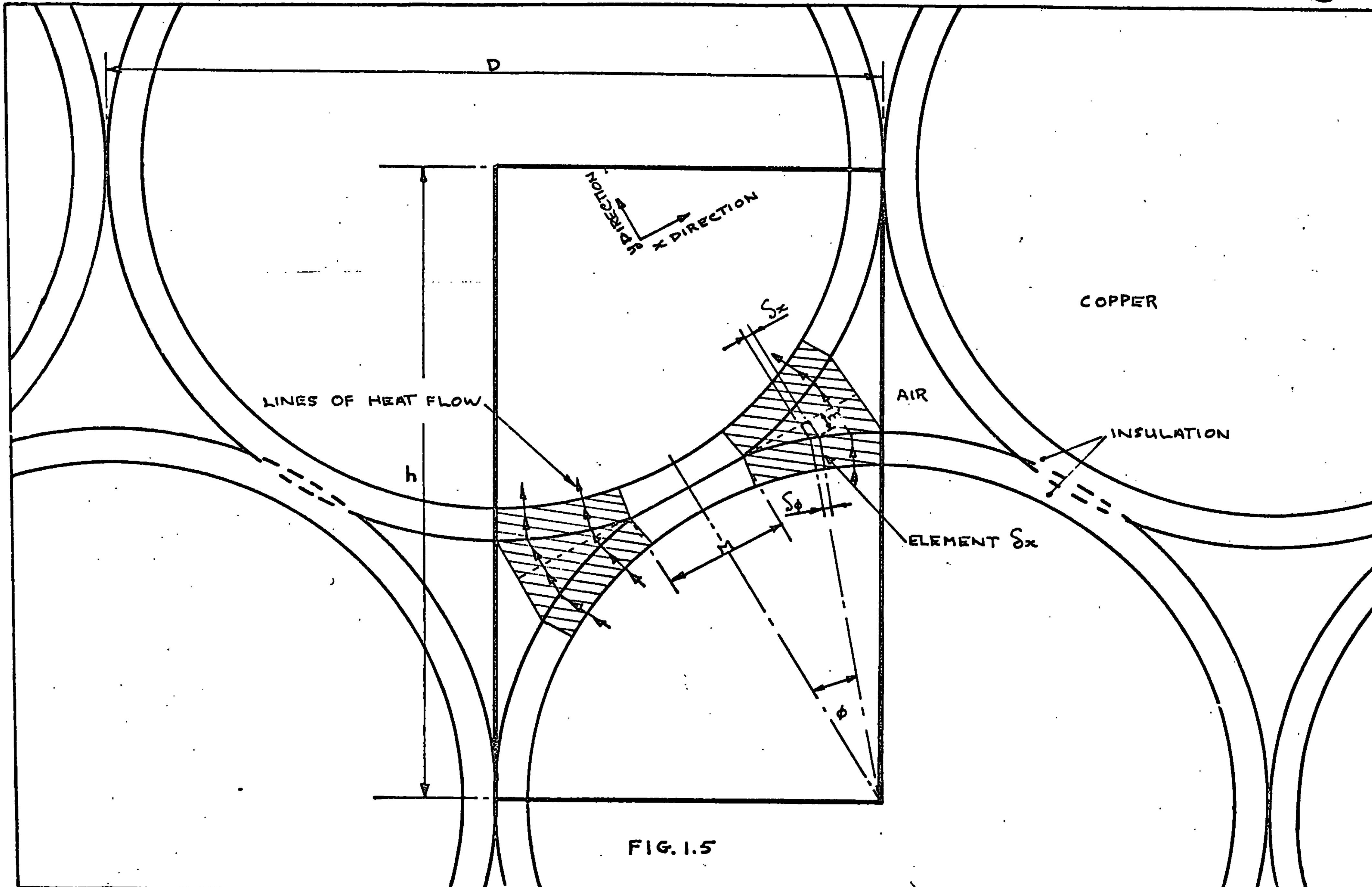
D
h
y DIRECTION
x DIRECTION
COPPER
AIR
INSULATION
LINES OF HEAT FLOW
ELEMENT δx
δx
δφ
φ

FIG. 1.5

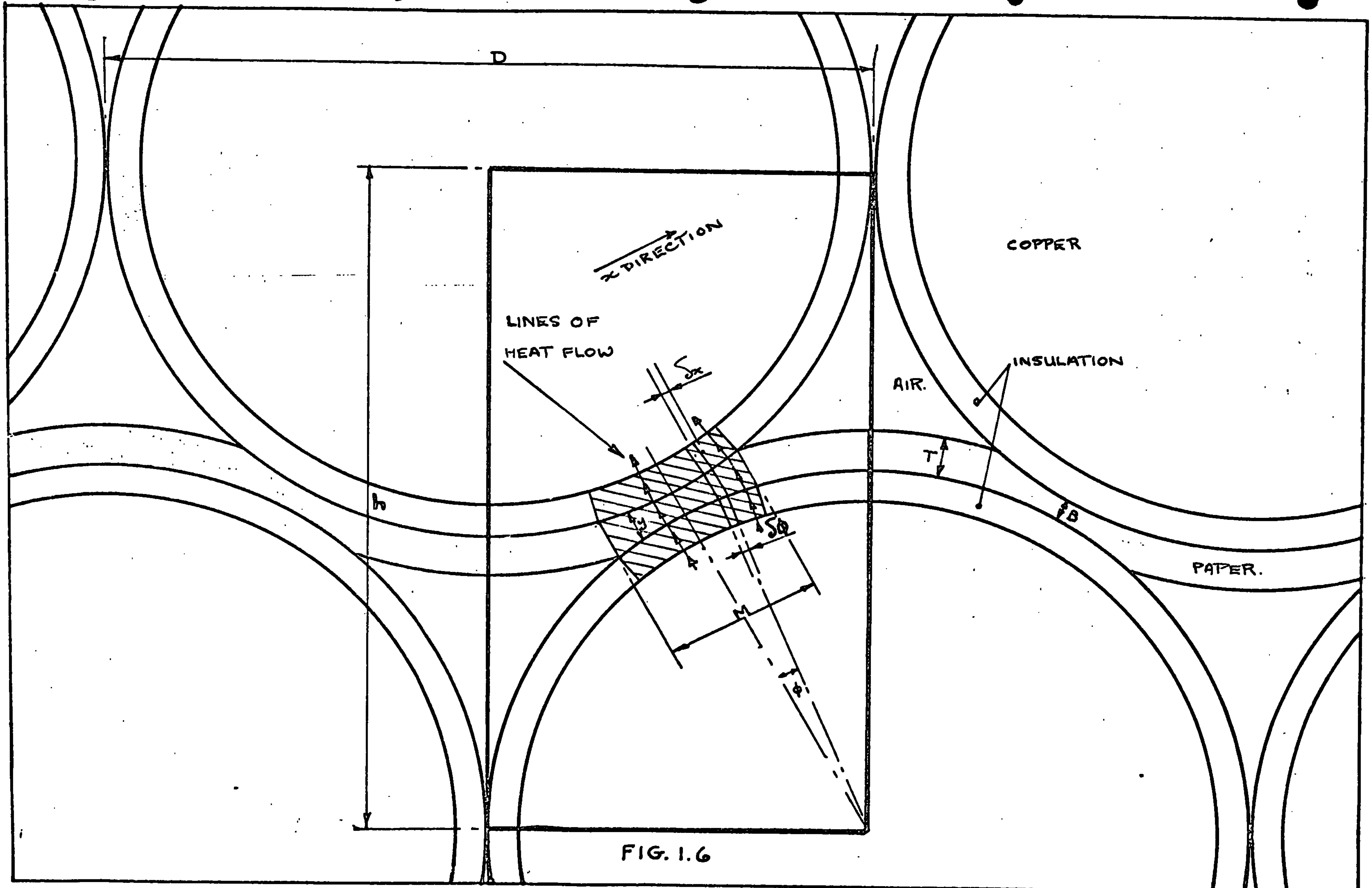
D
h
x DIRECTION
LINES OF
HEAT FLOW
δx
δy
δφ
M
φ
COPPER
INSULATION
AIR.
T
B
PAPER.

FIG. 1.6

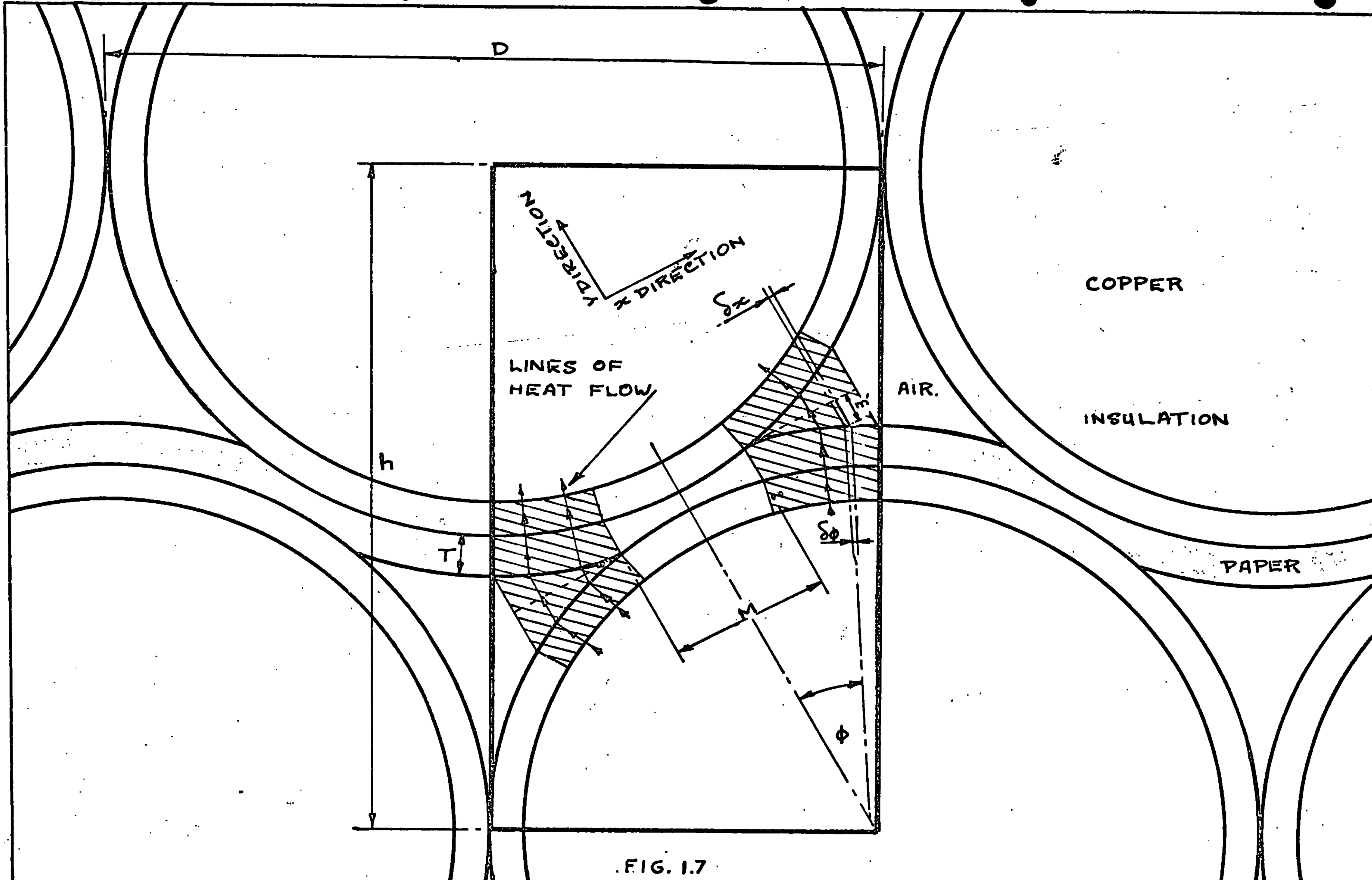

D
h
T
Y DIRECTION
x DIRECTION
δx
LINES OF
HEAT FLOW
E
AIR.
$\delta\phi$
M
ϕ
COPPER
INSULATION
PAPER

FIG. 1.7

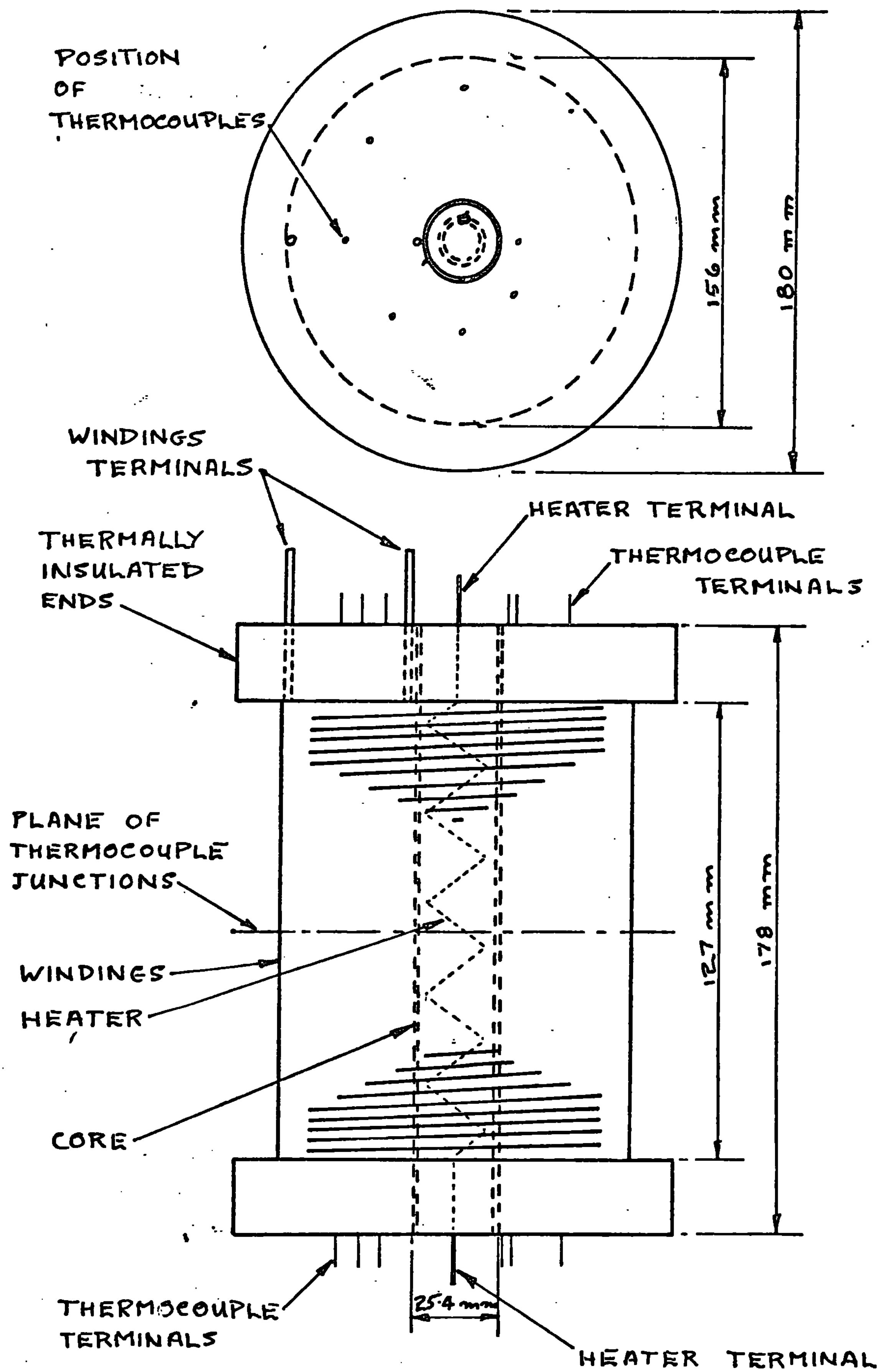

POSITION OF THERMOCOUPLES
156 mm
180 mm
WINDINGS TERMINALS
HEATER TERMINAL
THERMALLY INSULATED ENDS
THERMOCOUPLE TERMINALS
PLANE OF THERMOCOUPLE JUNCTIONS
WINDINGS
HEATER
CORE
127 mm
178 mm
THERMOCOUPLE TERMINALS
25·4 mm
HEATER TERMINAL

FIG. 2.1

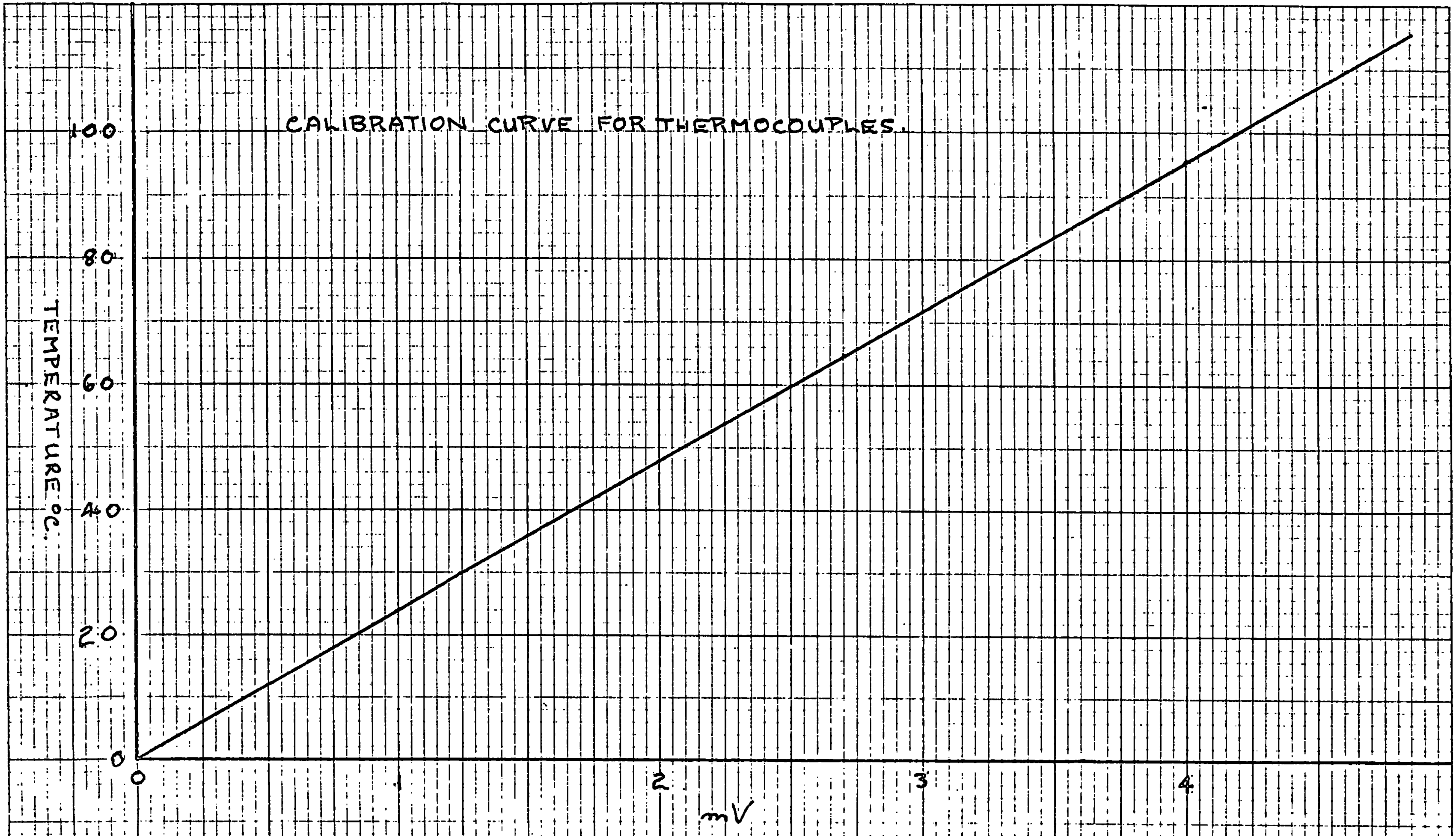
CALIBRATION CURVE FOR THERMOCOUPLES.
TEMPERATURE °C.
100
80
60
40
20
0
0
1
2
3
4
mV

FIG. 2.2

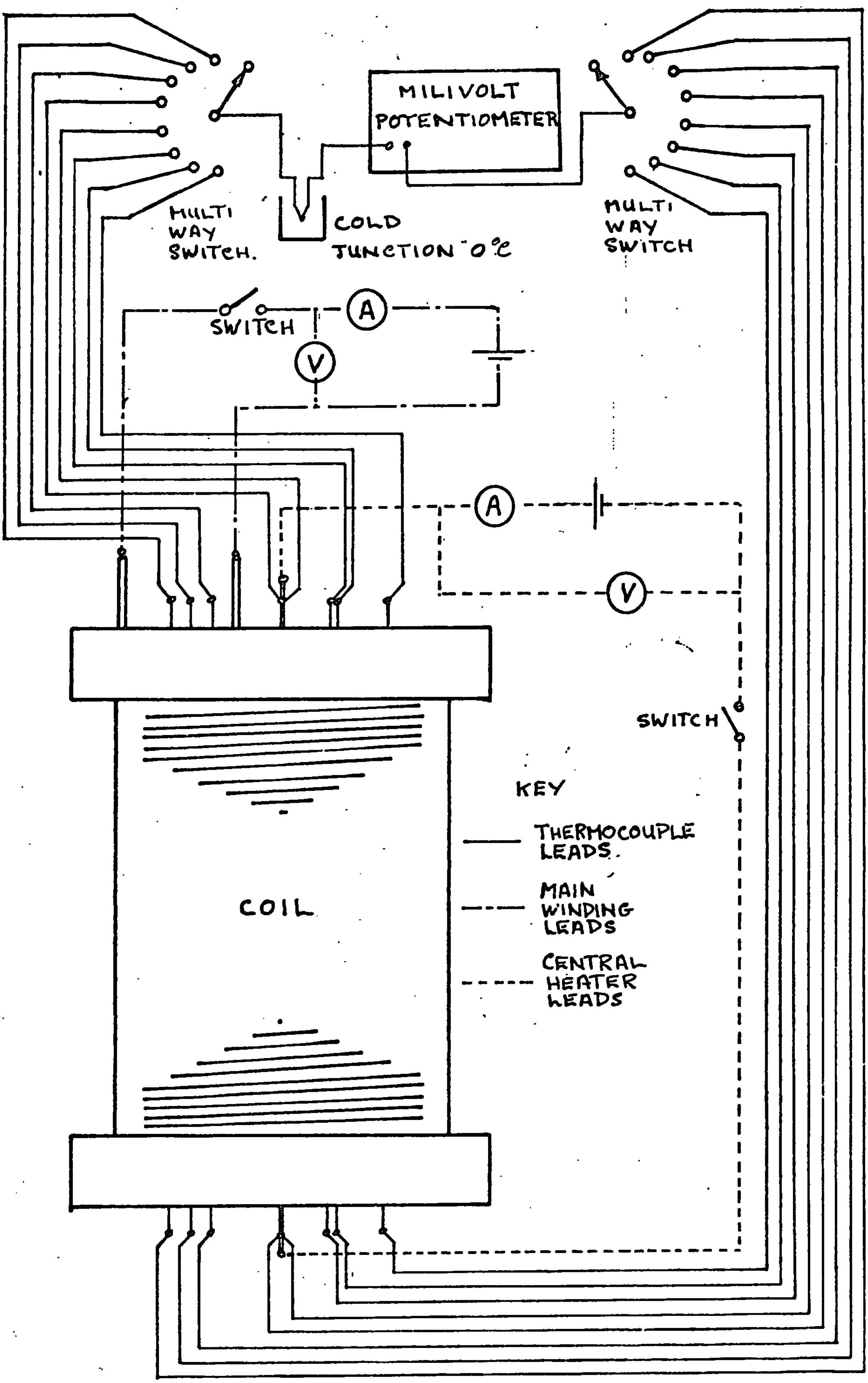

MILIVOLT POTENTIOMETER
MULTI WAY SWITCH.
COLD JUNCTION 0°C
MULTI WAY SWITCH
SWITCH
A
V
A
V
SWITCH
KEY
THERMOCOUPLE LEADS.
MAIN WINDING LEADS
CENTRAL HEATER LEADS
COIL

FIG. 2.3

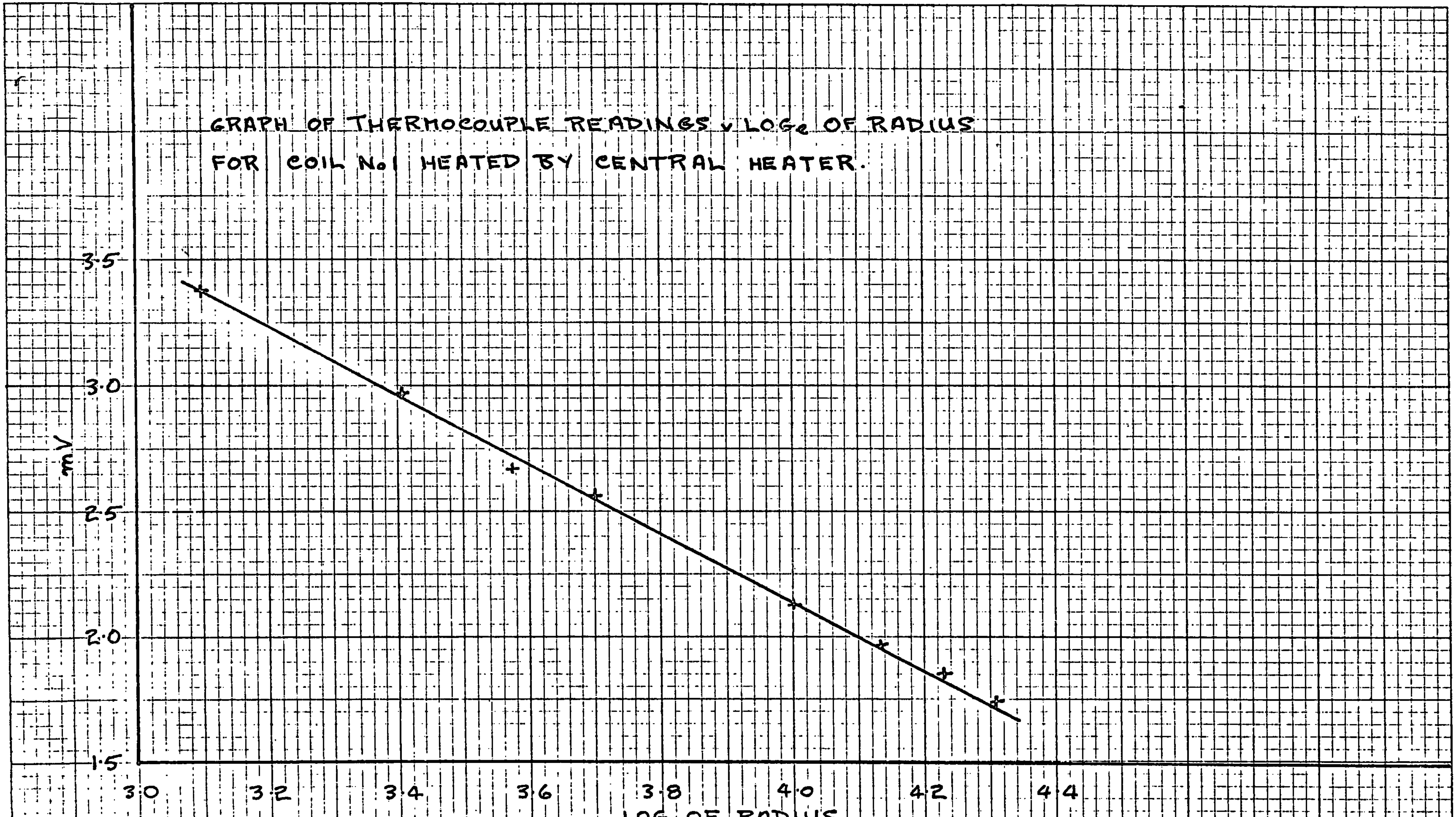

GRAPH OF THERMOCOUPLE READINGS v LOGe OF RADIUS
FOR COIL No 1 HEATED BY CENTRAL HEATER.
3·5
3·0
2·5
2·0
1·5
mV
3·0
3·2
3·4
3·6
3·8
4·0
4·2
4·4
LOG OF RADIUS.

FIG. 2.4

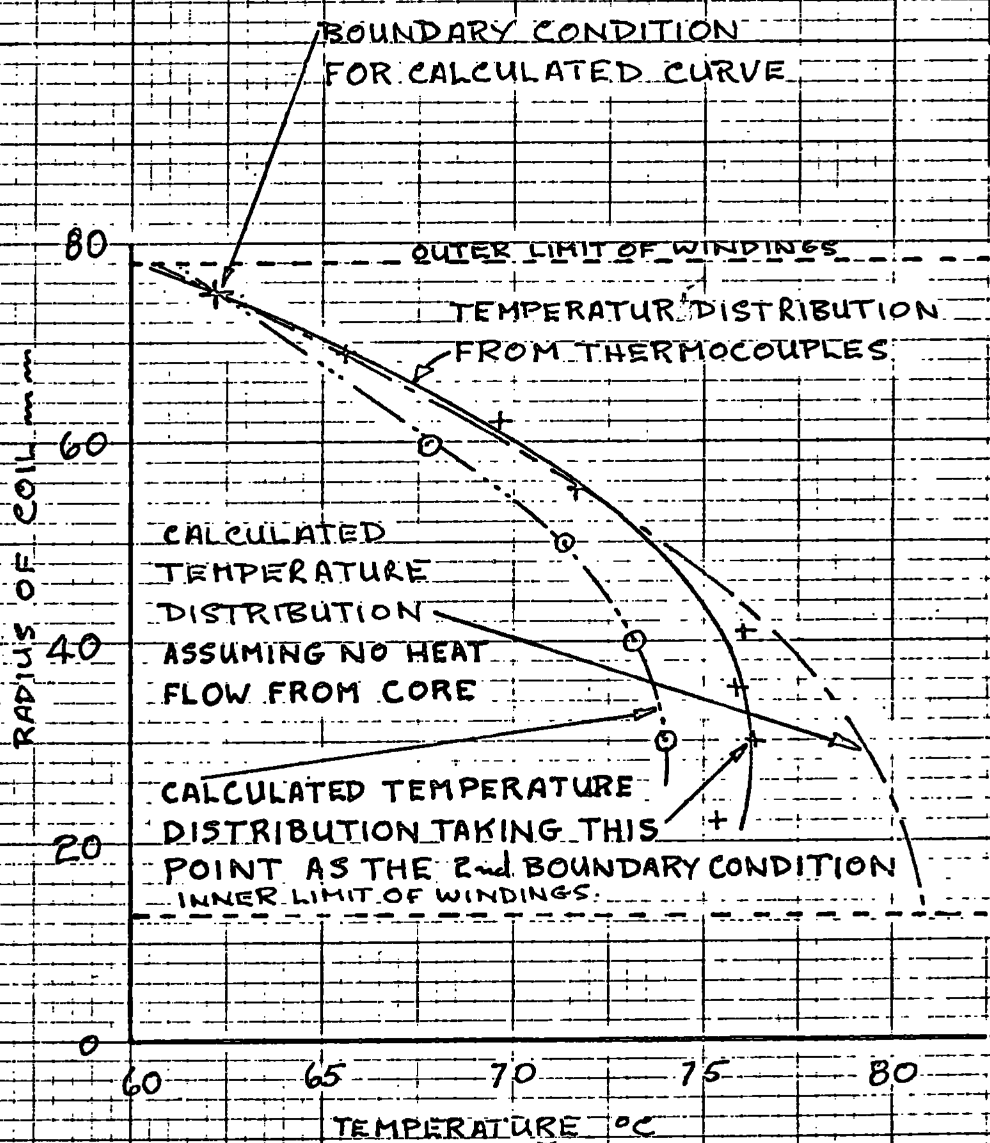

BOUNDARY CONDITION FOR CALCULATED CURVE
OUTER LIMIT OF WINDINGS
TEMPERATUR DISTRIBUTION FROM THERMOCOUPLES
CALCULATED TEMPERATURE DISTRIBUTION ASSUMING NO HEAT FLOW FROM CORE
CALCULATED TEMPERATURE DISTRIBUTION TAKING THIS POINT AS THE 2nd BOUNDARY CONDITION
INNER LIMIT OF WINDINGS
RADIUS OF COIL mm
80
60
40
20
0
60
65
70
75
80
TEMPERATURE °C

FIG. 2.5

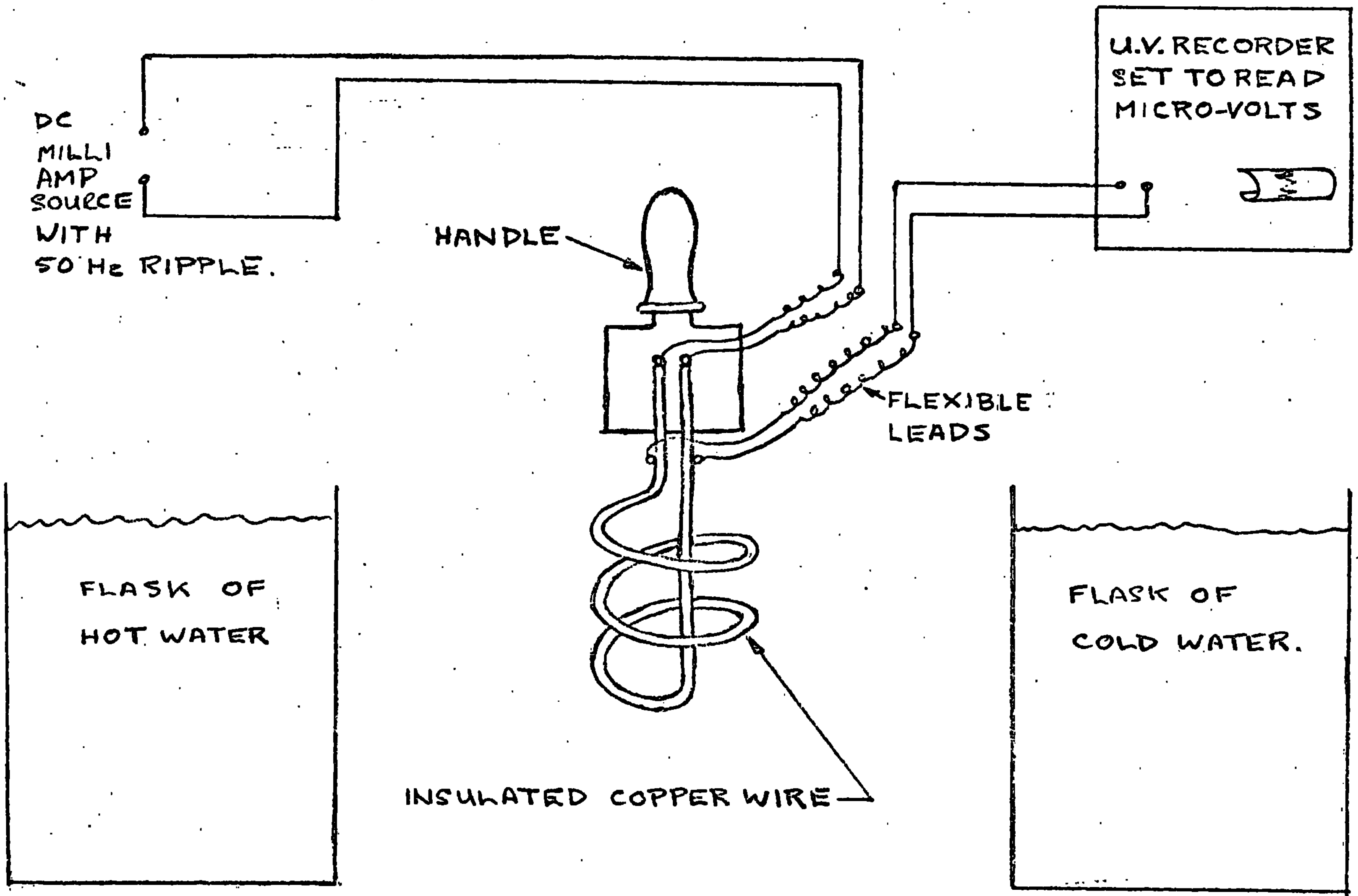
DC
MILLI
AMP
SOURCE
WITH
50 Hz RIPPLE.
HANDLE
U.V. RECORDER
SET TO READ
MICRO-VOLTS
FLEXIBLE
LEADS
FLASK OF
HOT WATER
INSULATED COPPER WIRE
FLASK OF
COLD WATER.

FIG. 2.6

TRACING OF THE U.V. RECORDING FOR No 1 COIL WIRE

NOTE: THE REPEAT TEST WAS IDENTICAL

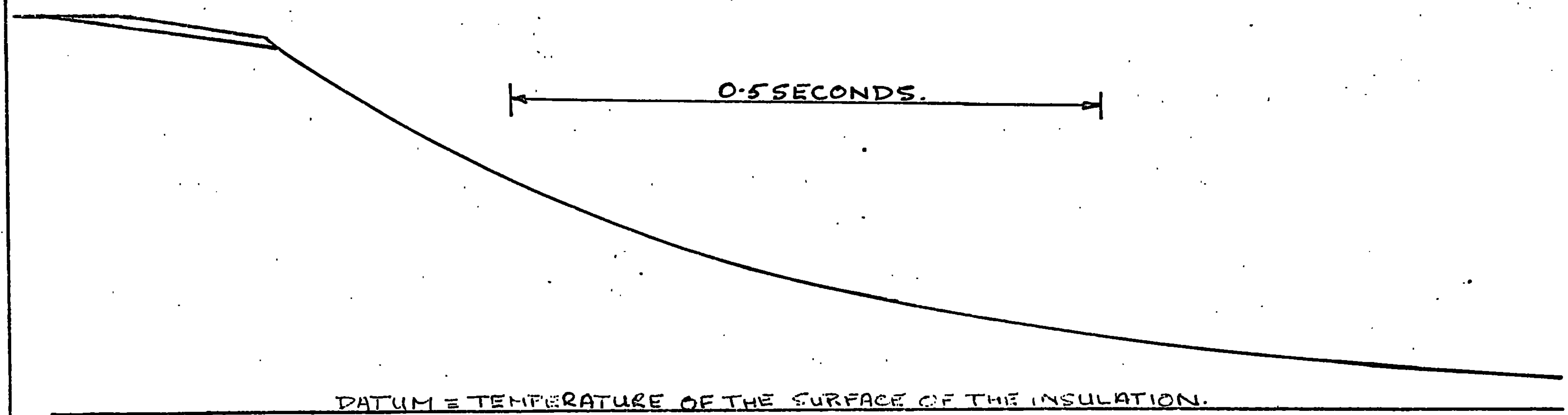

FIG. 2.7

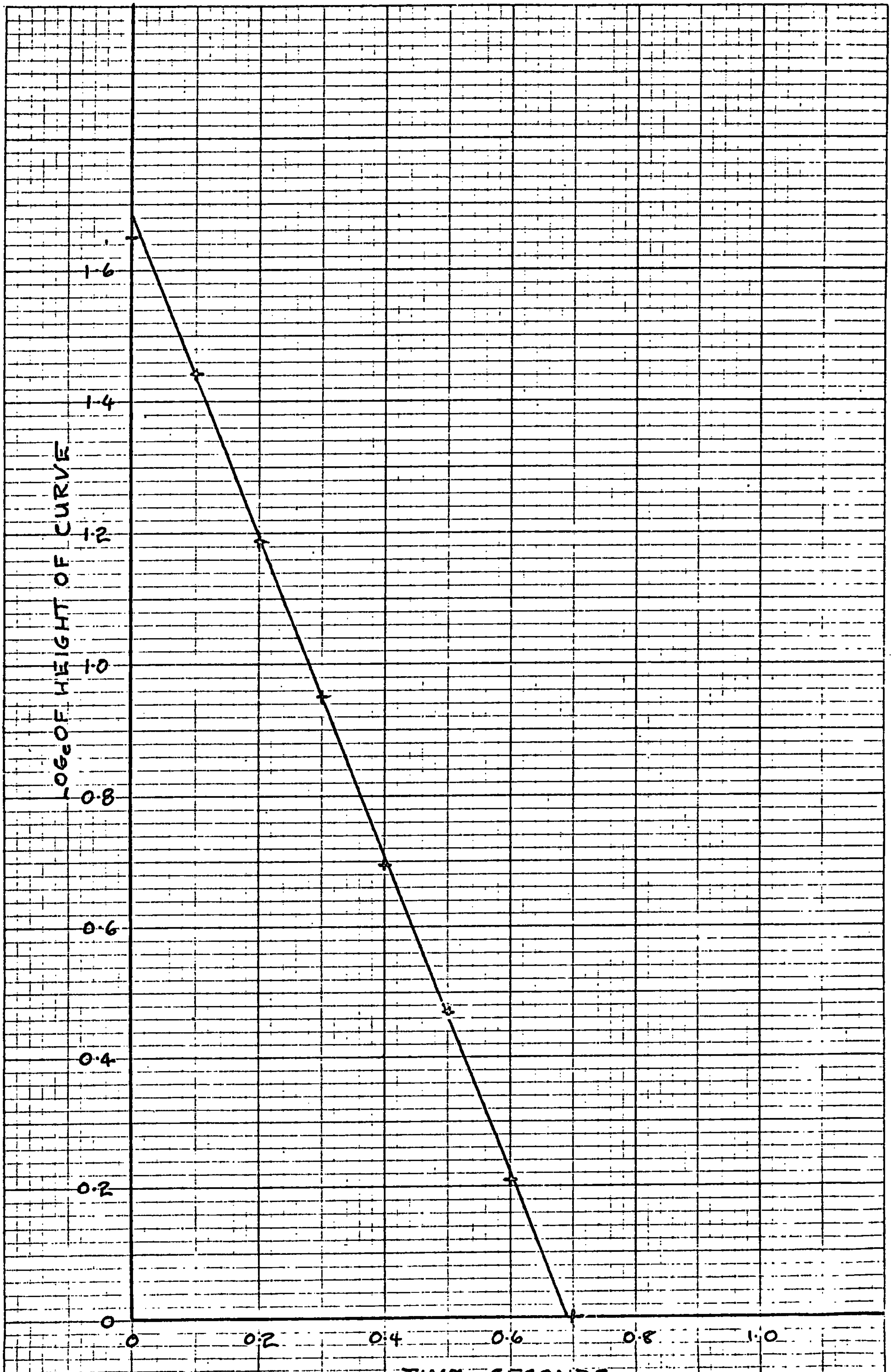
LOGe OF HEIGHT OF CURVE
1·6
1·4
1·2
1·0
0·8
0·6
0·4
0·2
0
0
0·2
0·4
0·6
0·8
1·0
TIME SECONDS
FIG. 2.8

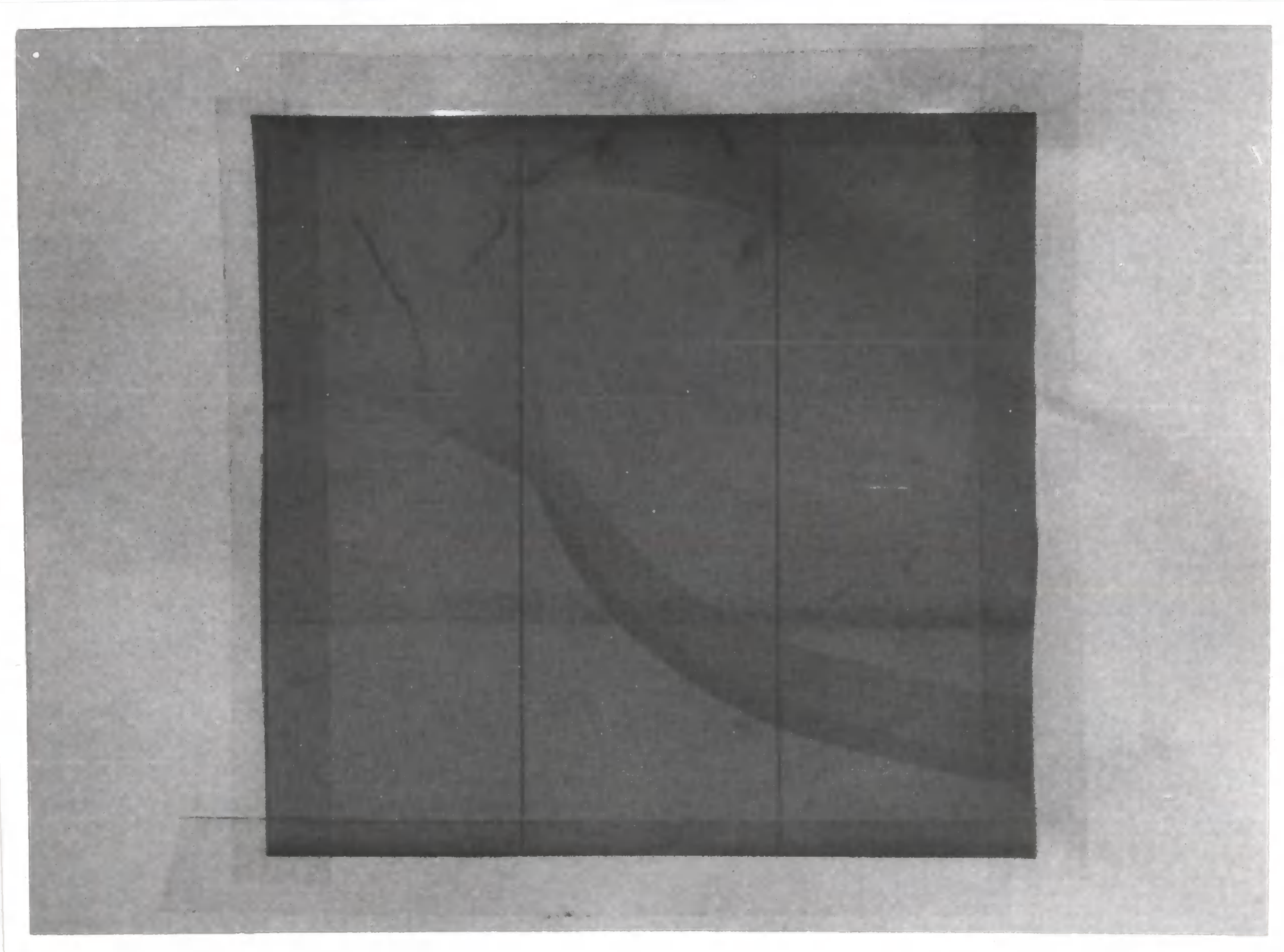

FIG. 2.9

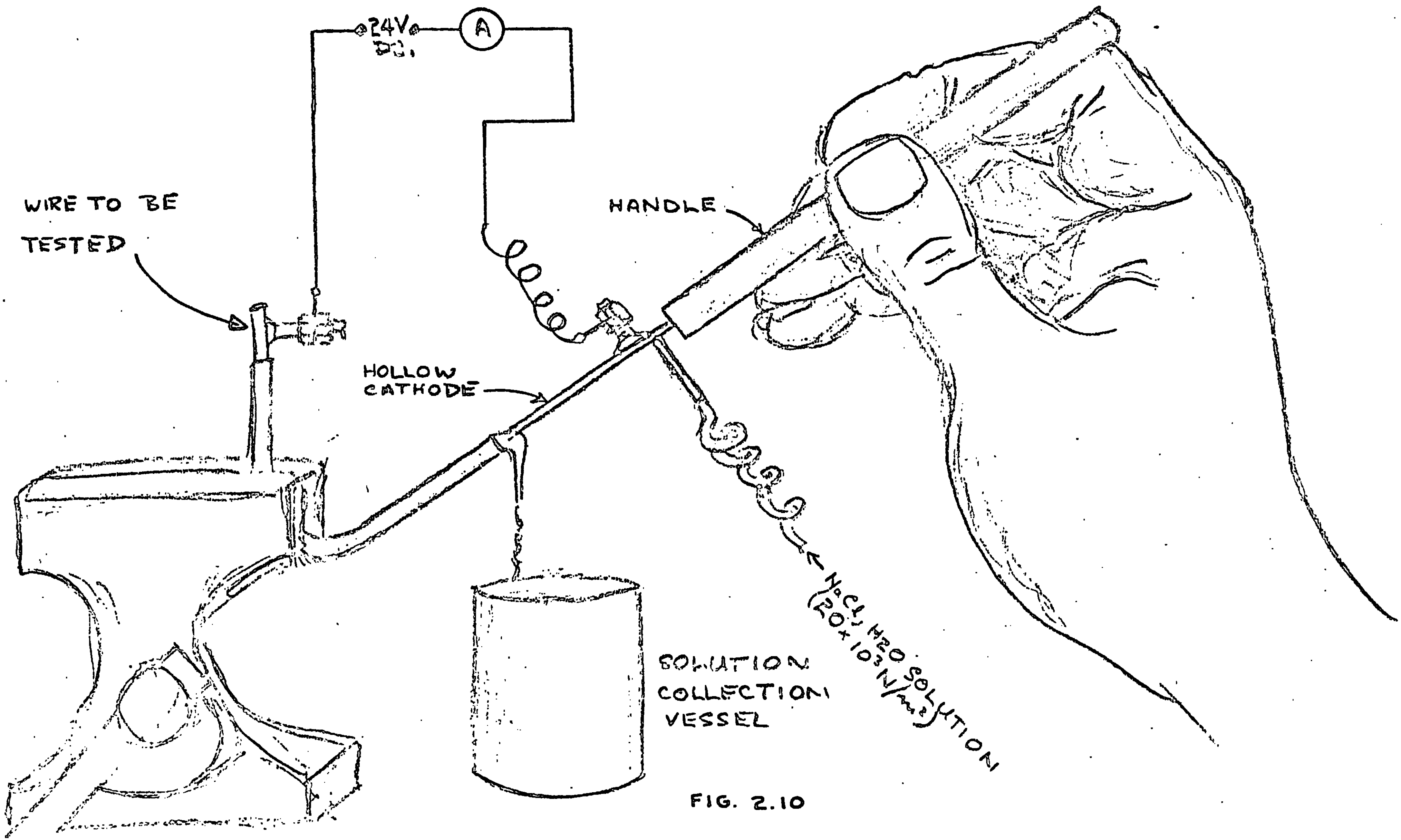
24V D.C.
A
WIRE TO BE TESTED
HANDLE
HOLLOW CATHODE
NaCl, H2O SOLUTION (20×10³ N/m²)
SOLUTION COLLECTION VESSEL

FIG. 2.10

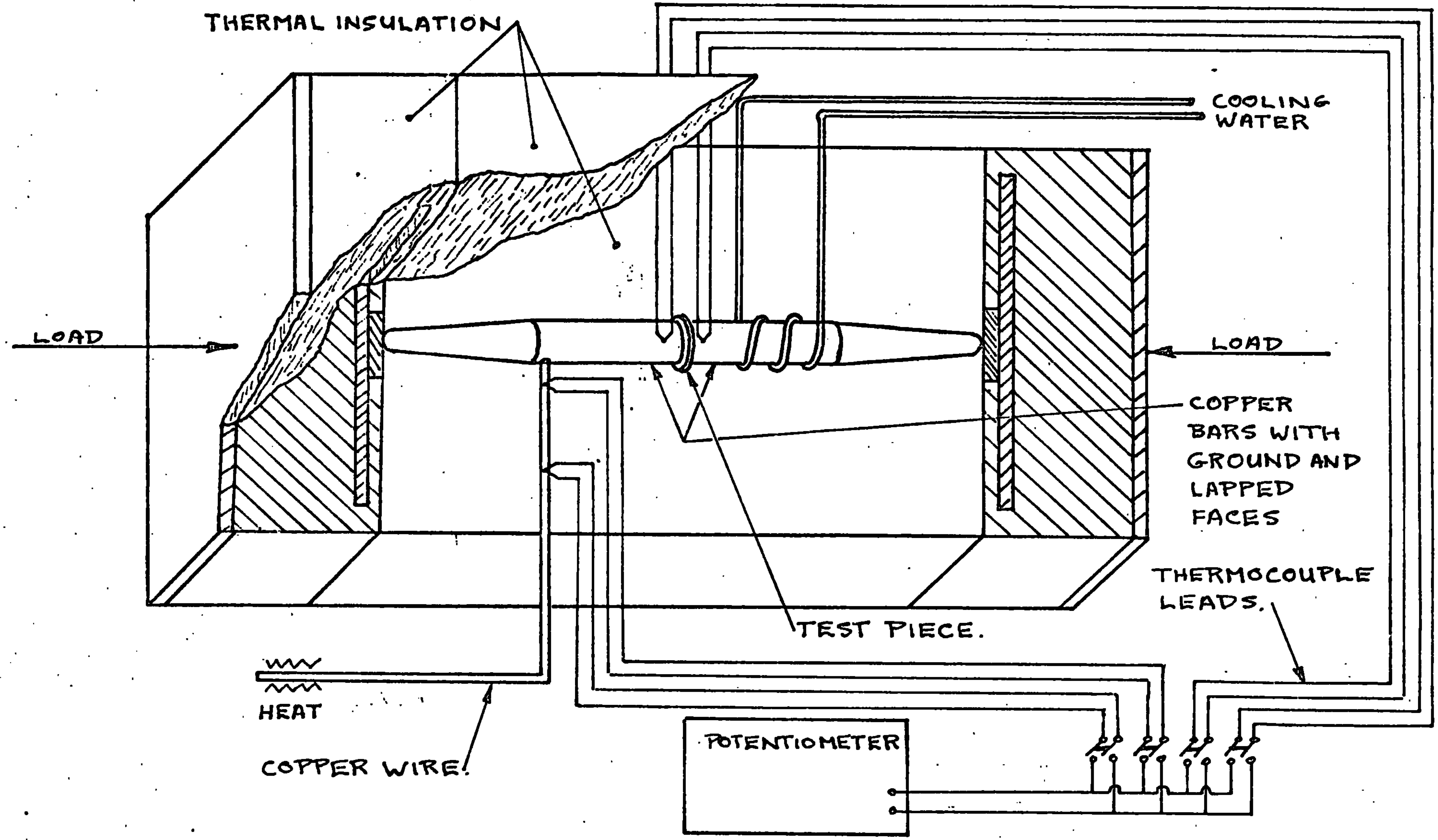
THERMAL INSULATION
COOLING WATER
LOAD
LOAD
COPPER BARS WITH GROUND AND LAPPED FACES
THERMOCOUPLE LEADS.
TEST PIECE.
HEAT
COPPER WIRE.
POTENTIOMETER

FIG. 2.11

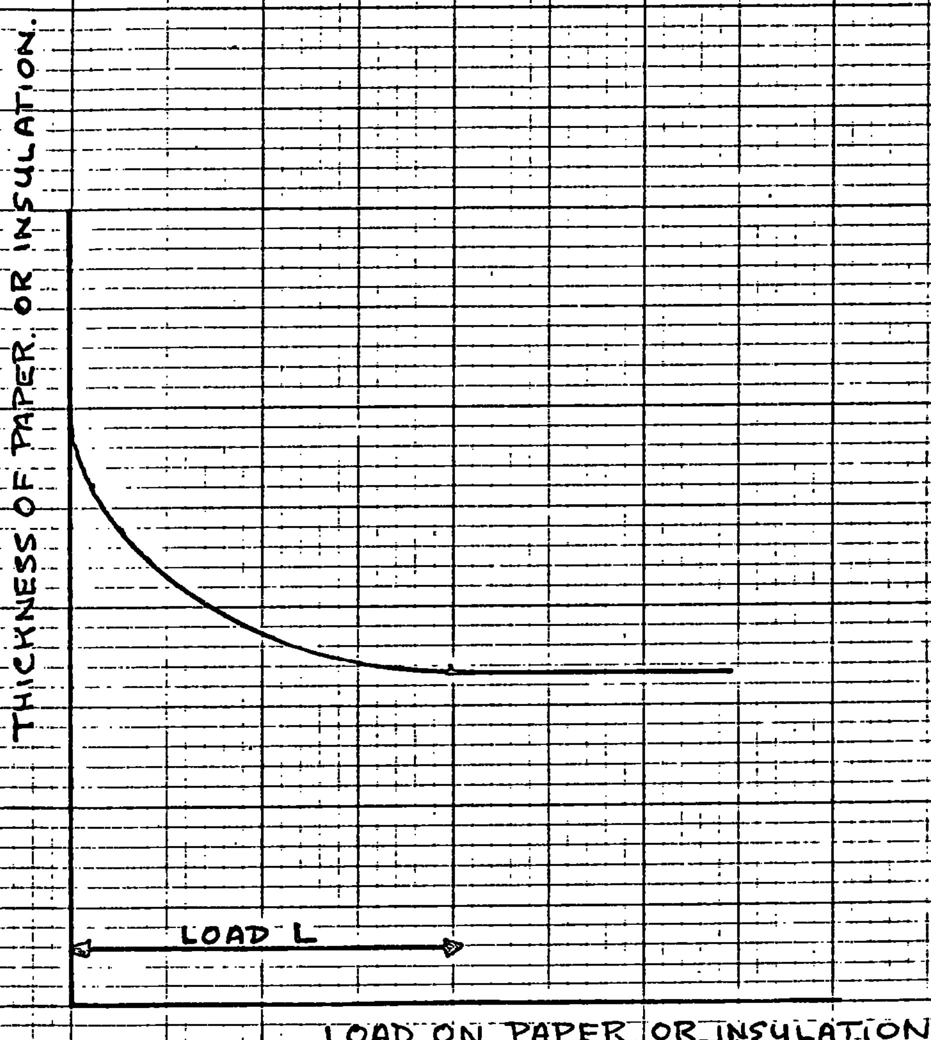
THICKNESS OF PAPER OR INSULATION.
LOAD L
LOAD ON PAPER OR INSULATION

FIG 2.12

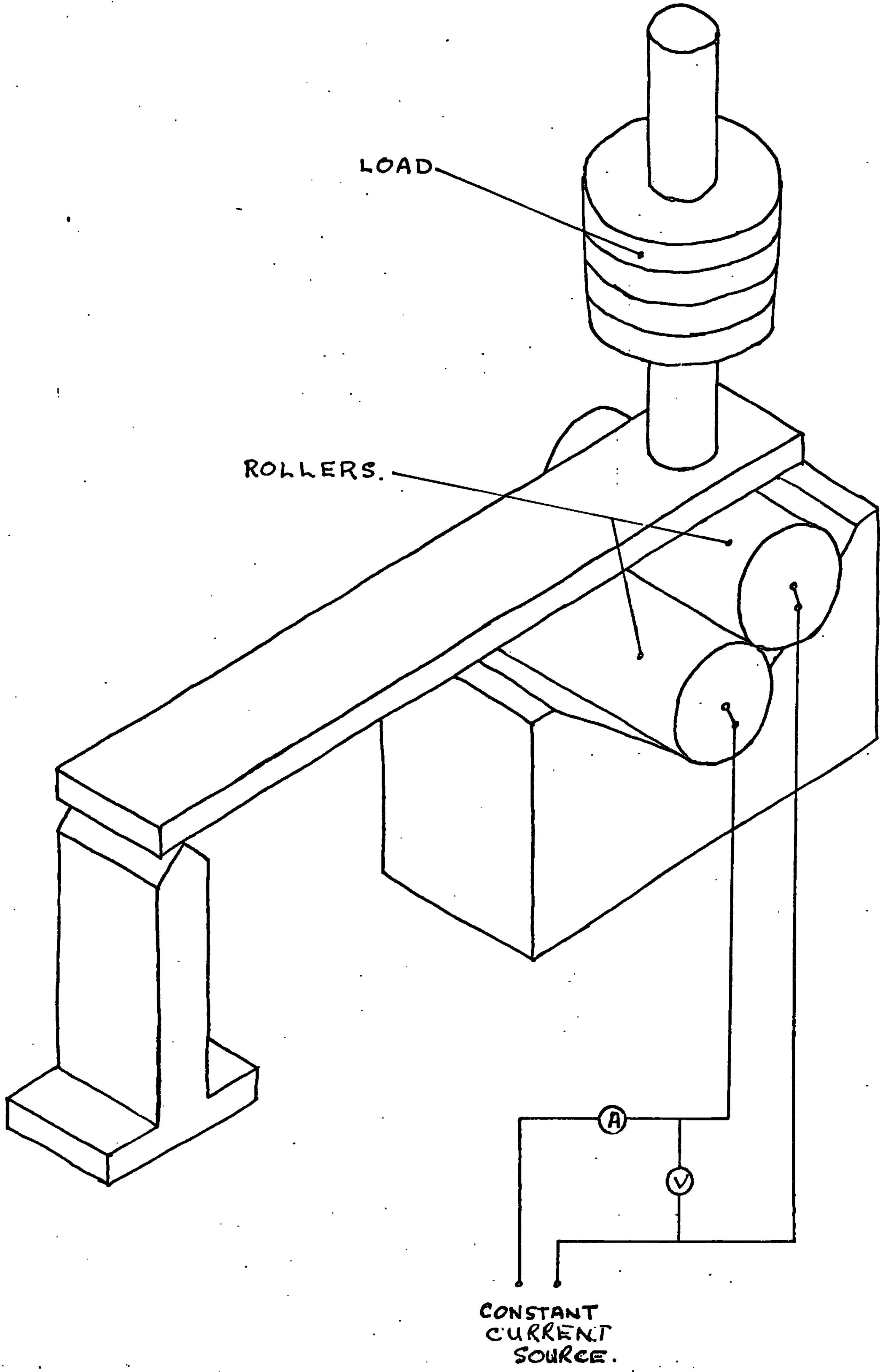

FIG. 2.13

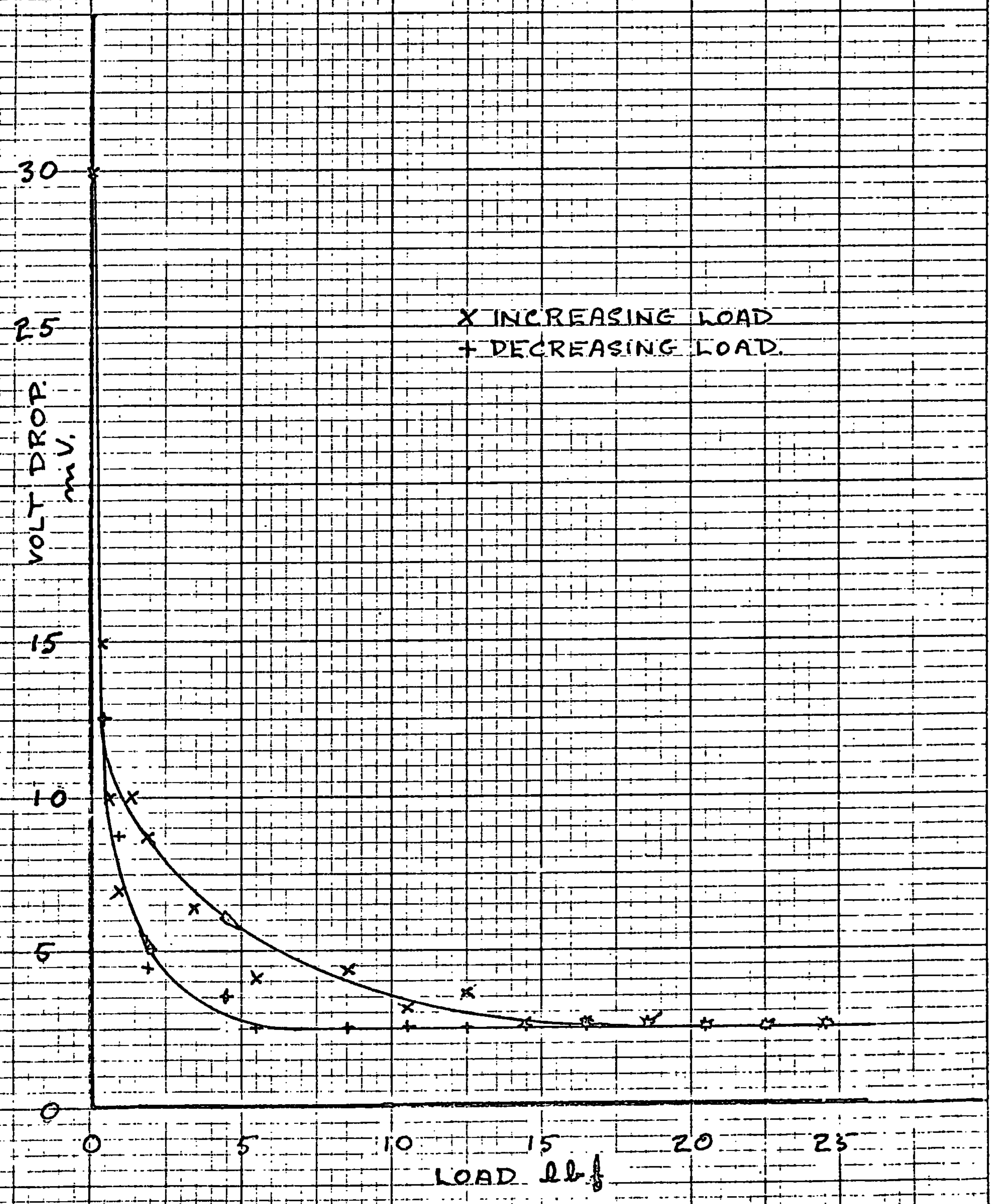

X INCREASING LOAD
+ DECREASING LOAD.
VOLT DROP.
mV.
30
25
15
10
5
0
0
5
10
15
20
25
LOAD lbf

FIG. 2.14

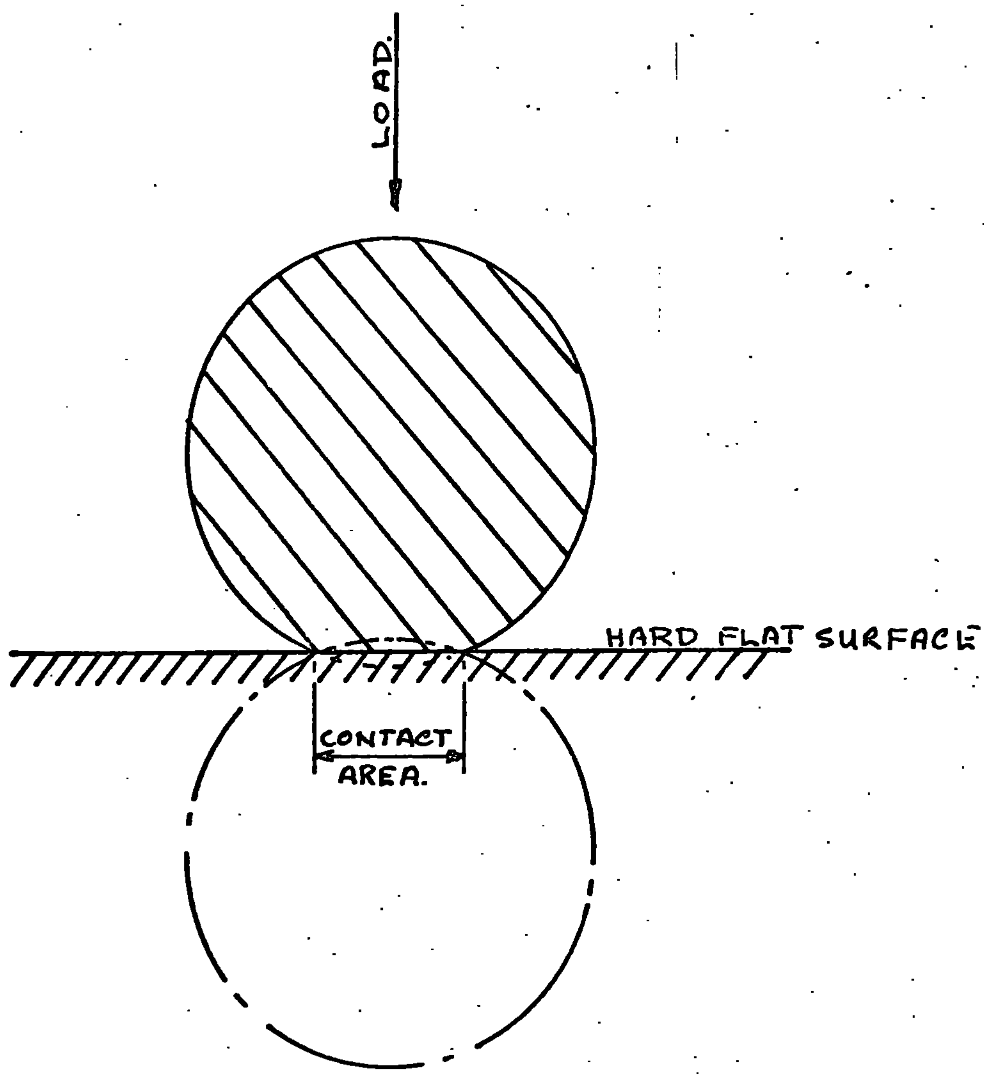

The sketch illustrates how the contact area would be the same for one wire pressed against another or against a hard flat surface of high Youngs modulus

FIG. 2.15

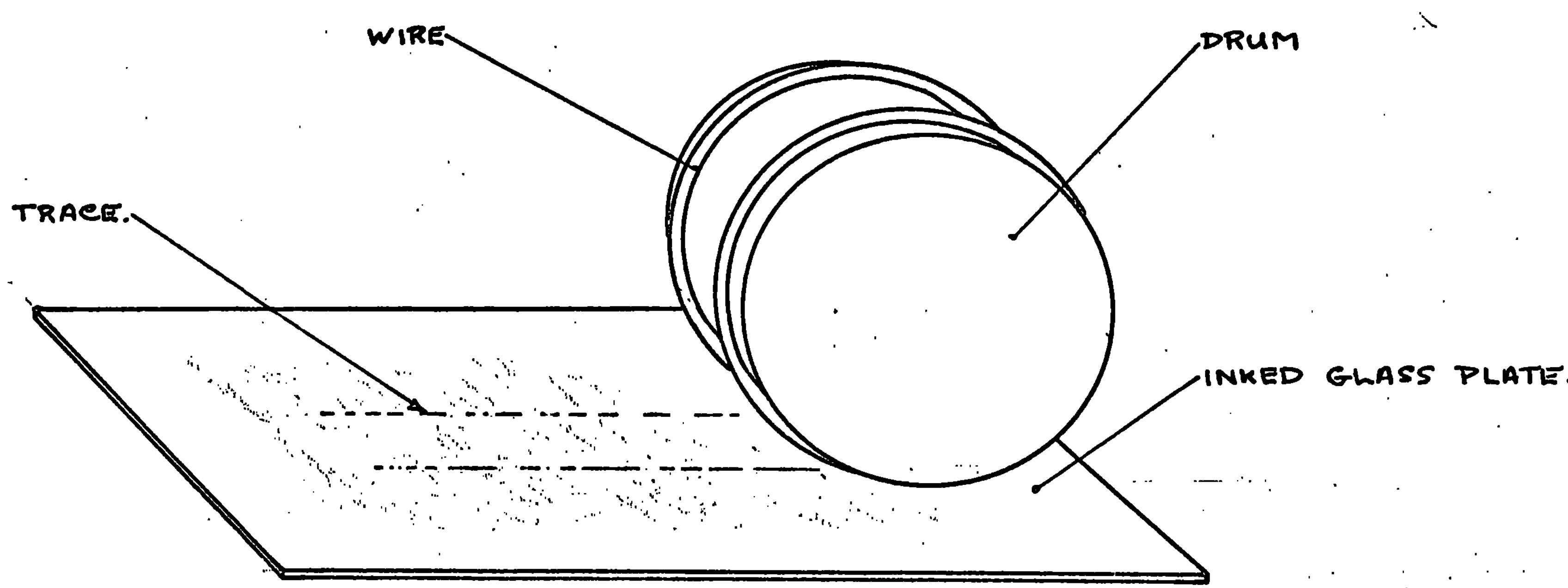

FIG. 2.16

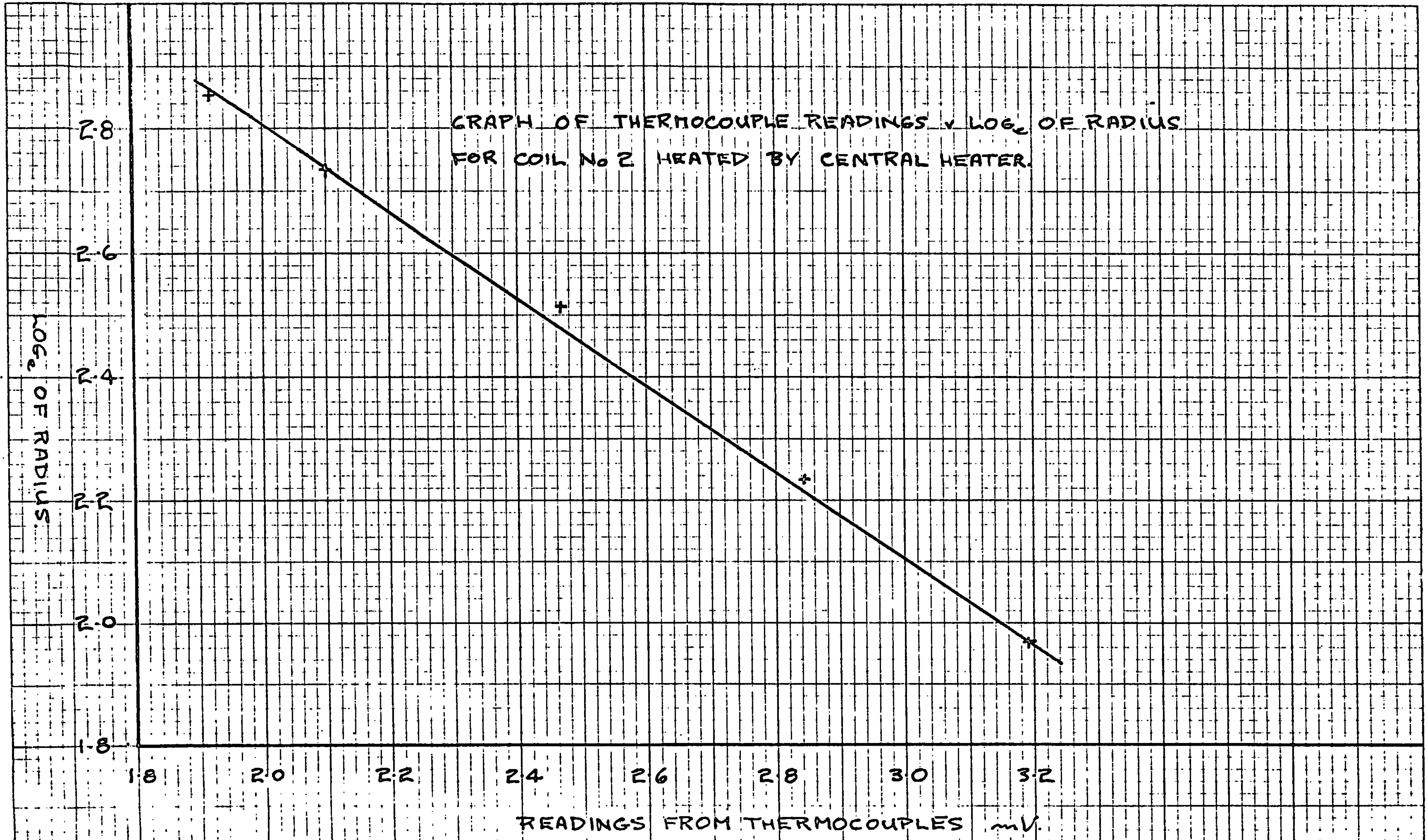

GRAPH OF THERMOCOUPLE READINGS v LOG$_e$ OF RADIUS
FOR COIL No 2 HEATED BY CENTRAL HEATER.
2·8
2·6
2·4
2·2
2·0
1·8
LOG$_e$ OF RADIUS.
1·8
2·0
2·2
2·4
2·6
2·8
3·0
3·2
READINGS FROM THERMOCOUPLES mV.

FIG. 3.1

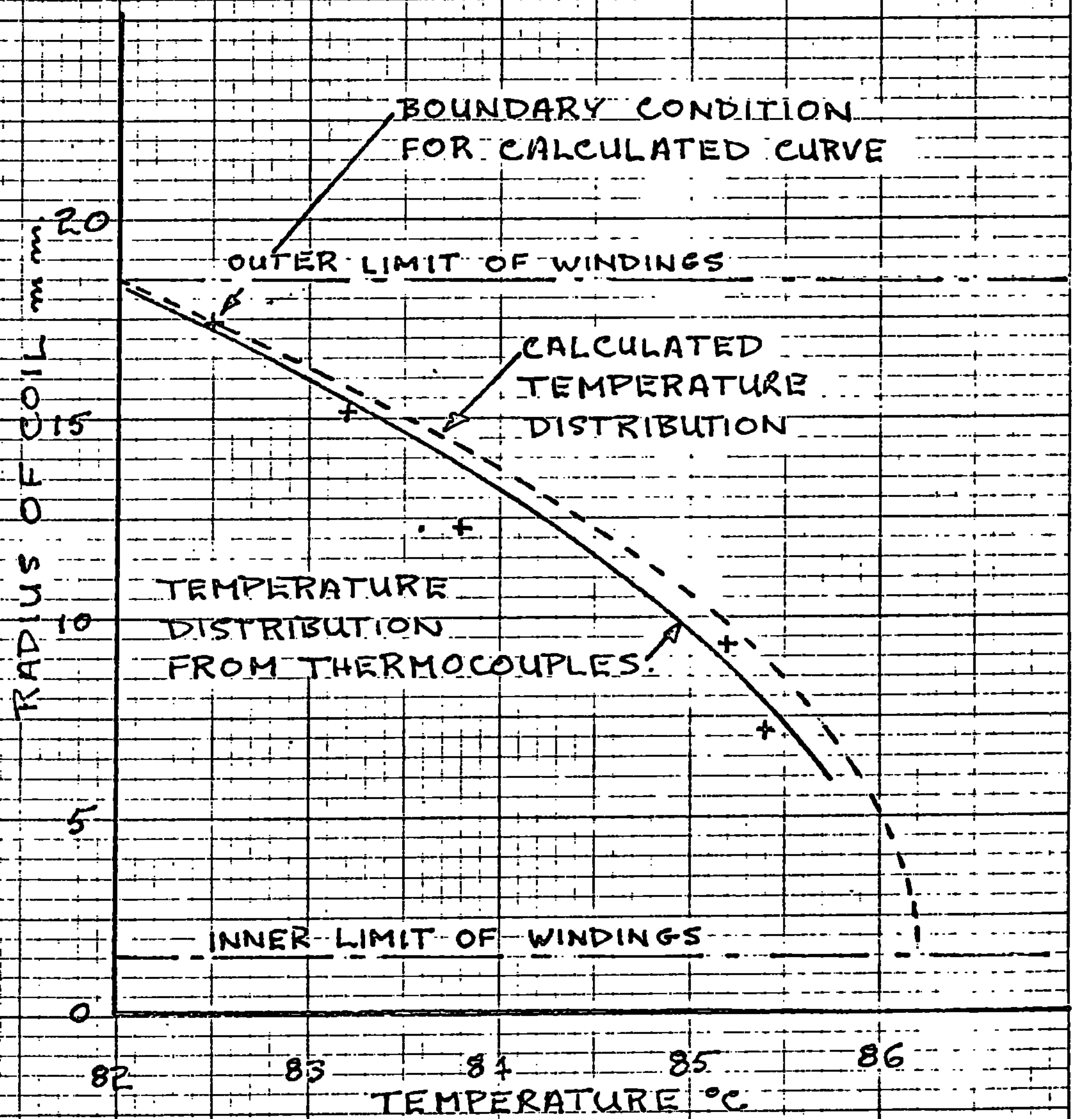
BOUNDARY CONDITION FOR CALCULATED CURVE
OUTER LIMIT OF WINDINGS
CALCULATED TEMPERATURE DISTRIBUTION
TEMPERATURE DISTRIBUTION FROM THERMOCOUPLES
INNER LIMIT OF WINDINGS
RADIUS OF COIL mm
20
15
10
5
0
82
83
84
85
86
TEMPERATURE °C

FIG.3.2

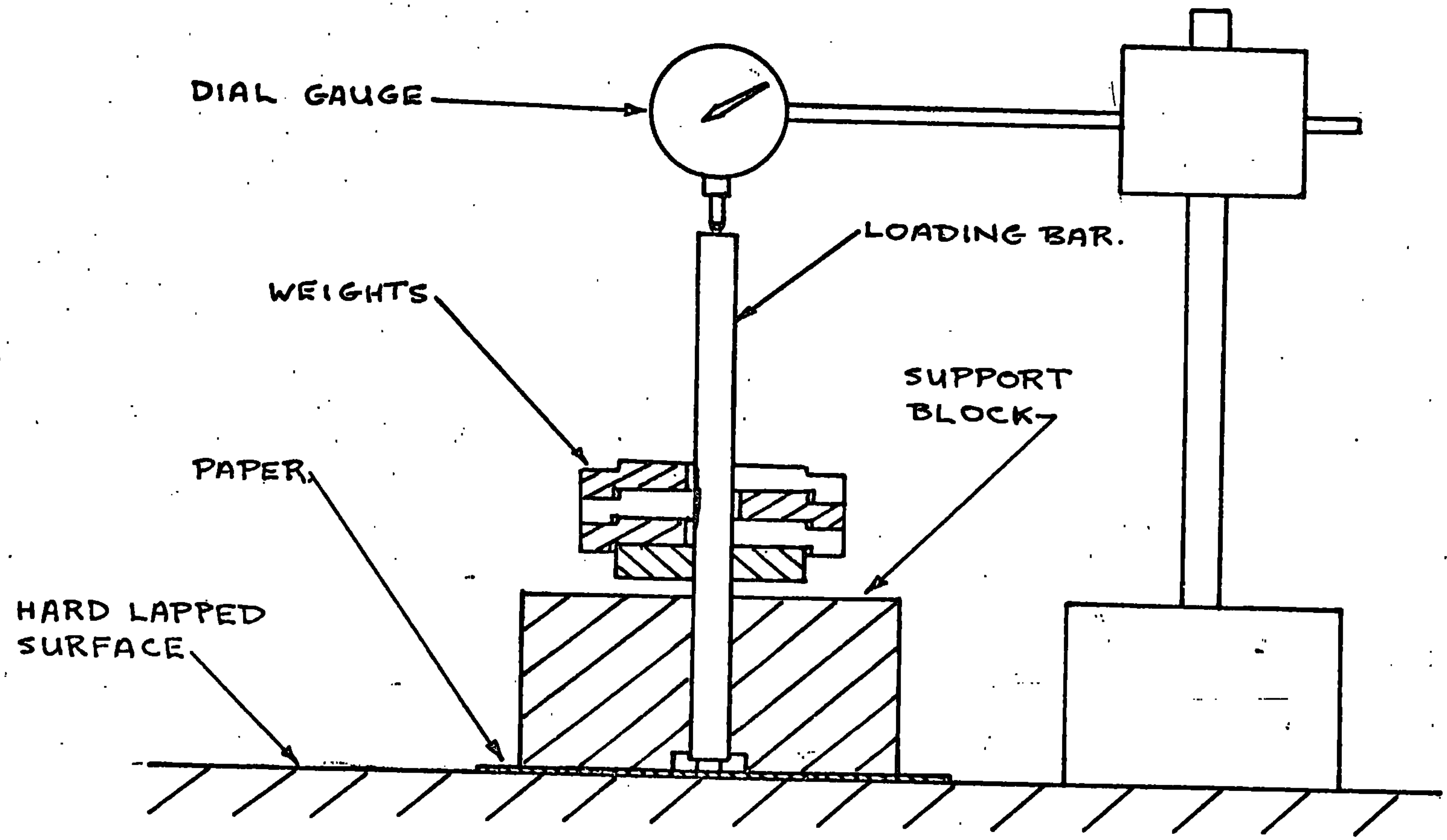
DIAL GAUGE
LOADING BAR.
WEIGHTS
SUPPORT
BLOCK
PAPER
HARD LAPPED
SURFACE

FIG. 3.3

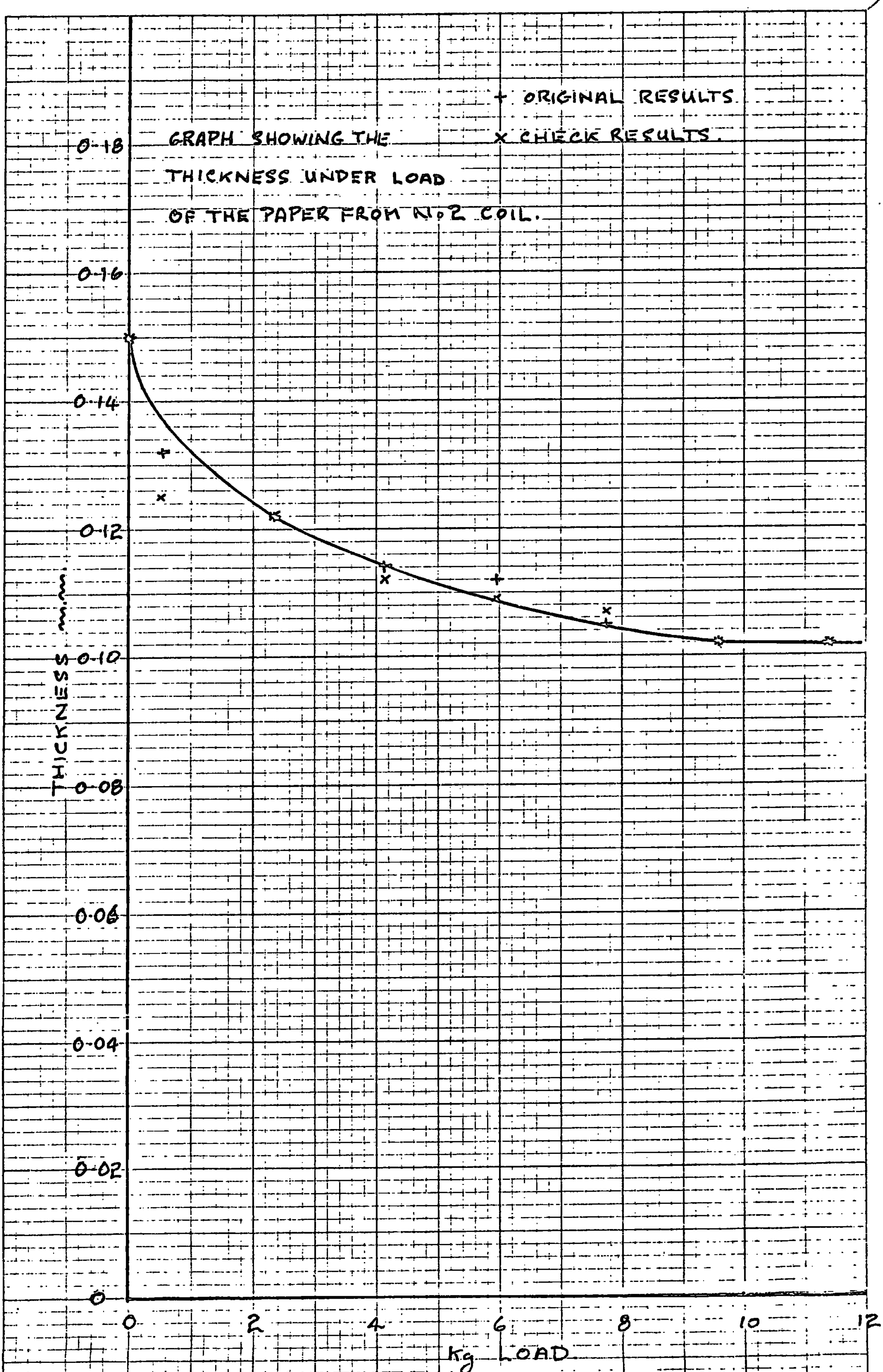
+ ORIGINAL RESULTS
× CHECK RESULTS.
GRAPH SHOWING THE
THICKNESS UNDER LOAD
OF THE PAPER FROM No 2 COIL.
0·18
0·16
0·14
0·12
0·10
0·08
0·06
0·04
0·02
0
THICKNESS m.m
0
2
4
6
8
10
12
Kg LOAD

FIG. 3. 4

TRACING OF THE UV RECORDING FOR No2 COIL WIRE.

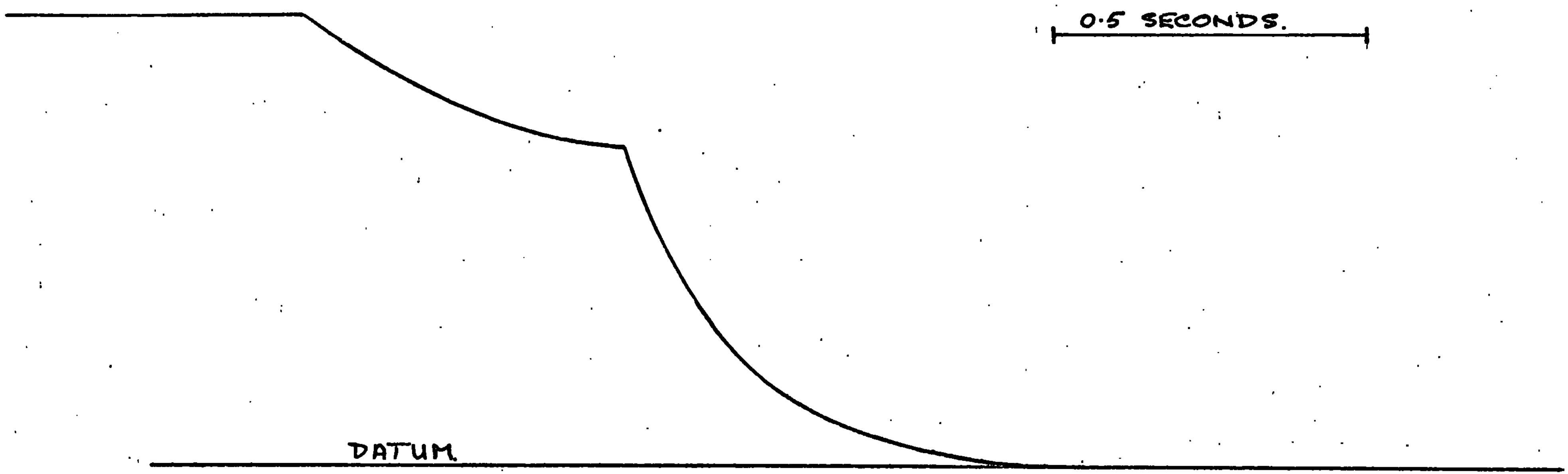

FIG. 3.5

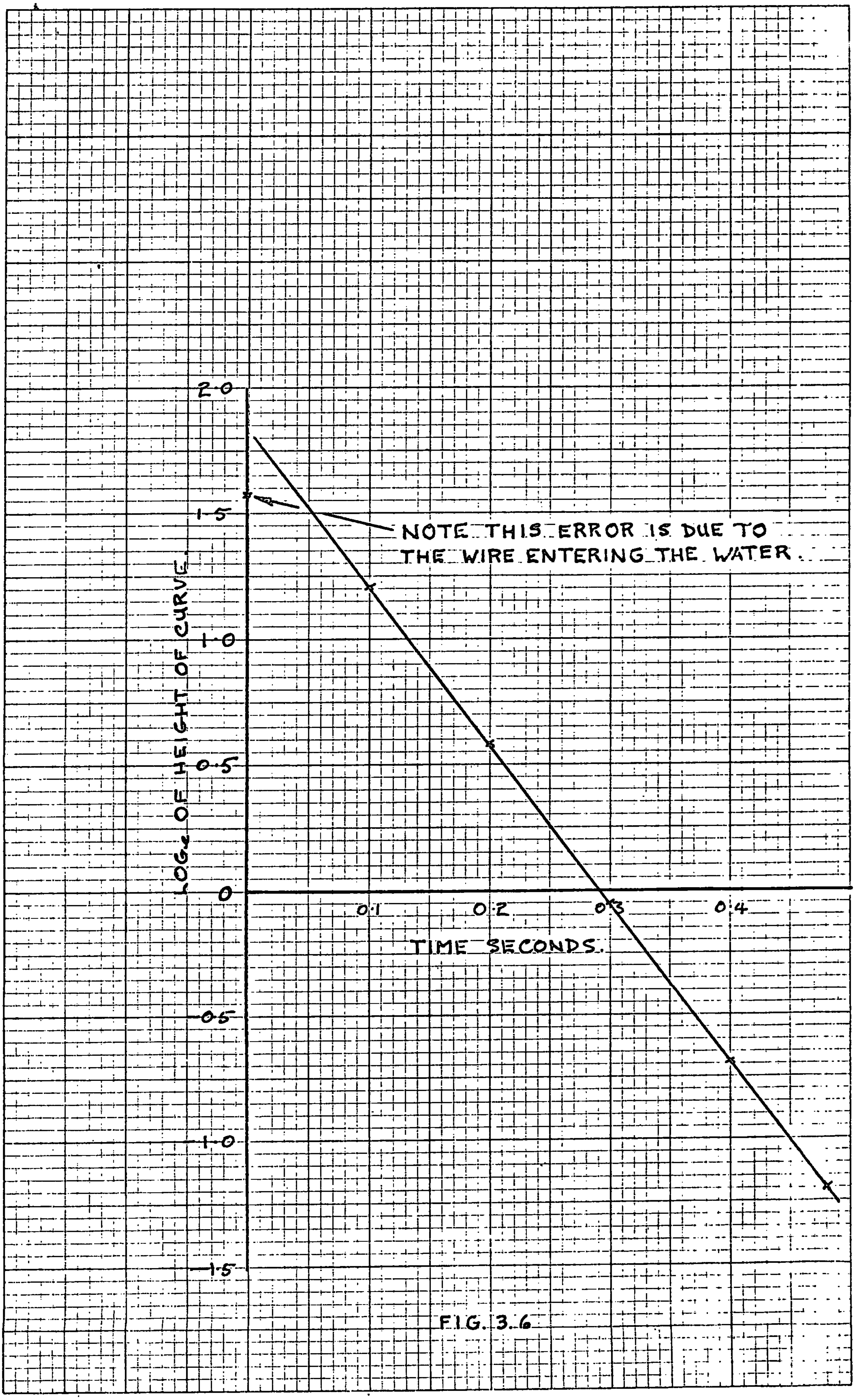
NOTE THIS ERROR IS DUE TO THE WIRE ENTERING THE WATER.
LOG$_e$ OF HEIGHT OF CURVE
TIME SECONDS.
2·0
1·5
1·0
0·5
0
-0·5
-1·0
-1·5
0·1
0·2
0·3
0·4

FIG. 3.6

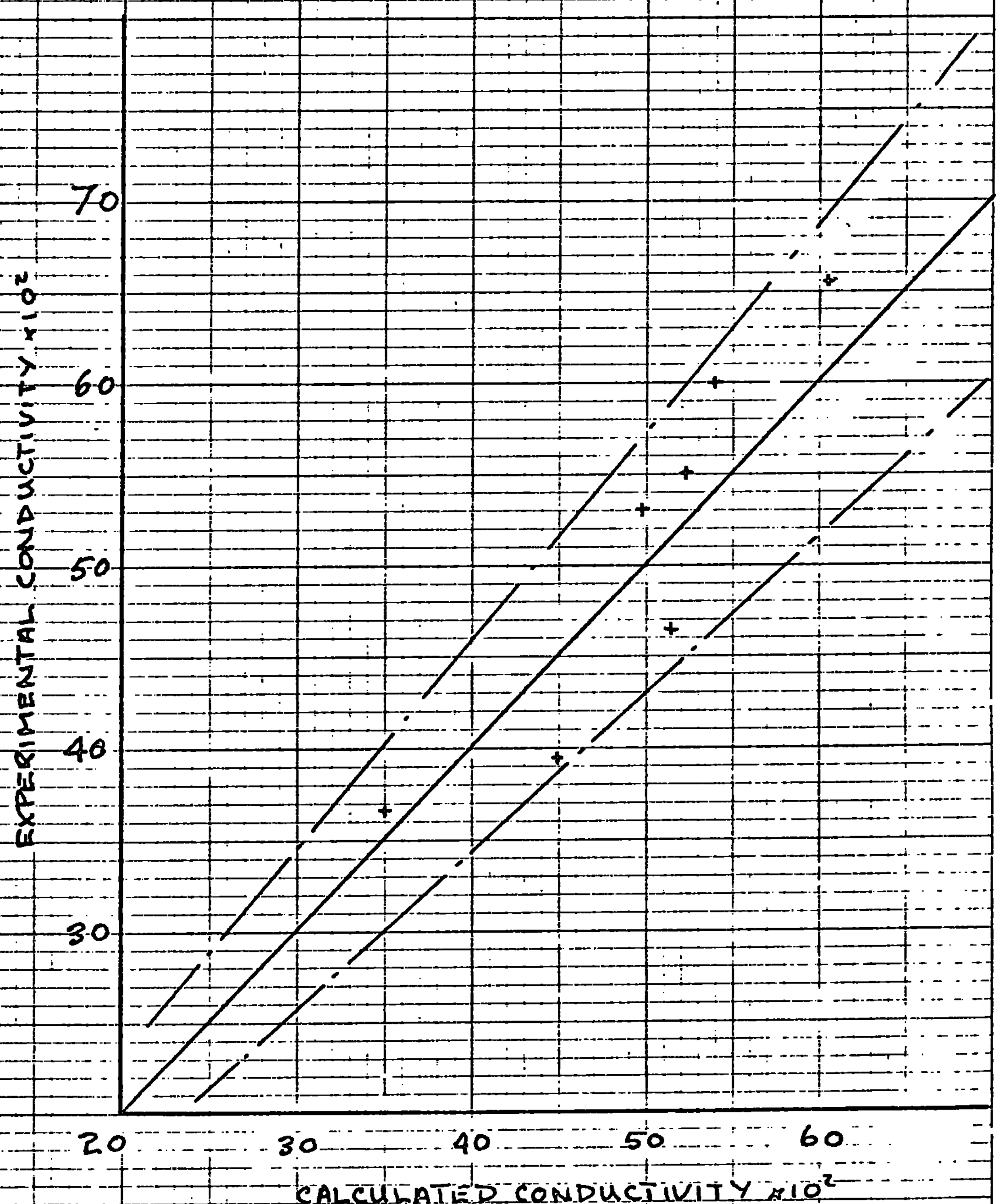
EXPERIMENTAL CONDUCTIVITY x10²
70
60
50
40
30
20
30
40
50
60
CALCULATED CONDUCTIVITY x10²

FIG. 3.7

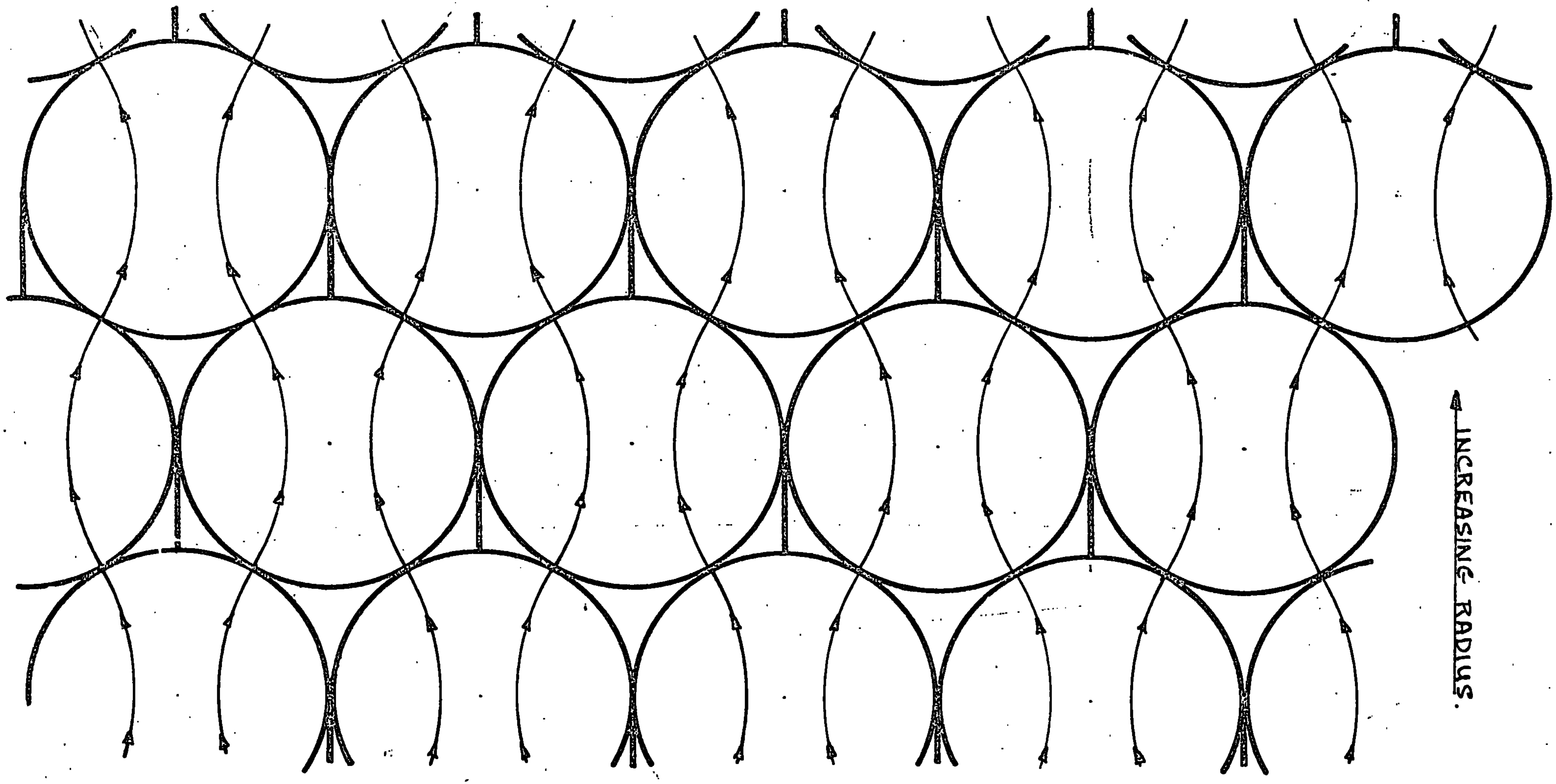

SECTION THROUGH COIL SHOWING
LINES OF HEAT FLOW. (RADIAL)

FIG. 4.1

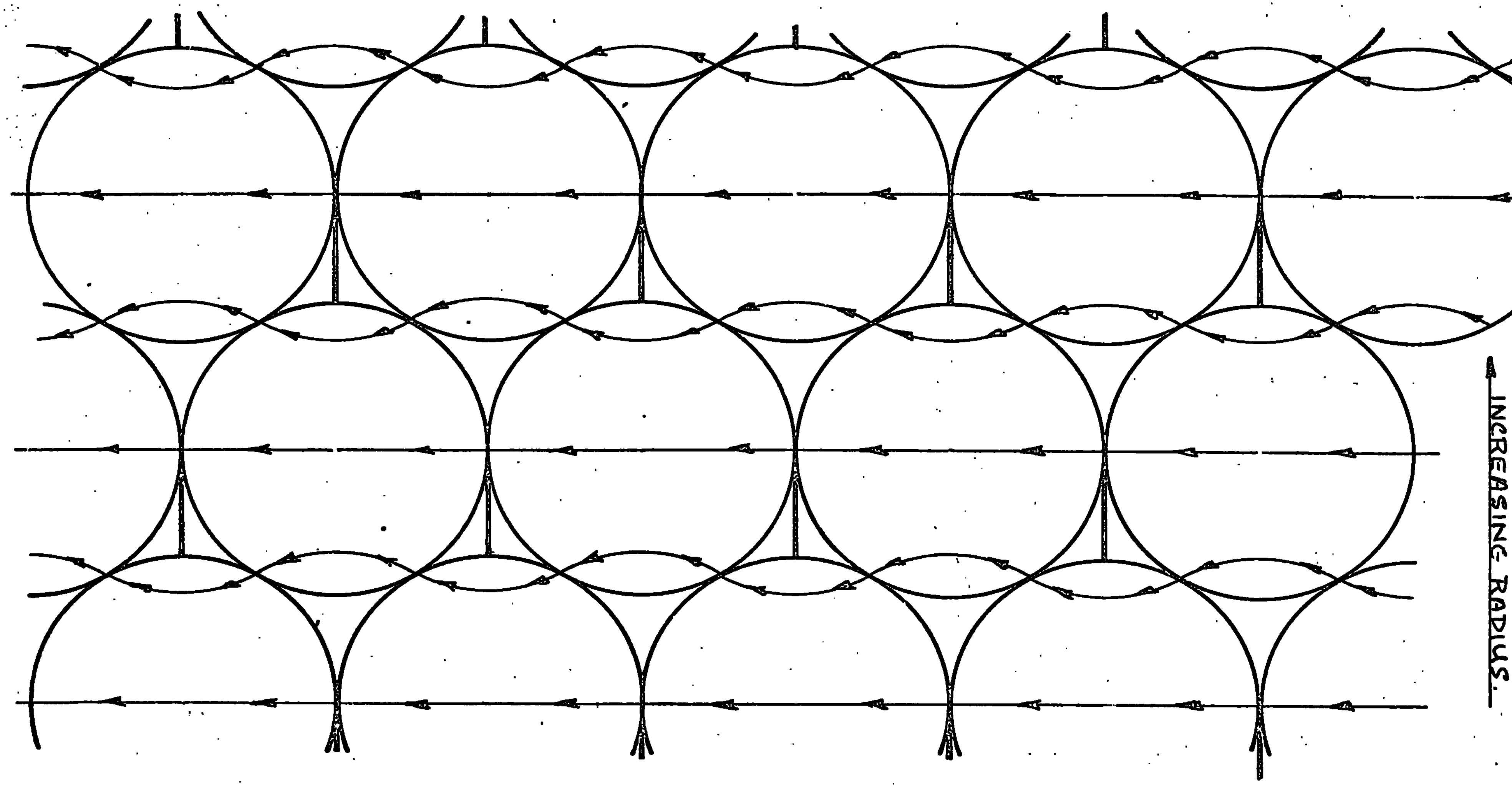

SECTION THROUGH COIL SHOWING
LINES OF HEAT FLOW (AXIAL)

FIG. 4.2

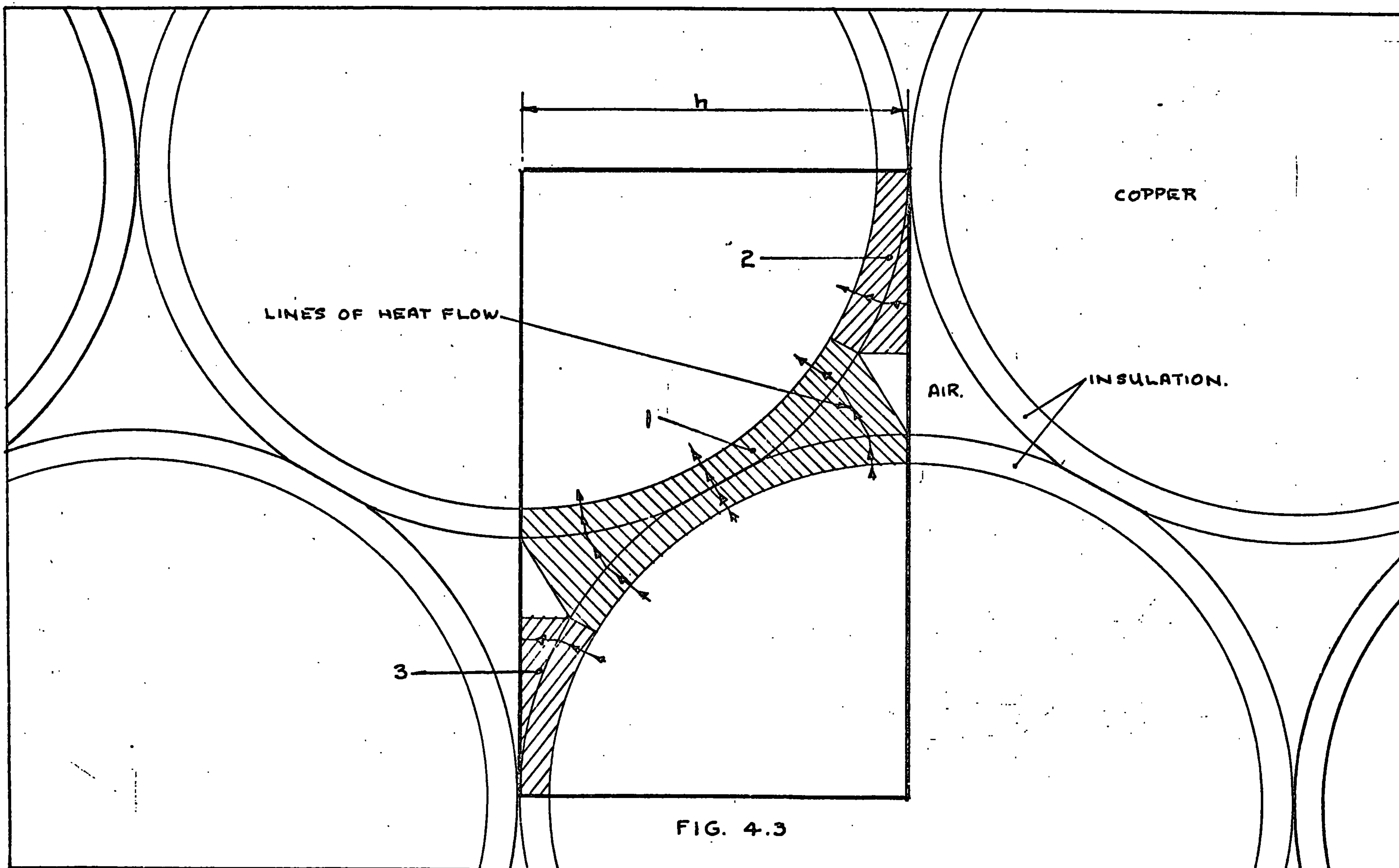

FIG. 4.3

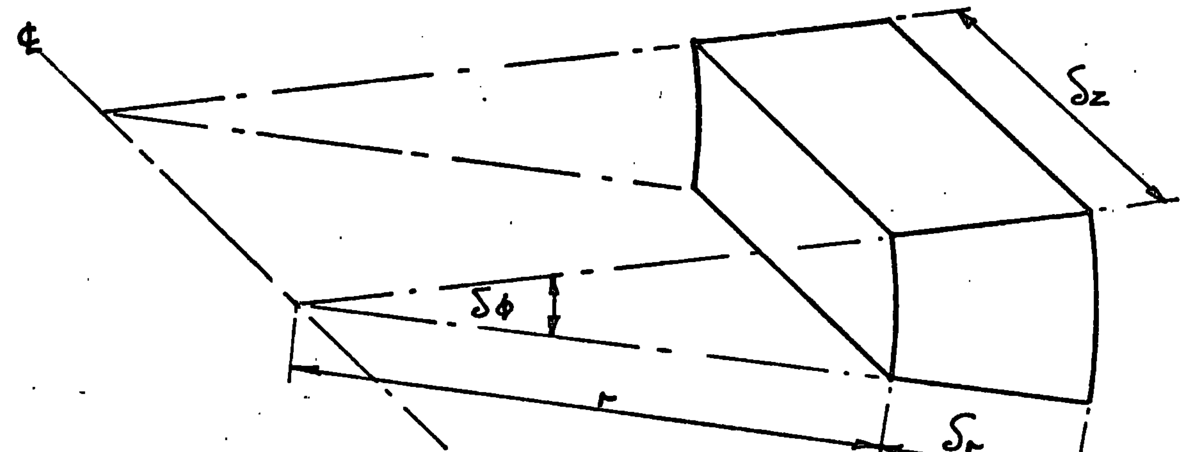

FIG. 4.4

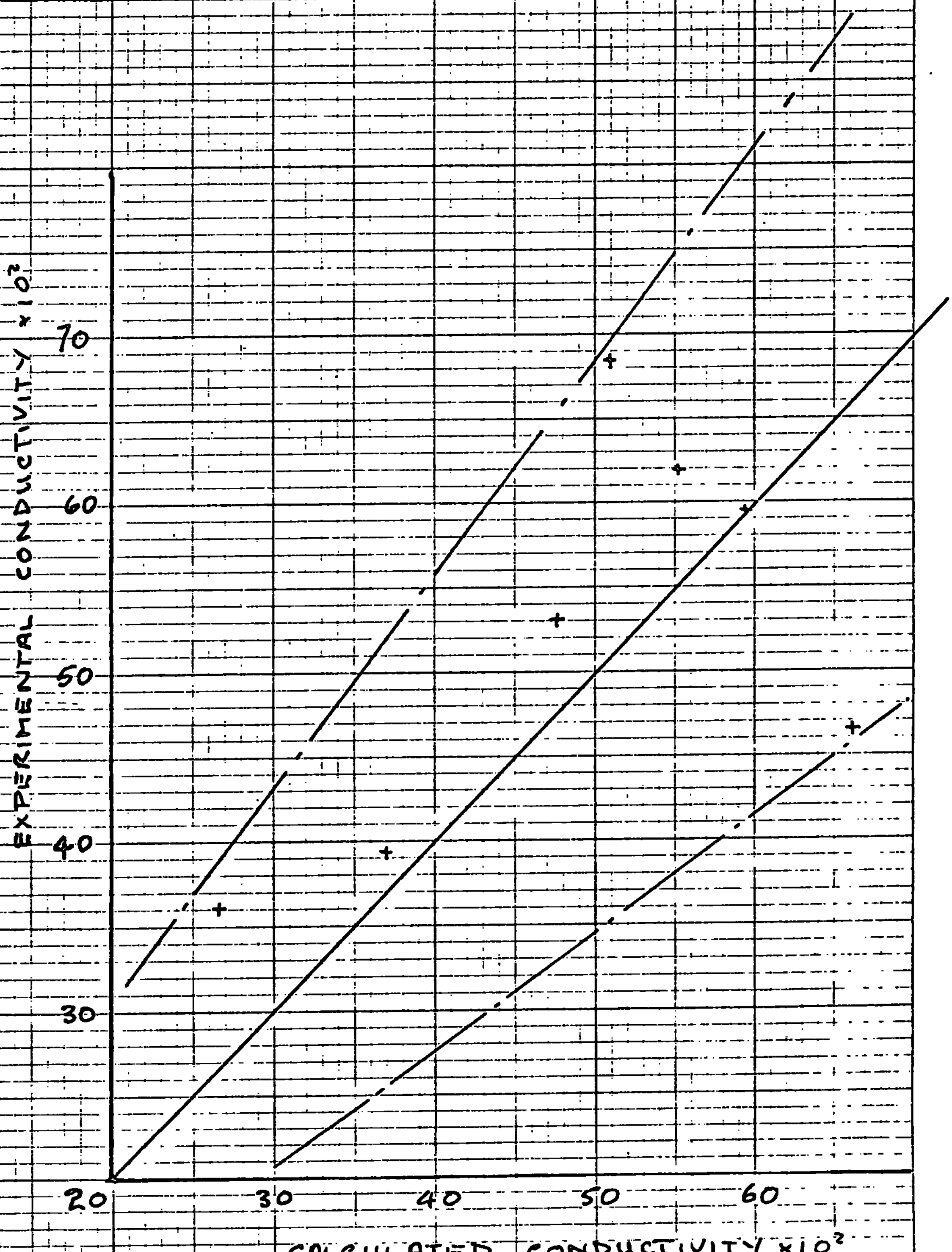

EXPERIMENTAL CONDUCTIVITY ×10²
70
60
50
40
30
20
30
40
50
60
CALCULATED CONDUCTIVITY ×10²

FIG. 5.1